RESPONSE TO REQUEST FOR ADDITIONAL INFORMATION

3/27/2014

US-APWR Design Certification

Mitsubishi Heavy Industries

Docket No. 52-021

RAI NO.:	**NO. 1050-7218 REVISION 3**
SRP SECTION:	**03.07.02 – Seismic System Analysis**
APPLICATION SECTION:	**3.7.2**
DATE OF RAI ISSUE:	**08/30/2013**

QUESTION NO. 03.07.02-229:

Section 03.3.8 of MUAP-10006 (R3) refers to the estimation of maximum displacements relative to the free field motion and basemat. These relative displacements are used in the verification of gaps between the containment internal structure (CIS), prestressed concrete containment vessel (PCCV) and reactor building (R/B), as described in Section 03.4.4, and verification of gaps between the R/B Complex and adjacent non-seismic Category I structures, which is not included in the report.

To assist the staff in its review, the applicant is requested to provide the following additional information:

(1) Provide a detailed discussion of how relative displacements are obtained from ACS SASSI. Is this done in the time domain or frequency domain? Is baseline correction performed? Are total displacements computed first, and then subtracted to obtain relative displacements?

(2) Section 03.4.4 indicates the gap between R/B and PCCV is 4 inches. The largest "coupled displacement" between R/B and PCCV is computed as 3.165 inches (1.728-inch displacement of the R/B plus 1.437-inch displacement of the PCCV). This results in a remaining clearance of only 0.835 inches (4 inches minus 3.165 inches). While this report section discusses the use of conservative seismic analysis assumptions, an independent staff calculation indicates the potential for reduced design margin in the seismic gap. The staff calculation, based on ASCE 43-05, Section 7.3 (Seismic Separation) made use of the applicants computed relative displacements and resulted in a required seismic gap greater than 4 inches.

Based on this observation, staff requests the applicant to describe the acceptance criteria used for the design of the seismic gap(s) between the R/B and PCCV.

ANSWER:

Below is MHI's response as discussed with the Nuclear Regulatory Commission (NRC) staff during the Design Certification Document (DCD) Tier 2, Section 3.7 and Section 3.8 Audits conducted in September 23-27 and November 4, 2013, respectively. The information provided in Section 03.3.8 of MUAP-10006 (R3) for the gaps between the Reactor Building R/B and the prestressed concrete containment vessel (PCCV), and the PCCV and the Containment Internal Structure (CIS) is superseded with the information provided herein.

(1) ACS SASSI RELDISP module is used to compute the relative displacements between the output node and the reference point (node). The relative displacements are computed in the frequency domain based on the displacement transfer function difference between the output node and the reference node; the results are transferred to the time domain using an inverse Fast Fourier Transform. No baseline correction is performed since the displacements are not obtained from integrating the acceleration time histories in the time domain. The following procedure is used to compute the relative displacement between the two points in the ACS SASSI RELDISP module:

a) Obtain the interpolated absolute acceleration complex transfer functions at the output node and the reference node.

b) Compute the relative acceleration transfer functions through taking the difference of the complex transfer functions of the output node and the reference node.

c) Compute the relative displacement transfer functions in complex frequency by dividing the relative acceleration transfer functions by $-\omega^2$, where ω is circular frequency.

d) Compute Fourier transforms of the relative displacement using the relative displacement transfer functions convolved with the Fourier of the input acceleration.

e) Compute the relative displacements in the time domain through the inverse Fourier transform of the relative displacement Fourier transforms

The evaluation of the seismic gap clearances between the R/B and the PCCV, and the PCCV and the CIS consider that the buildings are supported on a common basemat. The gap clearances are evaluated through post processing the relative displacement components obtained from the ACS SASSI RELDISP module. After the relative displacement time history responses between two points in the structures, due to excitation from the three components of the seismic excitations, are obtained using the ACS SASSI RELDISP module, they are combined as described in item 2) of this response to evaluate the gap clearance between two structures.

(2) The gap between the R/B and the PCCV is designed to be 4 (four) inches. If the remaining gap clearance during the CSDRS earthquake is equal to or greater than 2 (two) inches, the 4 inch designed gap is considered adequate to prevent collision of the buildings. The two inch gap clearance represents a Factor of Safety (FOS) of 2 (two) for the designed gap. The FOS is defined as the gap (4 inches) divided by the seismic relative displacement of the two buildings. The gap design margin requirement, i.e. requiring FOS of 2.0 is consistent with Section 7.3 of ASCE 43-05.

Section 7.3 of ASCE 43-05 specifies the minimum separation of δ between adjacent structures calculated as follows

$$\Delta = 2.0(\Delta_1{}^2 + \Delta_2{}^2)^{\frac{1}{2}}$$

Where Δ_1 and Δ_2 are the maximum elastically computed displacement, relative to the base of the foundation of each structure, along the same axis for the adjacent structures. This method is conservative for evaluation of the gaps between the R/B, the PCCV and the CIS that are supported on a common basemat foundation. The seismic responses of the R/B, the PCCV and the CIS are correlated since they are subject to the same earthquake excitations through the common basemat. Instead of computing the maximum displacements relative to the foundation separately for each of the structures and combining the two maximum relative displacements using ASCE 43-05 formula above, the gap variation between the structures due to seismic excitation could be evaluated directly through the displacement response time histories of the points at the perimeter of one structure relative to the points at the perimeter of the adjacent structure. Therefore, this direct relative displacement time history method is used to evaluate the maximum relative displacement, and the minimum remaining gap clearance, between the two structures. The approach for the R/B and the PCCV gap evaluation is described as follows:

Step 1 Select a point (A) at the perimeter of the PCCV and locate its counter point (B) on the R/B. The two points are located at approximately the same elevation (with one exception noted in the results table) and are approximately aligned at the same radial line from the center of the PCCV. The finite element meshes are not the same at the interface between the PCCV and the R/B so the nodes A and B, are not exactly at the same location but close enough so that there would be insignificant differences in any computation of displacements. Compute the displacement time history of point A relative to point B, i.e., direct relative displacement time history. The ACS SASSI RELDISP module is used to compute these relative displacements. The two horizontal displacement time histories in the global Cartesian coordinate system are obtained for each of the three components of the seismic input.

Step 2 Algebraically combine the horizontal displacements from the three components of the seismic input in the time domain to obtain the combined horizontal relative displacement responses. This algebraic combination is performed four times to consider the sign phases of the inputs. Thus, let X, Y and Z represent the horizontal responses due to the two horizontal and one vertical inputs, respectively, the following four combinations of the directional responses are considered: X+Y+Z, X+Y-Z, X-Y+Z and X-Y-Z. Compute the relative displacement time histories by computing the components in the radial direction of the two horizontal displacements obtained at Step 3. The radial direction is from the centerline of the PCCV to point A. The maximum values of the relative displacement time histories are then determined by scanning and selecting the largest value.

Step 3 Repeat Steps 1 to 4 for the twelve SSI cases (six soil profiles, cracked and uncracked concrete stiffness conditions). The enveloped values of the maxima from the relative displacement time histories from the twelve cases are reported in Table 1.

Table 1 presents the minimum remaining clearance between the R/B and the PCCV during CSDRS excitation. The locations at the perimeters are defined by the elevation and the azimuth with zero degree to the North and positive being counter clockwise (CCW). As indicated in Table 1, for the ten locations that are evaluated, the minimum remaining gap clearance is 2.271 inches and corresponding Factor of Safety is 2.3. Therefore, the 4 inch gap between the PCCV and the R/B is considered adequate to prevent collision during CSDRS excitation.

The gap between the PCCV and CIS is designed to be 4 (four) inches. The same approach as described above for the R/B and the PCCV is used to evaluate the clearance between the PCCV and the CIS. Thermal expansion of the CIS due to the load combination of operating plus accidental thermal is accounted for in the evaluation of the clearance between the PCCV and the CIS. Table 2 presents the minimum remaining clearance between the CIS and the PCCV resulting from combining the seismic and operating plus accidental thermal displacements. The locations at the perimeters are defined by the elevation and the azimuth with zero degree to the North and positive being counter clockwise (CCW). As indicated in Table 2, for the six locations that are evaluated, the minimum remaining clearance is 2.02 inches and corresponding Factor of Safety is 2.0. Therefore, the 4 inch gap between PCCV and CIS is considered adequate to prevent collision during CSDRS excitation combined with accidental thermal condition.

Table 1 PCCV-R/B Clearance

Location		Maximum Relative Displacement (inch)	Remaining Clearance (inch)	Factor of Safety
Degrees CCW North	Elevation (ft)			
0	114			
35	100			
74	100			
107	100			
142	100			
180	114			
218	131			
253	100			
286	114			
323	114			

Table 2 PCCV-CIS Clearance

Location		Maximum Relative Displacement (inch)*	Remaining Clearance (inch)	Factor of Safety
Degrees CCW North	Elevation (ft)			
0	76			
55	76			
114	76			
180	76			
246	76			
305	76			

* include [ ] inches thermal displacement

Impact on DCD

DCD subsection 3.7.2 will be revised as shown in Attachment 1.

Impact on R-COLA

There is no impact on the R-COLA.

Impact on PRA

There is no impact on the PRA.

Impact on Technical/Topical Report

Technical Report MUAP-10006, Rev. 3 section 03.3.8 and 03.4.4 will be revised as shown in Attachment 2.

QUESTION NO. 03.07.02-230:

DCD Subsection 3.7.1.1 states that the COL applicant will perform site-specific analysis of the US-APWR standard plant seismic Category I structures. Further, DCD Section 3.7.5, COL Information Item **3.7(23)** states that the COL Applicant will verify that the results of the site-specific soil structure interaction (SSI) analysis for the broadened in-structure response spectrum (ISRS) are enveloped by the US-APWR standard design.

Staff review of COL item 3.7(23) finds that it is not clear whether the ISRS described in MUAP-10006 (R3), Appendix 3-B, are intended to serve as points of comparison for the COL. Staff notes that SRP Section 3.7.1 (II.) (4), "COL Application Referencing an ESP and CD," specifies that a COL will compare responses at key locations in the structure to the standard design in-structure responses. Staff review finds that the DCD is not clear whether the nodal locations identified in MUAP-10006 (R3), Appendix 3-B are intended to serve as these key locations. Based on the above, the staff requests the applicant to provide the following additional information:

(a) Identify the US-APWR key locations for making site-specific ISRS comparisons to the standard plant design. The basis for the selection of the locations should also be described. The key locations should be clearly described in the DCD.

(b) Include in the DCD plots of ISRS (in three directions) for each key location and include on each plot the results for each soil profile case.

ANSWER:

The detailed information requested for Item (a) is contained in the response to RAI 950-6575 Questions 03.07.02-12. The basis for selection is to identify nodes that describe the structure response and for locations of major equipment.

The detail requested in Item (b) will be included in MUAP-10006 as an Appendix. See Attachment 2 for the mark-up of MUAP-10006 (R3).

DCD Rev. 4 Section 3.7.2.4.5 is also revised to reference the new MUAP-10006 Appendix.

Impact on DCD

Attachment 1 provides a mark-up to DCD Section 3.7.2.4.5.

Impact on R-COLA

There is no impact on the R-COLA.

Impact on PRA

There is no impact on the PRA.

Impact on Technical/Topical Report

MUAP-10006 (R3) is revised to incorporate Appendix 3-F. See Attachment 3 for mark-up of MUAP-10006 (R3).

This completes MHI's response to the NRC's question.

subgrade. The responses obtained from the SSI analyses of these generic soil profiles define the standard design ISRS up to a frequency of approximately 5 Hz. The seismic responses obtained from the analyses performed for the rock profiles 900-200, 900-100 and 2032-100 are dominated by the dynamic properties of the structures. The responses for these generic rock sites define the design basis ISRS at higher frequencies.

Table 03.4.3-1 through Table 03.4.3-6 of Technical Report MUAP-10006 (Reference 3.7-48) provide weighted average floor accelerations for the R/B Complex structures that are calculated from the results of the site-independent SSI analyses. These weighted average accelerations are the envelope of the results obtained from the SSI analyses for the six generic site profiles of the model with full (uncracked concrete) stiffness properties and the model with reduced (cracked concrete) stiffness properties. Figure 03.4.3-1 through Figure 03.4.3-12 of Technical Report MUAP-10006 (Reference 3.7-48) show shear force diagrams calculated using the weighted average floor accelerations in the two horizontal directions. Table 03.4.3-7 of Technical Report MUAP-10006 (Reference 3.7-48) provides a comparison of the base reaction results calculated from the twelve different site-independent SSI analyses. The comparison shows that maximum base shears are from the SSI analysis of full stiffness model for hard rock site 2032-100. The maximum vertical base reaction is from the SSI analyses of reduced stiffness model for 900-200 generic rock profile.

The site independent SSI analyses of R/B Complex also provide results for the maximum displacements relative to the free field motion and the building basemat. These maximum relative displacements are calculated by following the methodology described in Section 03.3.8 of Technical Report MUAP-10006 (Reference 3.7-48). ~~The maximum displacements due to three directions of the input motion are combined using the SRSS method.~~ Tables 03.4.4-1 and 03.4.4-2 of Technical Report MUAP-10006 (Reference 3.7-48) present the envelope of the results from the site-independent SSI analyses for maximum displacements for different locations at the PCCV - R/B and PCCV - CIS interfaces. The adequacy of the 4 inch gaps between the PCCV - R/B and PCCV - CIS are evaluated based on the largest coupled seismic displacement conservatively calculated. The maximum relative seismic displacements of ~~3.2~~1.73 and 1.~~6~~98 inches are obtained for the gaps at the R/B-PCCV and PCCV-CIS interfaces, respectively. This results in clearances of ~~0.8~~2.27 and 2.~~4~~02 inches respectively. Therefore the gaps of 4 inches are adequate.

DCD_03.07.02-229

DCD_03.07.02-229

DCD_03.07.02-229

Subsection 3.7.2.5 discusses development of ISRS based on the results of the site-independent seismic analyses for the US-APWR standard plant.

3.7.2.3 Procedures Used for Analytical Modeling

3.7.2.3.1 General Discussion of Analytical Models

The procedures used for development of analytical models for seismic analysis are consistent with the procedures and guidelines of SRP 3.7.2, Section II.3 (Reference 3.7-16). Structural element mass and stiffness characteristics, as well as load and tributary masses, and damping characteristics, are incorporated into the models.

The Dynamic FE model of the R/B complex is developed and validated using ANSYS (Reference 3.7-21) and then translated into SASSI (Reference 3.7-17) format. The

for the broadened ISRS are enveloped by the US-APWR standard design. This is accomplished by comparing site specific ISRS results for all locations provided in Appendix 3~~B~~F of MUAP-10006 (Reference 3.7-48) and ensuring the site-independent results in MUAP-10006 bound the site-specific results. DCD_03.07.02-230

Simplified SSI modeling approaches, such as a lumped parameter model, can be employed for the site-specific seismic response analyses of seismic category I and II buildings and structures that are not part of the US-APWR standard design if it is demonstrated that for the specific site conditions the following applies:

- The basemats are much stiffer than the supporting subgrade
- The SSI impedance functions remain relatively constant in the range of frequencies important for the design
- The consideration of basemat embedment yields conservative results

In accordance with SRP 3.7.2 (Reference 3.7-16), Section II.4, fixed base response analysis can be performed if the basemats are supported by subgrades having a shear wave velocity of 8,000 ft/s or higher, under the entire surface of the foundation.

3.7.2.5 Development of Floor Response Spectra

The SASSI analyses provide results for the response of the R/B complex due to the three directional design input ground motion for both the cracked and uncracked R/B complex models for each of the generic soil profiles. ISRS are generated for various areas of the R/B complex in accordance with RG 1.122 (Reference 3.7-26) to serve as the seismic design basis for the design of pipe and equipment. The ISRS may be developed from the SASSI ARS data for any node location or damping values, or for variable damping where permitted by ASME Code Case N411-1, as discussed in RG 1.61 (Reference 3.7-15). At selected node locations, ARS in the three orthogonal directions are calculated for each of the three orthogonal directions of the input ground motion from time histories generated by SASSI. The ARS are calculated at 301 frequency points equally distributed on the logarithmic scale at the range of frequency from 0.1 Hz to 100 Hz. The ARS for particular damping value obtained for the three directions of the input ground motion are then combined using the Square Root Sum of the Squares (SRSS) method as follows:

$$ARS_X = \sqrt{ARS_{XX}^2 + ARS_{YX}^2 + ARS_{ZX}^2}$$

$$ARS_Y = \sqrt{ARS_{XY}^2 + ARS_{YY}^2 + ARS_{ZY}^2}$$

$$ARS_Z = \sqrt{ARS_{XZ}^2 + ARS_{YZ}^2 + ARS_{ZZ}^2}$$

where:

B roof, which varies in elevation as shown on the general arrangement drawings in Section 1.2. However, to preclude seismic and structural interaction above the common basemat, the R/B is separated from the PCCV with a 4 in. minimum gap at all above-basemat locations. The gap has been sized to prevent contact between the R/B and PCCV super-structures even if the maximum translational and rotational displacements due to a seismic loading (and other loading) were to occur. The gap size has been determined by considering, at all potential interaction locations, the ~~absolute~~ summation of the deflection associated with each super-structure, obtained from the time history analysis results for those structures. DCD_03.07.02-229

3.7.2.9 Effects of Parameter Variations on Floor Response Spectra

To account for variations in the structural frequencies due to the uncertainties in parameters, such as material and mass properties of the structures, damping values, soil properties, SSI analysis techniques, and the seismic modeling methods, the ISRS are developed from six SSI soil profiles representing a range of soft soil to hard rock conditions and two structural stiffnesses representing cracked and uncracked conditions values. These 12 cases and 8 additional cases from SSSI analysis are enveloped and then broadened by ±15% as described in Section 3.7.2.5. Developing enveloping ISRS using this range of parameters and the CSDRS as an input motion creates a design envelop that will encompass most variations in site-specific conditions.

3.7.2.10 Use of Constant Vertical Static Factors

The plant design does not utilize constant vertical static factors in the seismic design. The vertical component of the seismic motion is obtained using one of the analysis methods described in Subsection 3.7.2.1. The vertical component is combined with the horizontal components of the seismic motion as described in Subsection 3.7.2.6.

3.7.2.11 Method Used to Account for Torsional Effects

Inertial torsional effects are inherently considered in the seismic analysis using a 3D FE model.The site-independent SSI analyses are performed using FE models described in Section 3.7.2.3 that represent the general layout of the building and explicity account for eccentricities between the center of mass and center of rigidities.

The structural members of category I and II buildings are designed for two types of torsional effects: (1) torsional responses captured in the seismic response analysis; and (2) accidental torsion. The accidental torsion considers torsional effects that are not captured in the seismic response analyses such as torsion that is due to incoherency (spatial variation) of the input ground motion, non vertically propagating incident waves, and/or accidental eccentricities. The accidental torsional effect is included in accordance with SRP 3.7.2 Section II (Reference 3.7-16) in the design of all seismic category I and II structures by use of the following process:

- The accidental torsional moments are computed by determining an additional building torsion equal to story shear force with a moment arm of +/- 5% of the plan dimension of the floor perpendicular to the direction of the applied motion. This computation is performed for both horizontal directions.

03.3.8 Computation of Maximum Displacement

The results obtained from the SSI analyses of the R/B complex model with reduced (cracked concrete) stiffness properties and full stiffness properties (uncracked concrete) are used to compute the maximum relative displacements. These results serve as the basis for evaluation of gaps between CIS, PCCV and R/B. ~~These maximum relative displacements are developed as follows:~~

~~1.Calculate maximum displacements relative to the basemat in each of the three response directions due to each of the 3-directional input motions from the SSI analyses of the R/B complex.~~

~~2.Apply the SRSS rule to combine the nodal maximum displacements due to the three directions of the earthquake calculated in Step 1.~~

~~3.Envelope the results of the SRSS combined maximum displacements from the SSI analyses of the six generic soil cases and the two structural stiffness levels~~

~~4.Compare maximum relative displacements at the perimeters of the buildings at elevations close to other structures to obtain contribution of elastic seismic displacements that serve for assessment of adequacy of gaps between buildings.~~

The evaluation of the seismic clearance between the R/B and the PCCV, and the PCCV and the CIS considers that the buildings are supported on a common basemat. The seismic responses of the R/B, the PCCV, and the CIS are correlated since they are subjected to the same earthquake excitations through the common basemat. The gap variation between the structures due to seismic excitation could be evaluated directly through the displacement of the points at the perimeter of on structure relative to the points at the perimeter of the adjacent structure. Therefore, this direct relative displacement time history method is used to evaluate the maximum relative displacement, and the remaining clearance, between the structures. The approach for the R/B and PCCV gap evaluation is described as follows:

1. Select a point (A) at the perimeter of the PCCV and locate its counter point (B) on the R/B. The two points are located at the approximately the same elevation and lined up approximately at the same radial line from the center of the PCCV. The finite element meshes are not aligned at the interface between the PCCV and R/B so the nodes A and B are not exactly at the same location but close enough so that there would be insignificant differences in any computation of displacement.
2. Compute the displacement time history of the point A relative to the point B, i.e., direct relative displacement time history. ACS SASSI RELDISP module is used to compute these relative displacements. The two horizontal displacement time histories in the global Cartesian coordinate system are obtained for each of the three components of seismic input.
3. Algebraically combine the horizontal displacement from the three components of the seismic input in the time domain to obtain the combined horizontal relative displacement responses. This algebraic combination is performed four times to consider the sign phases of the inputs. Thus, let X, Y, and Z represent the horizontal responses due to the two horizontal and one vertical inputs, respectively. The following four combinations of the directional responses are considered: X+Y+Z, X+Y-Z, X-Y+Z, and X-Y-Z.
4. Compute the relative displacement time histories by computing the components in the radial direction of the two horizontal displacements obtained at Step 3. The radial direction is from the centerline of the PCCV to point A. The maximum values of the

relative displacement time histories are then determined by scanning and selecting the largest value.

5. Repeat Steps 1 through 4 for the twelve SSI cases (six soil profiles, cracked and uncracked concrete conditions). The enveloped values of the maxima from the relative displacement time histories from the twelve cases are reported.

The same approach as described above for the R/B and the PCCV is used to evaluate the gap clearance between the PCCV and the CIS. But the thermal expansions of the CIS due to the load combination of operating plus accidental thermal are added to the seismic induced gap movement.

03.4.4 Maximum Relative Displacements

Based on the methodology described in Section 03.3.8, the maximum displacements relative to the free field motion and basemat were determined from the SSI analysis of the R/B complex.

The seismic gap between the R/B and the PCCV is designed to be 4 inches. If the remaining seismic clearance during an SSE seismic event is not smaller than 2 inches, the 4 inch gap is considered adequate to prevent collision of the two structures. The two inch clearance represents a Factor of Safety (FOS) of 2 for the designed seismic gap. The FOS is defined as the seismic gap divided by the seismic relative displacements of the two structures. The seismic gap design is consistent with the requirements of Section 7.3 of ASCE/SEI 43-05 (Reference 03-14).

Table 03.4.4-1 presents the minimum seismic remaining clearance between the R/B and the PCCV during earthquake excitation. The locations at the perimeters of the structures are defined by the elevation and the azimuth with 0 degrees on North and positive being Counter-Clockwise (CCW). As indicated in Table 03.4.4-1, the minimum remaining clearance is 2.271 inches and the corresponding factor of safety is 2.3. Therefore, the 4 inch seismic gap between the R/B and the PCCV is considered adequate to prevent collision during a seismic event.

The seismic gap between the PCCV and the CIS is also designed to be 4 inches. The same approach as described above for the R/B and the PCCV is used to evaluate the clearance between the PCCV and the CIS. But thermal expansions of the CIS due to load combination of operating plus accident thermal are added to the seismic induced gap movement.

Table 03.4.4-2 presents the minimum remaining clearance between the CIS and the PCCV resulting from the combination of seismic and operating plus accident thermal conditions. The locations at the perimeters of the structures are defined by the elevation and the azimuth with 0 degrees on North and positive being Counter-Clockwise (CCW). As indicated in Table 03.4.4-2, the minimum remaining clearance is 2.02 inches and corresponding factor of safety is 2.0. Therefore, the 4 inch seismic gap between the PCCV and the CIS is considered adequate to prevent collision during a seismic excitation combined with accident thermal conidtion.

~~The SRSS method was implemented to combine the motion inputs for determination of the nodal maximum displacements. The maximum displacement results envelope the maximum displacements of the soil cases analyzed. These results are tabulated in Table 03.4.4-1 and Table 03.4.4-2.~~

~~The angular orientations are approximate locations. Based on the available model nodes, angular orientations were selected based on the available nodes between adjacent structures. The orientation of the PCCV - R/B and PCCV - CIS interfaces is based on North as 0 degrees with positive being Clockwise (CW).~~

~~The results were reviewed to determine the maximum coincident displacements which would result in the smallest gap between the structures. A conservative approach was taken where the maximum displacement across all elevations at a location in a structure was determined. This maximum was then compared with the maximum determined from the adjacent structure at the similar angular location. Adding to the conservative approach, the displacements compared are not radial results that occur along the same vector, but are the maximum scalar value found through the SRSS.~~

~~Following this approach, the minimum clearance, based on an initial minimum 4-inch gap between structures, was determined from the displacement results relative to center of the basemat to occur at the following locations:~~

- ~~R/B-PCCV Interface - Table 03.4.4-1 shows that the largest coupled displacement of all the locations analyzed is 3.165 inches (1.728 inch displacement of R/B plus a 1.437-inch displacement of the PCCV) at 0 degrees CW of North for the cracked case. This results in a clearance of 0.835 inches (3.165 inches subtracted from the 4-inch gap).~~
- ~~PCCV-CIS Interface – shows that the largest coupled displacement of all the locations analyzed is 1.599 inches (1.030 inch displacement of the PCCV plus a 0.569 inch displacement of the CIS) at 300 degrees CW of North for the cracked case. This results in a clearance of 2.401 inches (1.599 inches subtracted from the 4-inch gap).~~

Table 03.4.4-1 PCCV - R/B ~~Maximum Relative Displacements - Basemat~~Clearance

Degrees CW North	Elevation (ft)	Cracked Displacement (in)		Uncracked Displacement (in)	
		R/B	PCCV	R/B	PCCV
0	114	1.728	1.437	1.015	0.881
35	100	0.787	1.208	0.455	0.733
74	100	0.725	1.247	0.386	0.727
~~107~~	~~100~~	~~0.657~~	~~1.249~~	~~0.334~~	~~0.719~~
142	100	0.694	1.237	0.332	0.756
180	114	0.867	1.454	0.425	0.897
218	131	0.976	1.612	0.493	0.971
253	100	0.949	1.253	0.517	0.720
286	114	1.550	1.481	0.949	0.864
323	114	1.487	1.474	0.875	0.900

Location		Maximum Relative Displacement (in)	Remaining Clearance (in)	Factor of Safety
Degrees CCW North	Elevation (ft)			
0	114	1.729	2.271	2.3
35	100	0.850	3.150	4.7
74	100	0.937	3.063	4.3
107	100	0.898	3.102	4.5
142	100	1.114	2.886	3.6
180	114	1.588	2.412	2.5
218	131	1.508	2.492	2.7
253	100	0.937	3.063	4.3
286	114	1.626	2.374	2.5
323	114	1.571	2.429	2.5

Table 03.4.4-2 PCCV - CIS ~~Maximum Relative Displacements - Basemat~~Clearance

Degrees CW North	Elevation (ft)	Cracked Difference (in)		Uncracked Difference (in)	
		PCCV	CIS	PCCV	CIS
0	75	0.992	0.549	0.610	0.406
60	75	0.930	0.557	0.556	0.407
120	75	0.950	0.558	0.544	0.401
180	75	0.990	0.568	0.603	0.403
245	75	0.953	0.572	0.550	0.410
300	75	1.030	0.569	0.607	0.415

Location		Maximum Relative Displacement (in)*	Remaining Clearance (in)	Factor of Safety
Degrees CCW North	Elevation (ft)			
0	76	1.935	2.065	2.1
55	76	1.782	2.218	2.2
114	76	1.818	2.182	2.2
180	76	1.964	2.036	2.0
246	76	1.759	2.241	2.3
305	76	1.980	2.020	2.0

* Inlcudes 1.097 in thermal displacement.

complex, these two buildings are too small and light to have any significant effect on the response of the much heavier and larger R/B complex.

The SSSI effects on ISRS are considered in the Standard Plant design by enveloping all twenty cases, twelve cases for SSI and eight cases for SSSI, as discussed at beginning of this section.

03.4.2 In-Structure Response Spectra (ISRS)

ISRS are generated at specific locations in the R/B complex following the methodology described in Section 03.3.6. Appendix 3-A provides figures showing the location within the R/B complex where the ISRS are developed. The 15% broadened envelope of the results obtained from the six generic soil profiles, cracked and uncracked , and both SSI and SSSI models, provide broad frequency ISRS. Appendix 3-B provides the design basis ISRS for a selection of equipment and structural locations throughout the R/B complex.

As an example, Figure 03.4.2-1 through Figure 03.3.4.2-3 present the design basis ISRS at the top of the Reactor Cavity for the NS, EW and Vertical directions, respectively. The top of the Reactor Cavity is comprised of eight structural nodes, presented in Table 3-A.1.1-1 and schematically in Figure 3-A.1.0-1. The design basis ISRS is developed with these eight structural nodes, using the process described in Section 03.3.6 and corresponding figures, Figure 03.3.6-1 through Figure 03.3.6-6.

Appendix 3-F provides the ISRS, at the same locations presented in Appendices 3-A and 3-B, for the purpose of comparison by a COL Applicant to determine if site-specific ISRS are bounded by the site-independent responses. The ISRS are presented for the cracked and uncracked cases separately for clarity of the Figures. Shown on each plot is the broadened envelope results as presented in Appendix 3-B, but without the ISRS valleys filled. Also shown are the 10 individual soil cases (6 for SSI and 4 for SSSI) for the cracked and uncracked cases, respectively.

03.4.3 Seismic Loads

The loads used for seismic design of R/B complex are developed following the methodology described in Section 03.3.7. The summary of weighted average floor accelerations of the PCCV, CIS, R/B, A/B, East PS/B and West PS/B are provided in Table 03.4.3-1 through Table 03.4.3-6. These Tables provide the cracked and uncracked results for the envelope of the six soil cases in all three directions. Figure 03.4.3-1 through Figure 03.4.3-12 present the story shear diagrams for these locations. The story shear diagrams present the comparison of the cracked (presented in dark blue) and uncracked (presented in pink) cases of the SSI model. The presented results (in kips) are the enveloped results of all six soil profiles. These values are representative design values, but will be confirmed during the design process. Table 03.4.3-7 provides the base shear forces at the bottom of the basemat. The table shows that 2032-100 is the governing soil case for all directional responses for both cracked and uncracked except for the cracked vertical response which is governed by the 900-200 soil case.

Figure 03.4.3-25 through Figure 03.4.3-27 present contour plots of the enveloped ZPA values at the R/B ground floor elevation. The plots for vertical acceleration contour are used to determine the out of plane accelerations for the slab design. The plots are created using ANSYS post-processing module (Reference 03-13).

Appendix 3-F

US-APWR ISRS Plots for COL Comparison

APPENDIX 3-E TABLE OF CONTENTS

LIST OF FIGURES

3-F.1.0 OBJECTIVE

This appendix presents the ISRS plots that serve as the basis for comparison by a COL Applicant. Appendix 3-A presents the critical structural locations of the ISRS presented herein.

3-F.2.0 US-APWR ISRS FOR COL COMPARISON

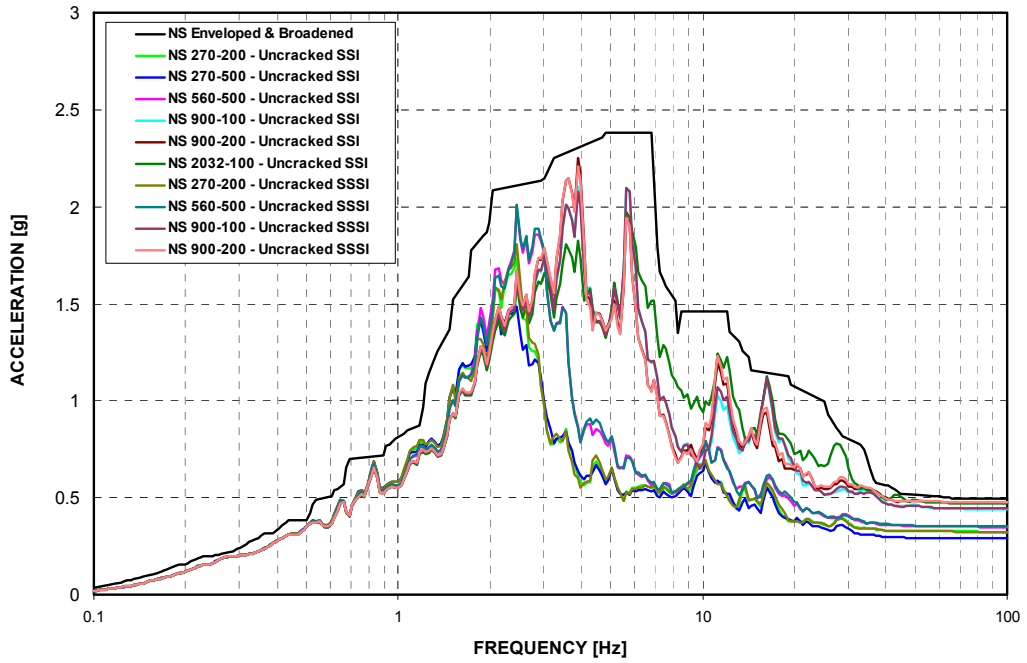

Figure 3-F.2.0-1 ISRS at Top of Reactor Cavity – 3% Damped Response in NS Direction (X) - Uncracked

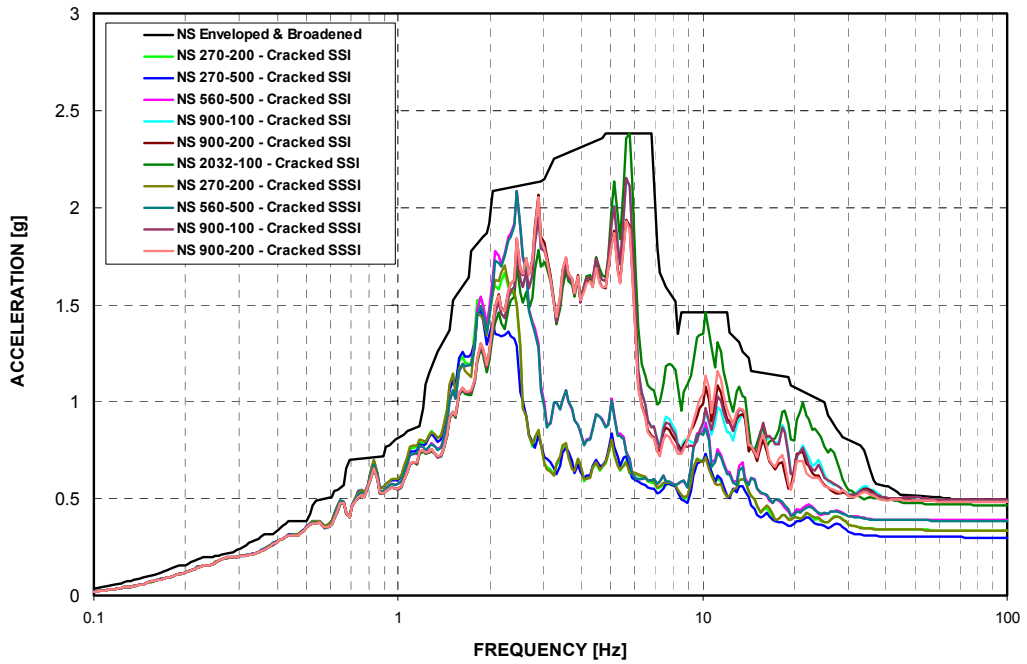

Figure 3-F.2.0-2 ISRS at Top of Reactor Cavity – 3% Damped Response in NS Direction (X) - Cracked

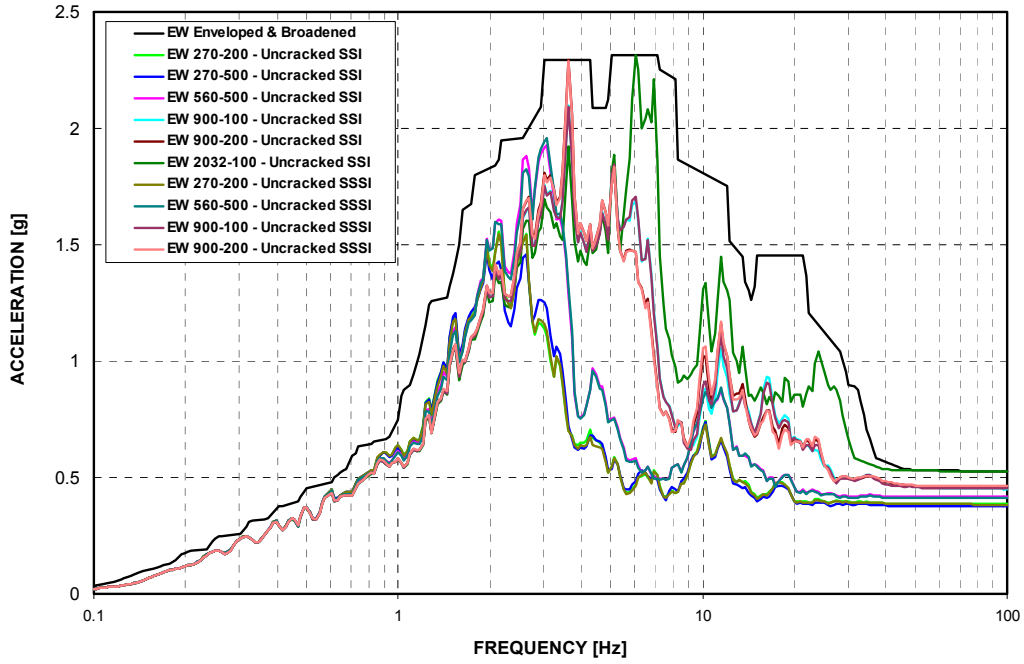

Figure 3-F.2.0-3 ISRS at Top of Reactor Cavity – 3% Damped Response in EW Direction (Y) - Uncracked

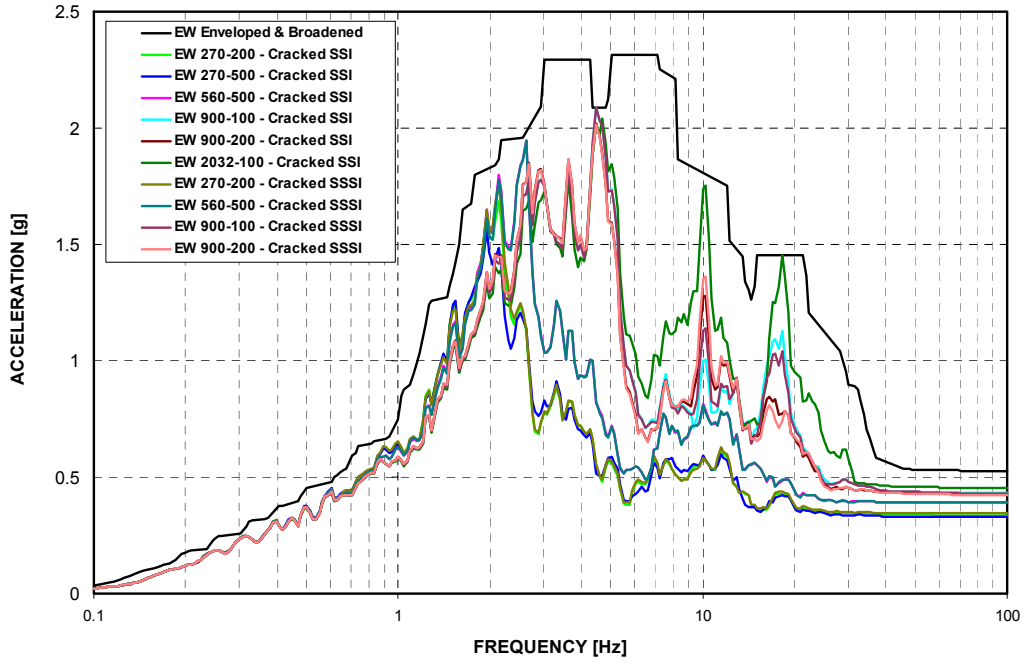

Figure 3-F.2.0-4 ISRS at Top of Reactor Cavity – 3% Damped Response in EW Direction (Y) - Cracked

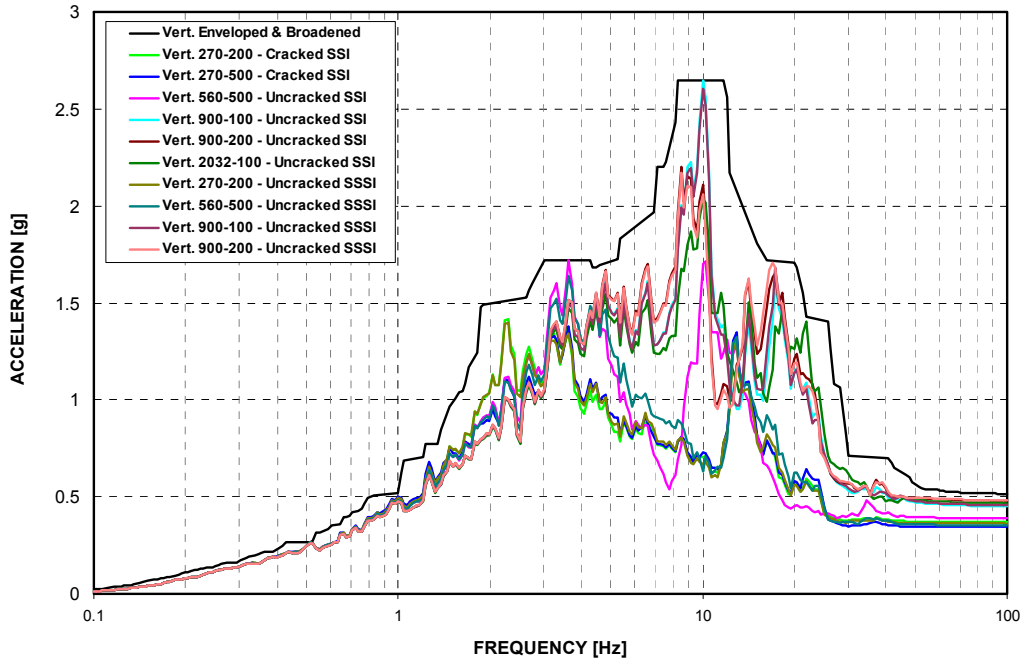

Figure 3-F.2.0-5 ISRS at Top of Reactor Cavity – 3% Damped Response in Vertical Direction (Z) - Uncracked

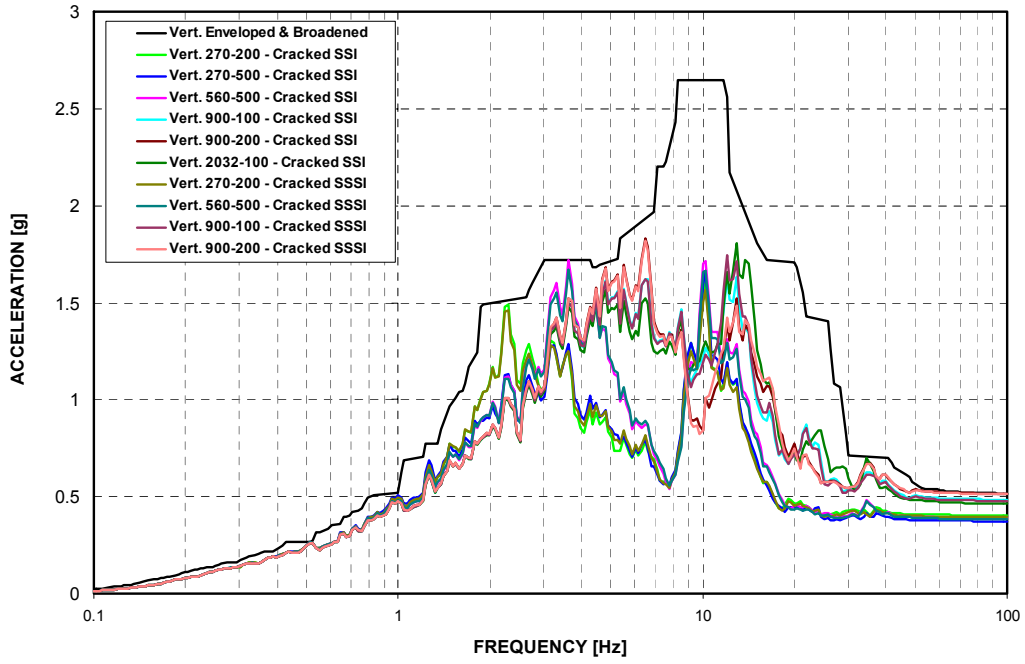

Figure 3-F.2.0-6 ISRS at Top of Reactor Cavity – 3% Damped Response in Vertical Direction (Z) - Cracked

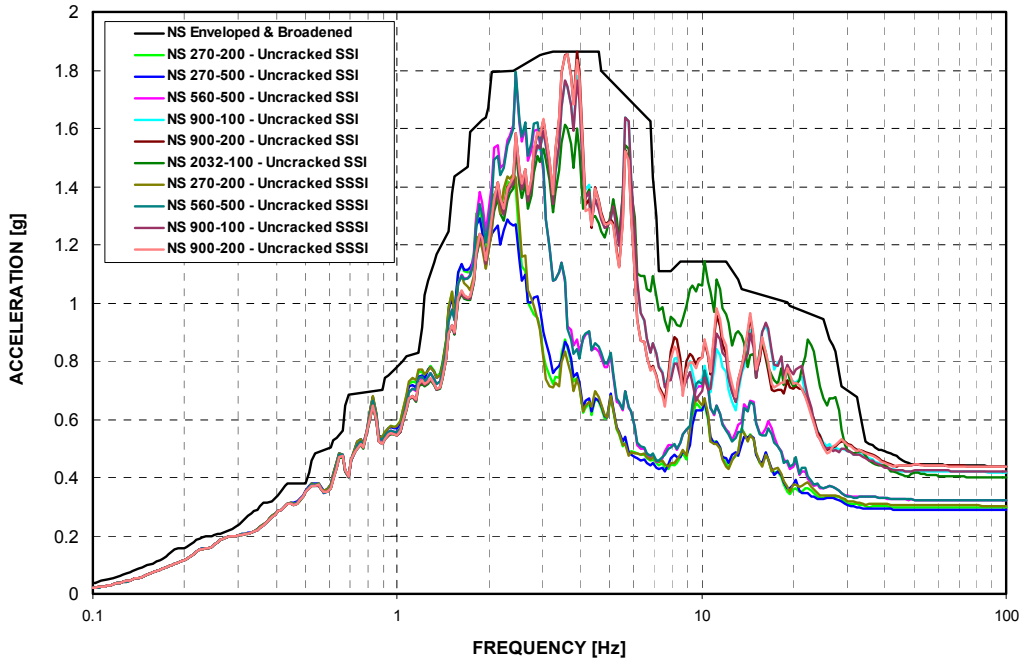

Figure 3-F.2.0-7 ISRS at Sump Strainer – 3% Damped Response in NS Direction (X) - Uncracked

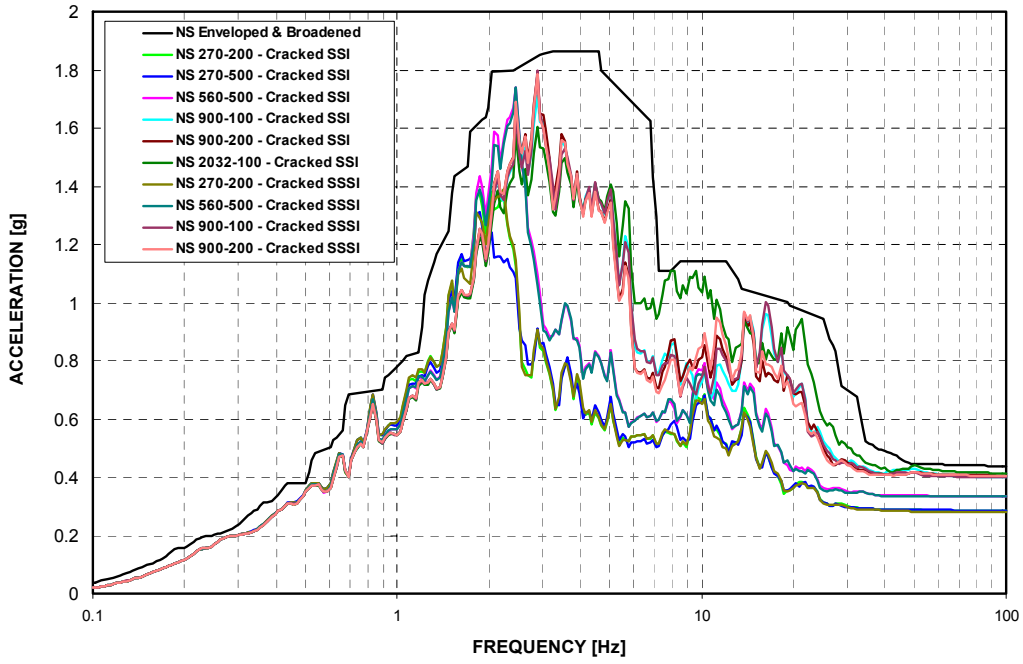

Figure 3-F.2.0-8 ISRS at Sump Strainer – 3% Damped Response in NS Direction (X) - Cracked

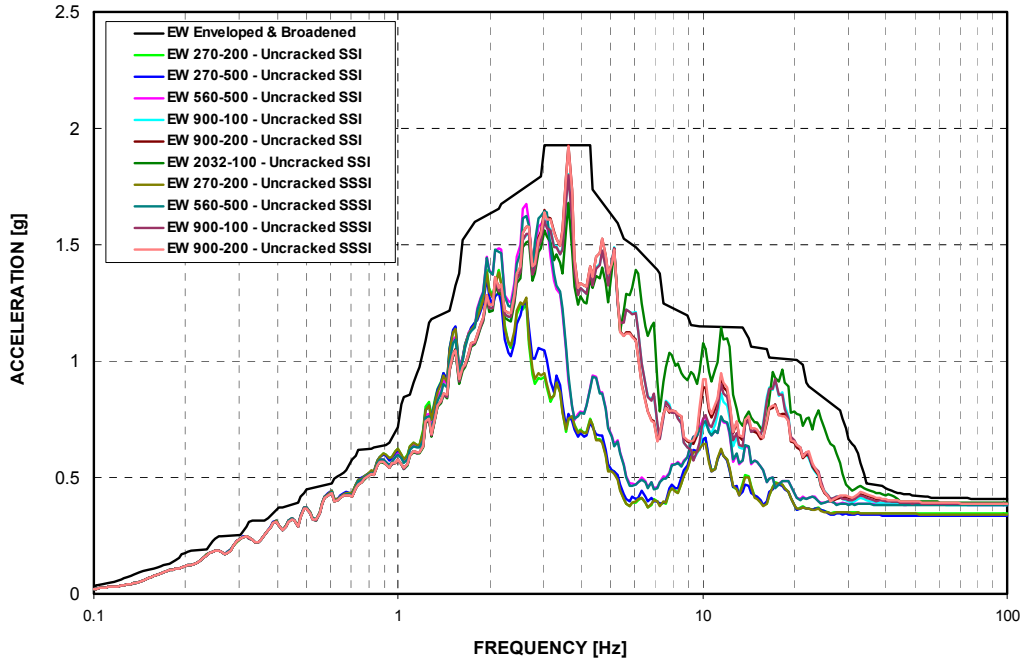

Figure 3-F.2.0-9 ISRS at Sump Strainer – 3% Damped Response in EW Direction (Y) - Uncracked

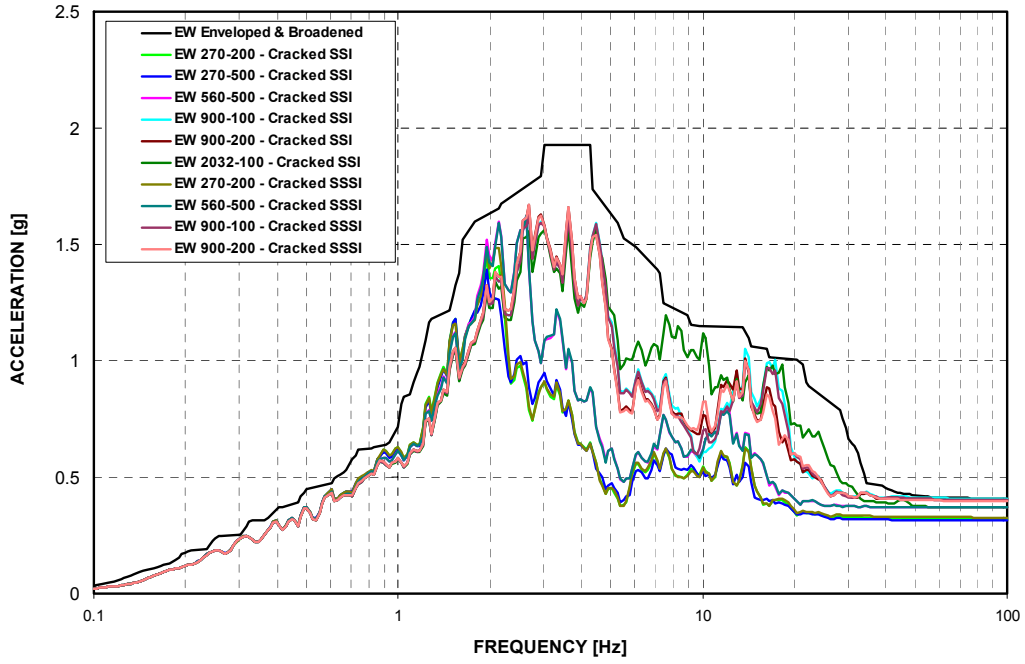

Figure 3-F.2.0-10 ISRS at Sump Strainer – 3% Damped Response in EW Direction (Y) - Cracked

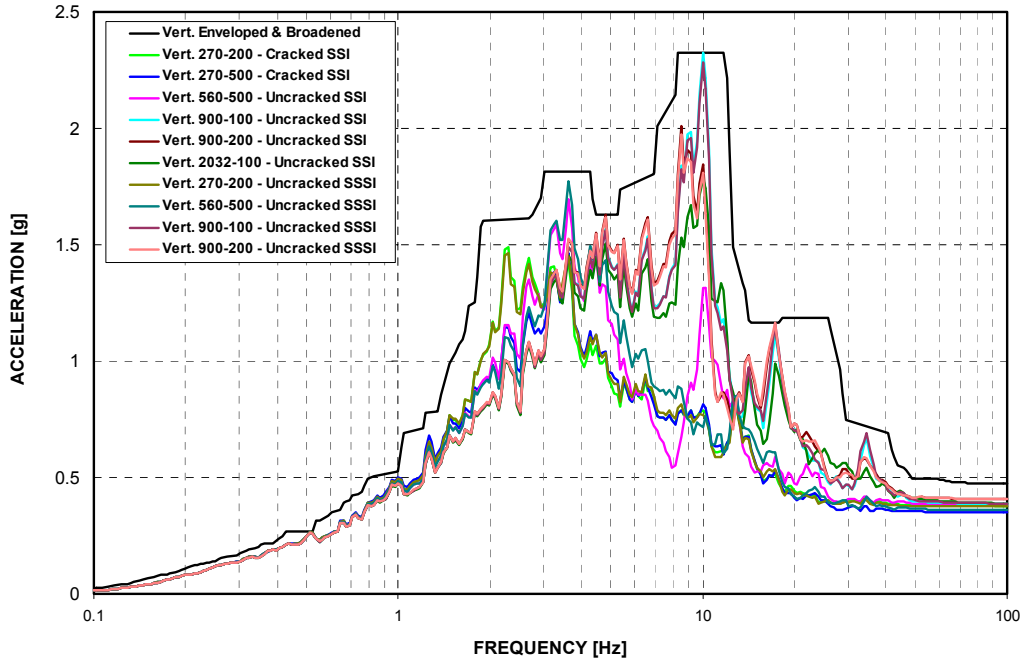

Figure 3-F.2.0-11 ISRS at Sump Strainer - 3% Damped Response in Vertical Direction (Z) - Uncracked

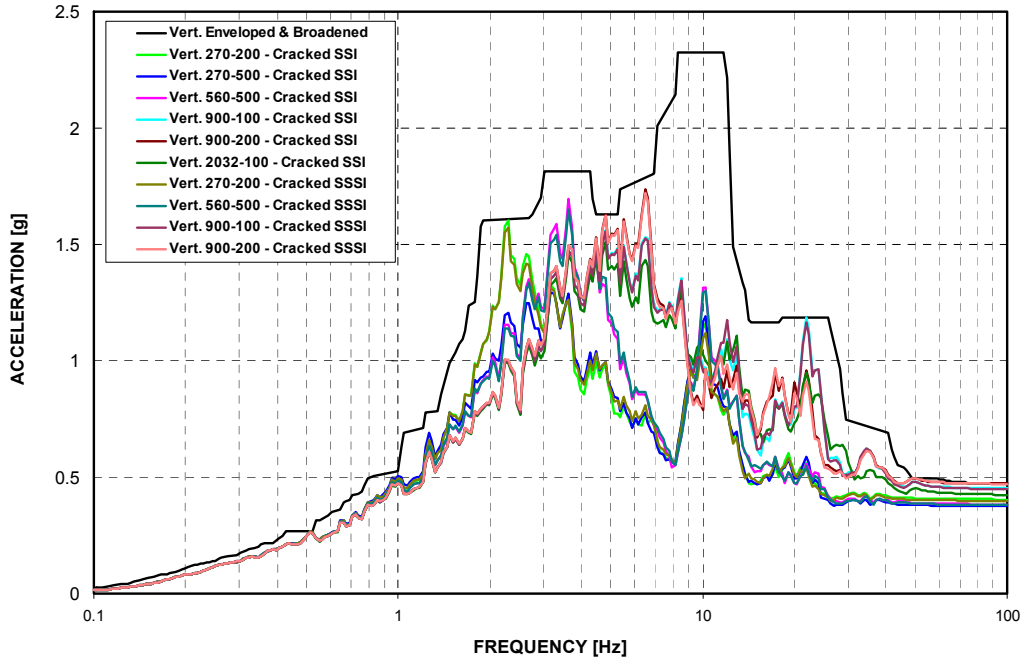

Figure 3-F.2.0-12 ISRS at Sump Strainer - 3% Damped Response in Vertical Direction (Z) - Cracked

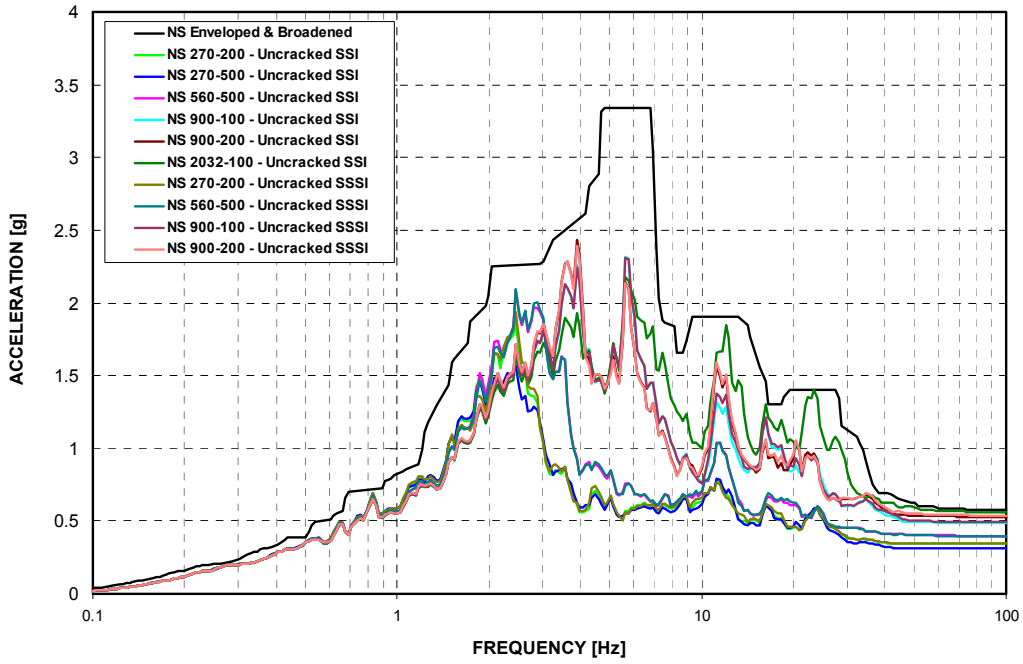

Figure 3-F.2.0-13 ISRS at SG Lower Supports - 3% Damped Response in NS Direction (X) - Uncracked

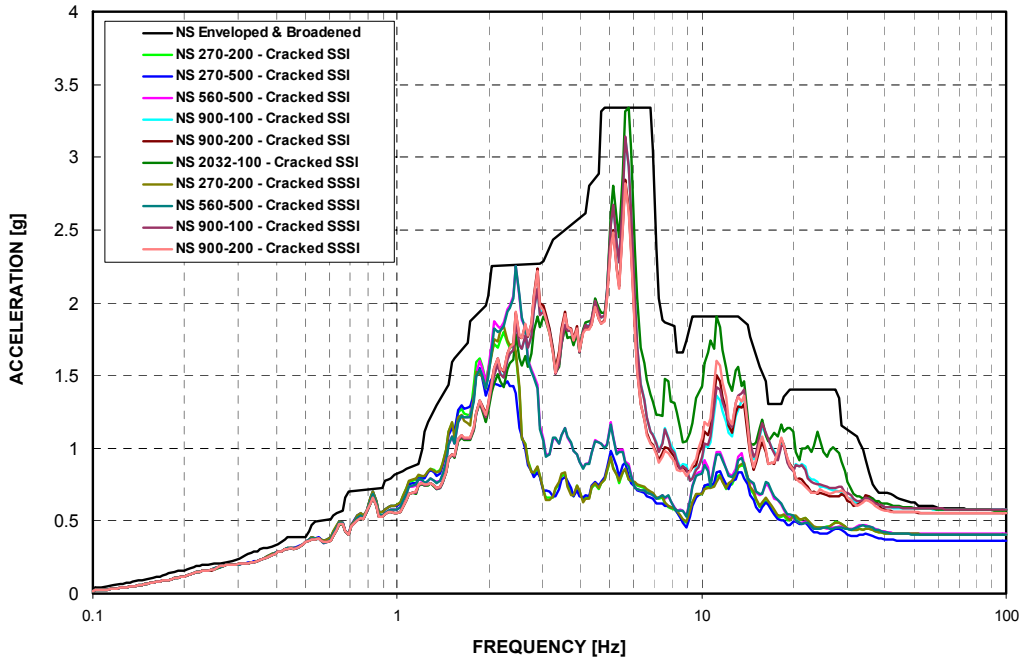

Figure 3-F.2.0-14 ISRS at SG Lower Supports - 3% Damped Response in NS Direction (X) - Cracked

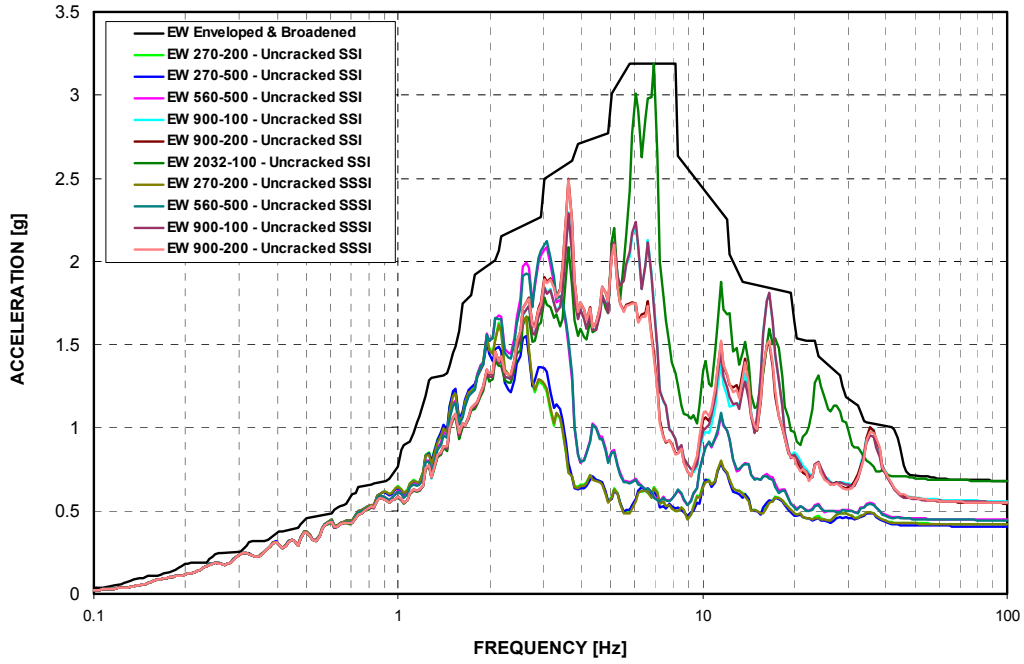

Figure 3-F.2.0-15 ISRS at SG Lower Supports - 3% Damped Response in EW Direction (Y) - Uncracked

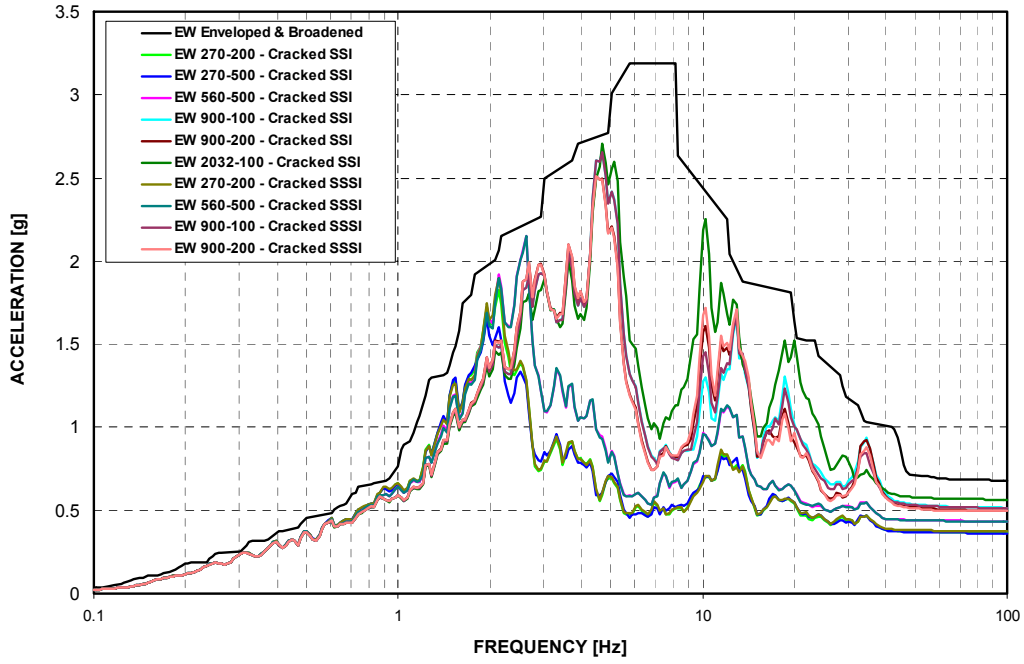

Figure 3-F.2.0-16 ISRS at SG Lower Supports - 3% Damped Response in EW Direction (Y) - Cracked

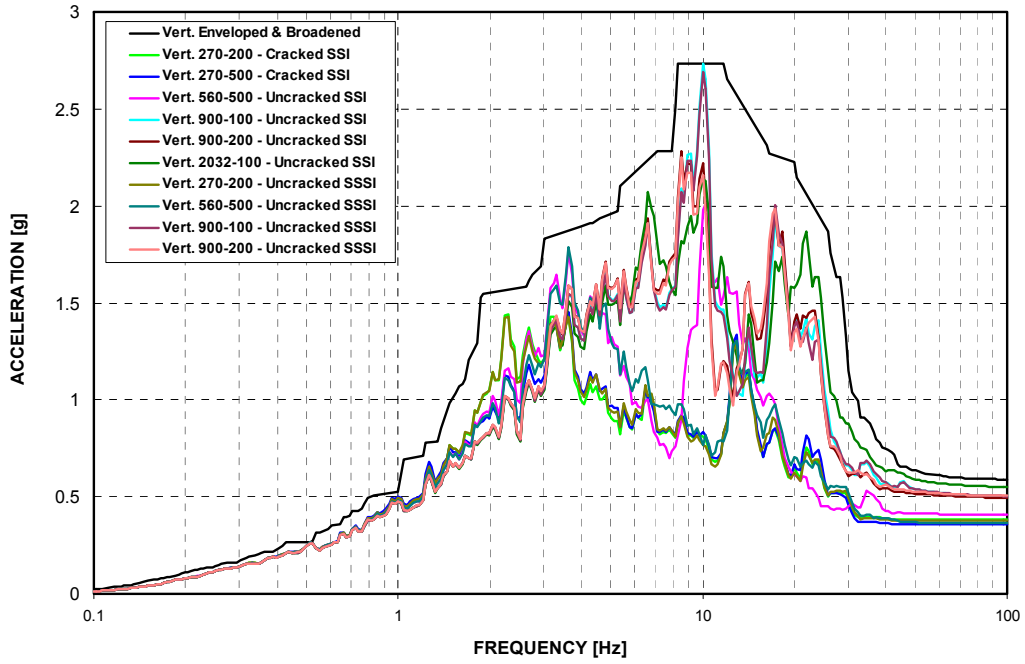

Figure 3-F.2.0-17 ISRS at SG Lower Supports - 3% Damped Response in Vertical Direction (Z) - Uncracked

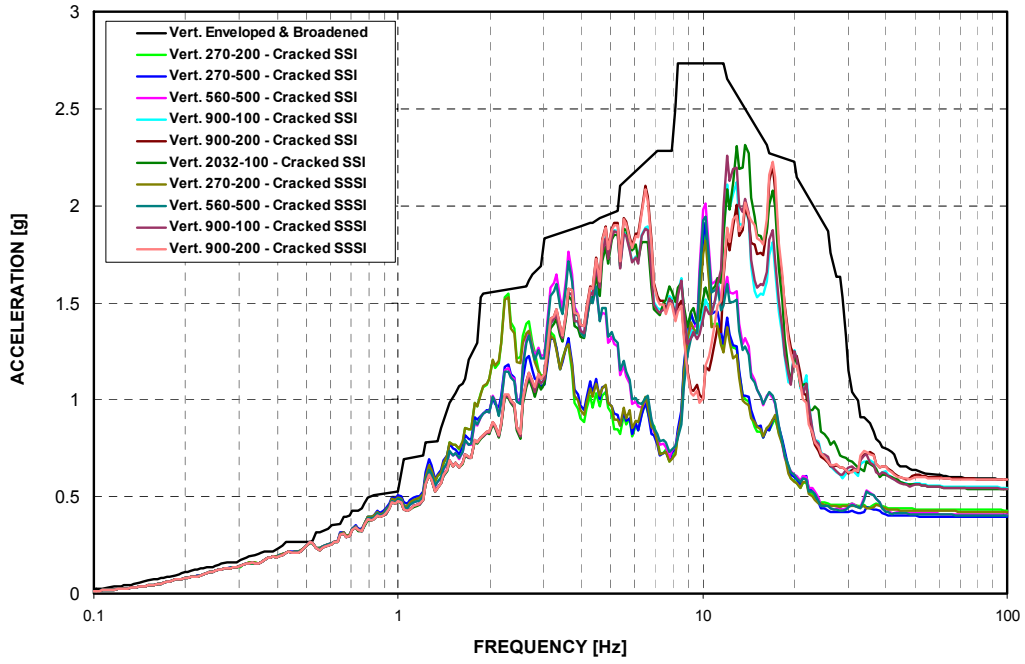

Figure 3-F.2.0-18 ISRS at SG Lower Supports - 3% Damped Response in Vertical Direction (Z) - Cracked

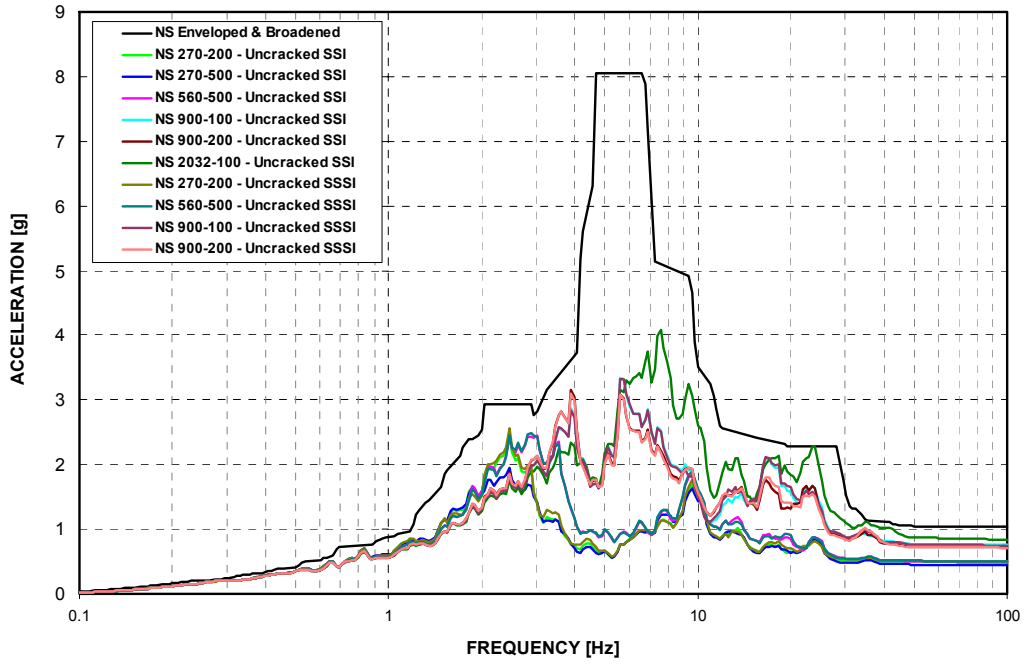

Figure 3-F.2.0-19 ISRS at SG Upper Supports - 3% Damped Response in NS Direction (X) - Uncracked

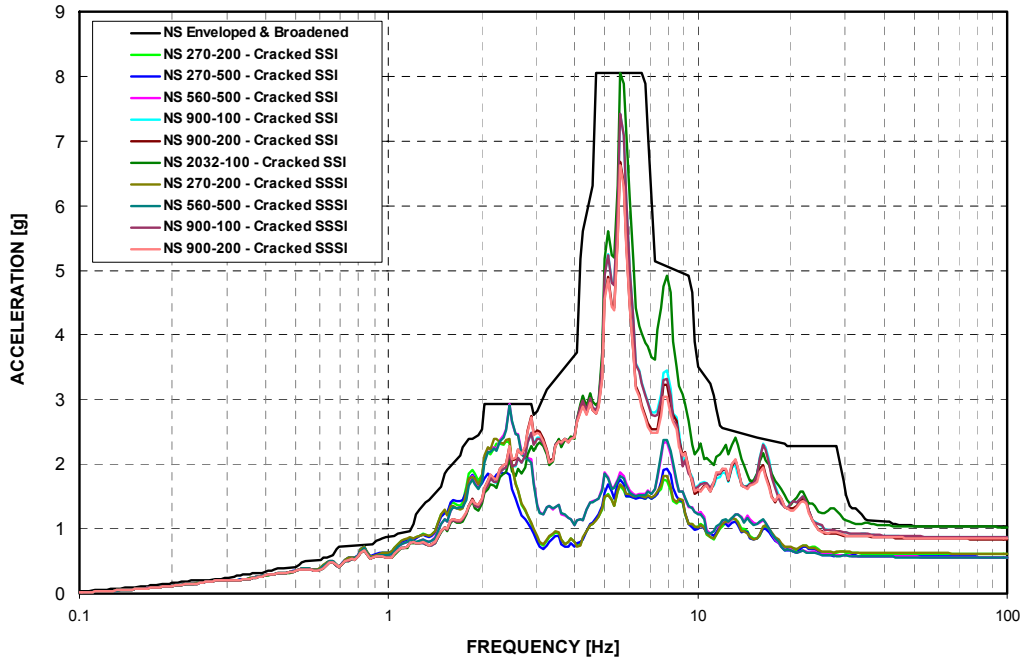

Figure 3-F.2.0-20 ISRS at SG Upper Supports - 3% Damped Response in NS Direction (X) - Cracked

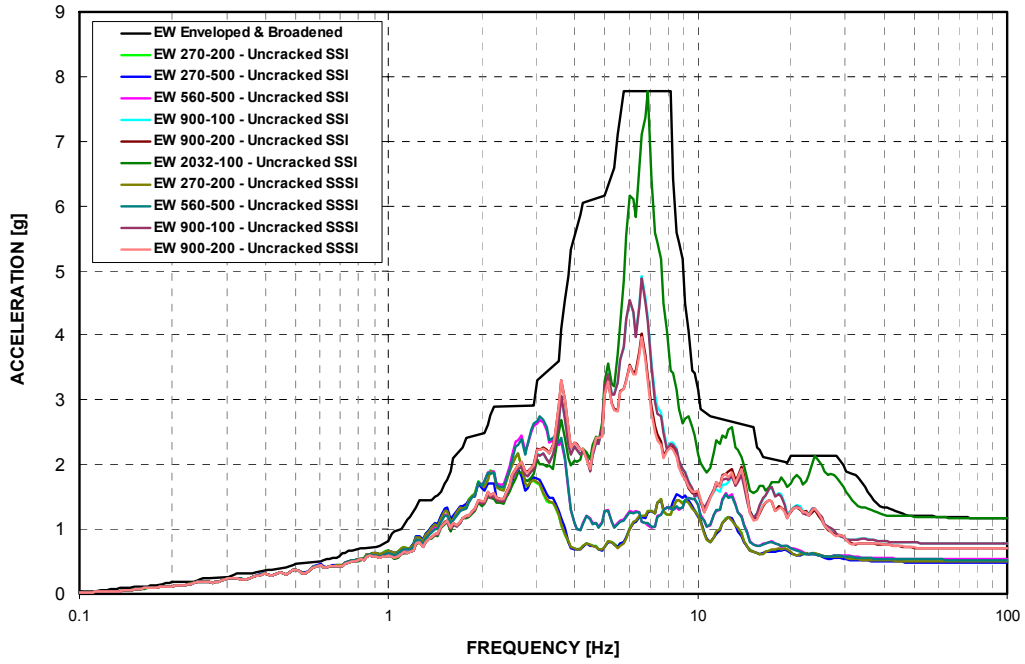

Figure 3-F.2.0-21 ISRS at SG Upper Supports - 3% Damped Response in EW Direction (Y) - Uncracked

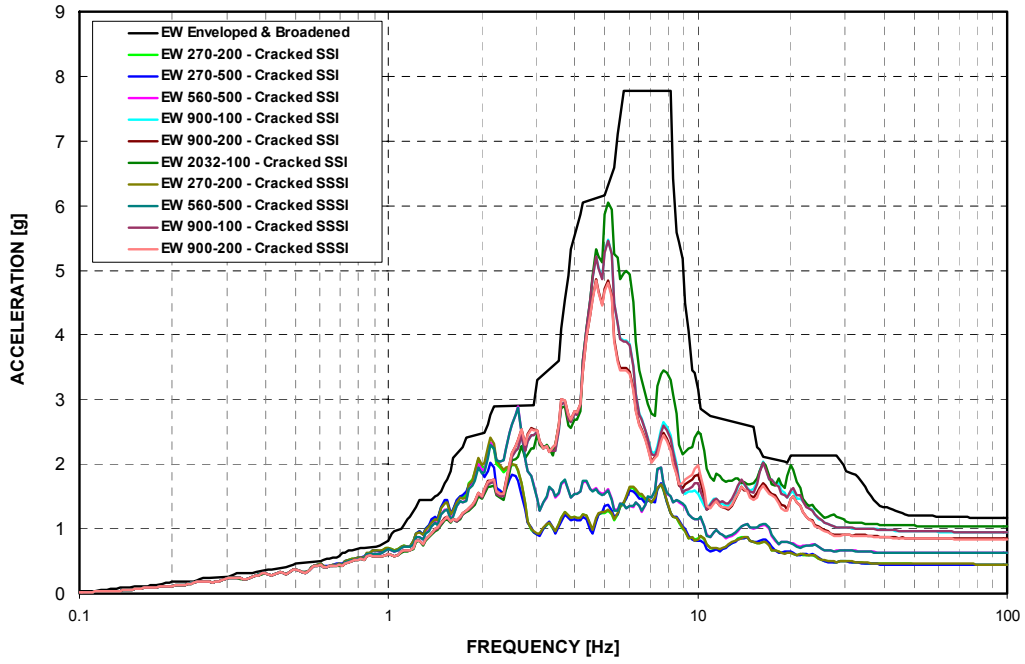

Figure 3-F.2.0-22 ISRS at SG Upper Supports - 3% Damped Response in EW Direction (Y) - Cracked

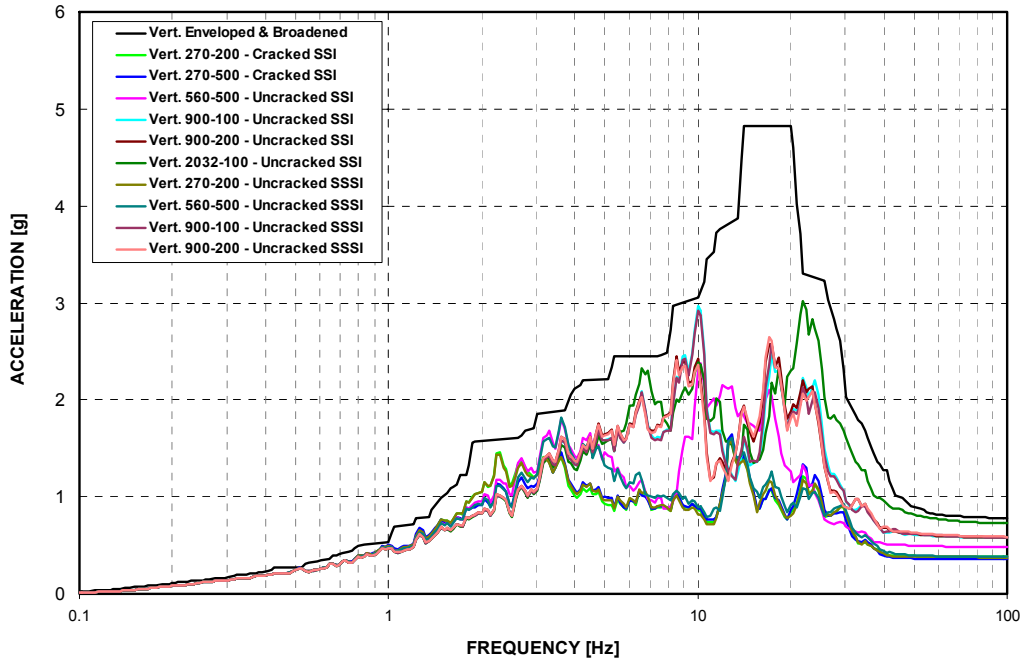

Figure 3-F.2.0-23 ISRS at SG Upper Supports - 3% Damped Response in Vertical Direction (Z) - Uncracked

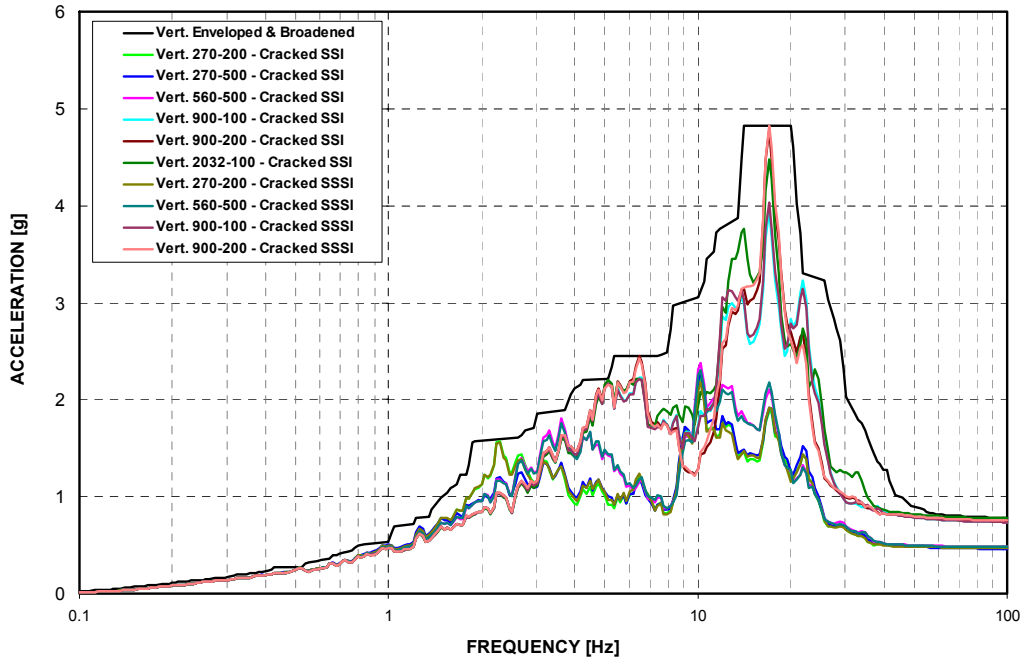

Figure 3-F.2.0-24 ISRS at SG Upper Supports - 3% Damped Response in Vertical Direction (Z) - Cracked

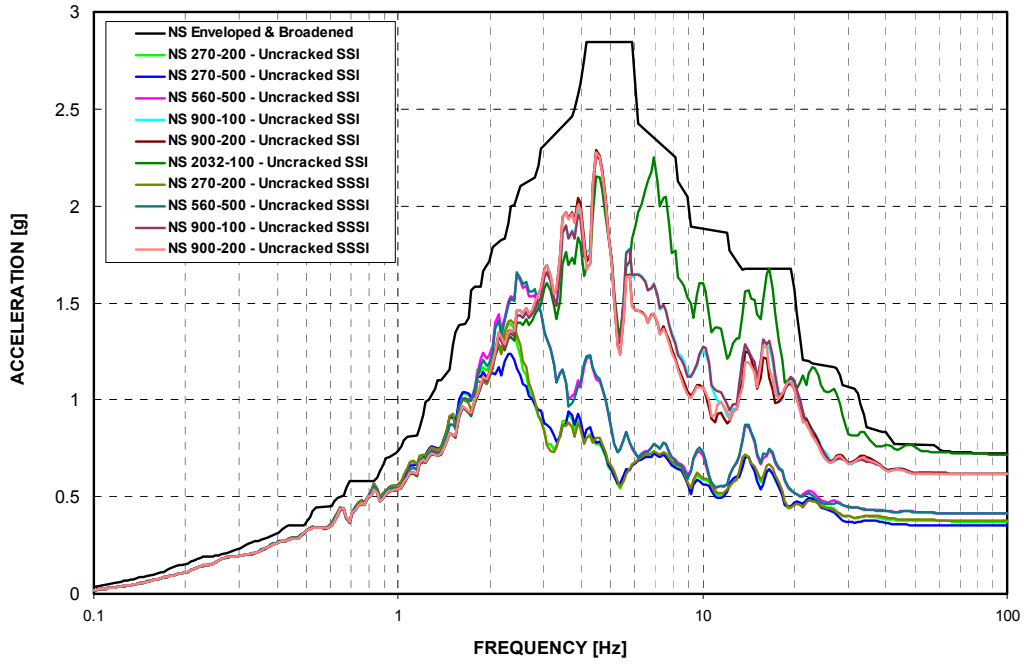

Figure 3-F.2.0-25 ISRS at SFP - 4% Damped Response in NS Direction (X) - Uncracked

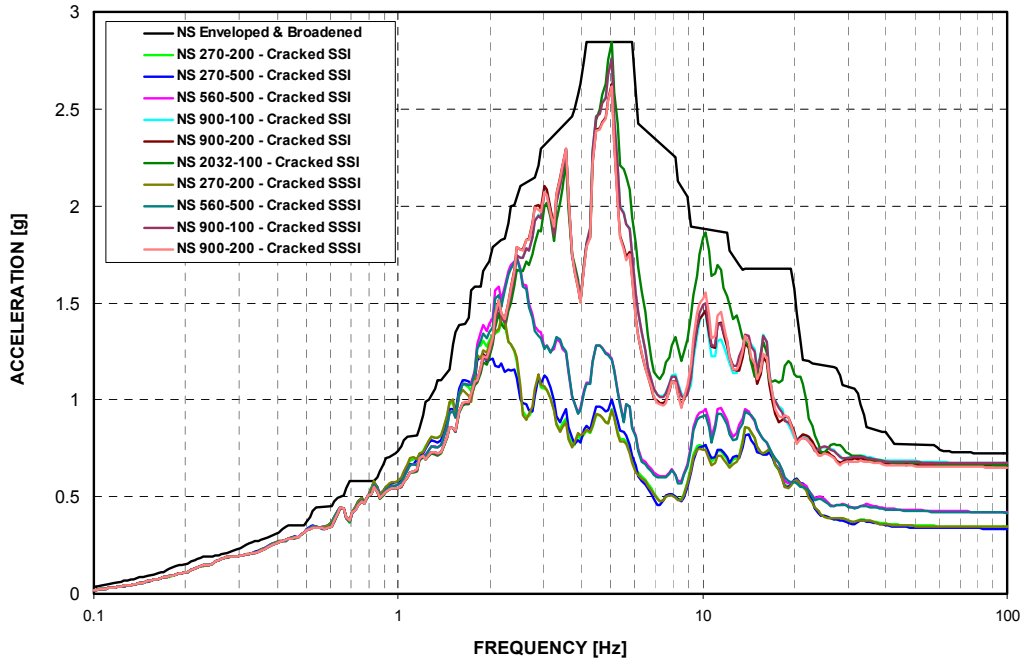

Figure 3-F.2.0-26 ISRS at SFP - 4% Damped Response in NS Direction (X) - Cracked

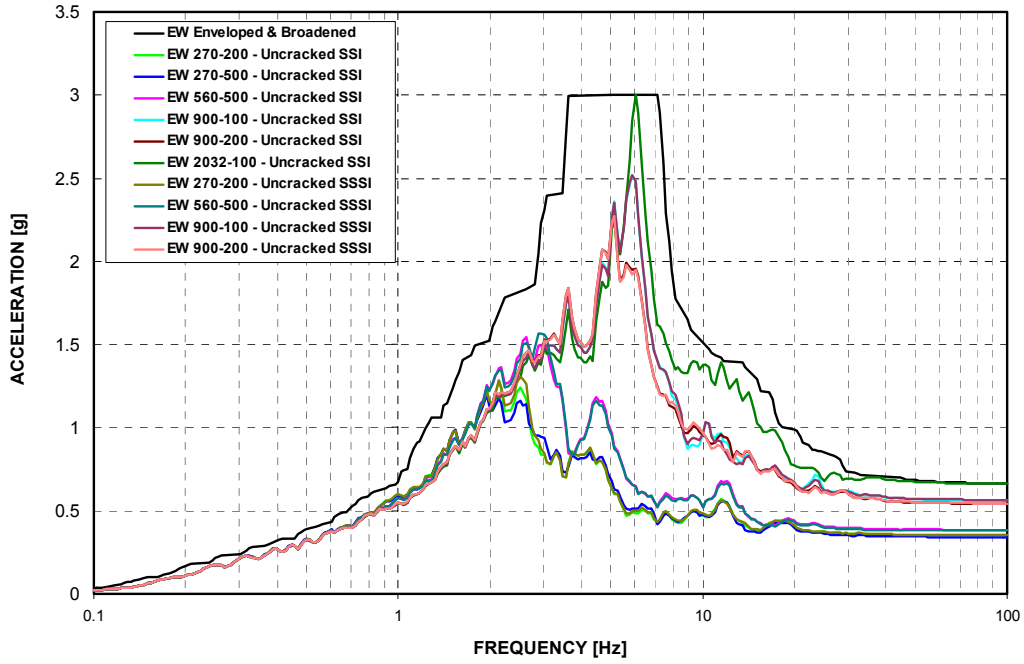

Figure 3-F.2.0-27 ISRS at SFP - 4% Damped Response in EW Direction (Y) - Uncracked

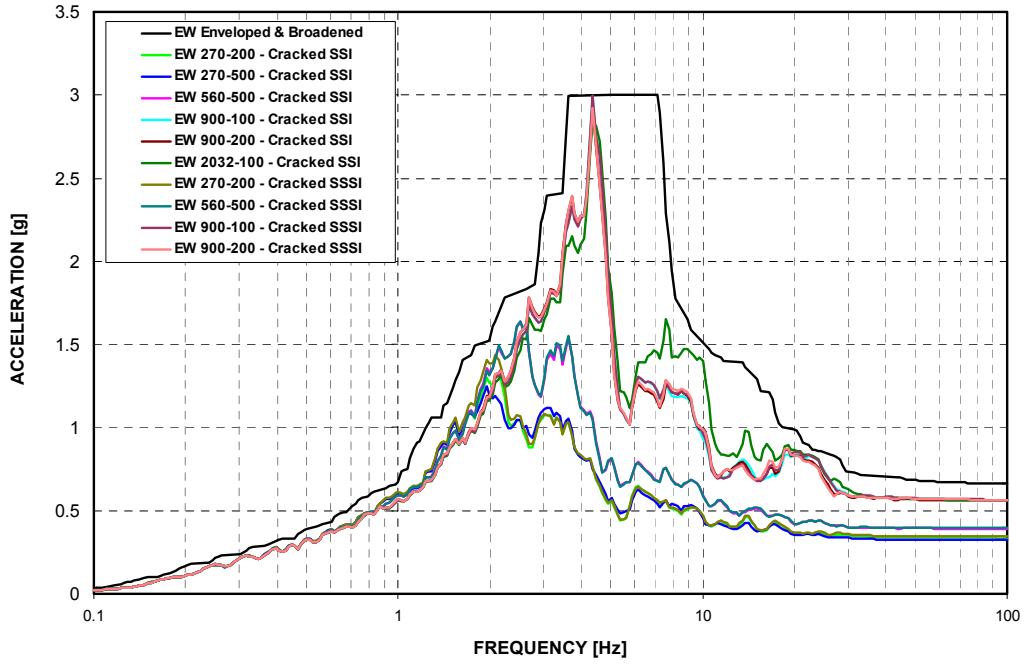

Figure 3-F.2.0-28 ISRS at SFP - 4% Damped Response in EW Direction (Y) - Cracked

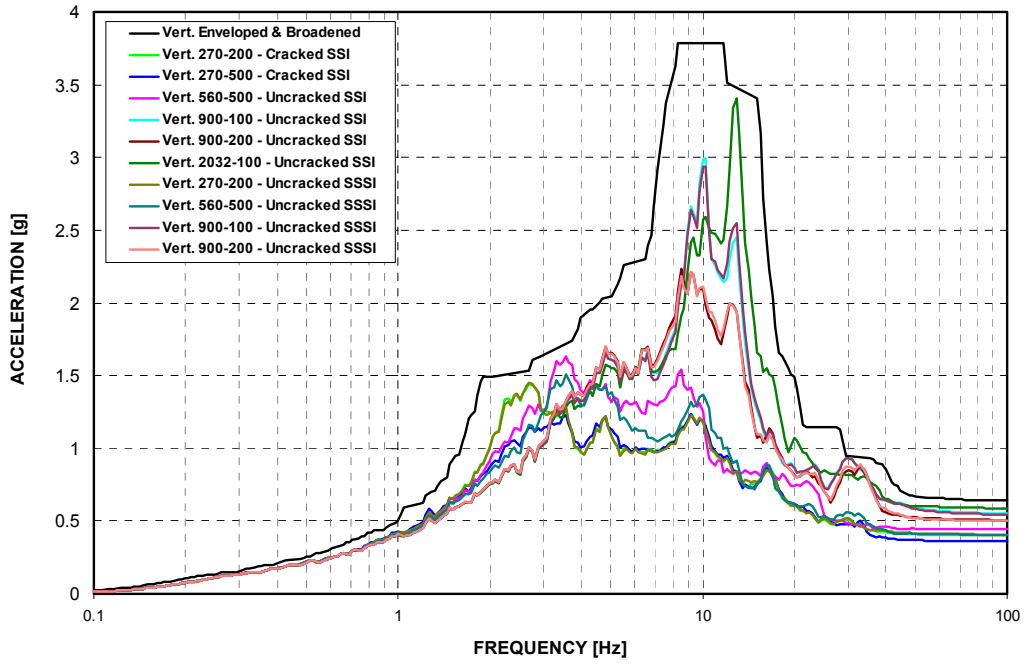

Figure 3-F.2.0-29 ISRS at SFP - 4% Damped Response in Vertical Direction (Z) - Uncracked

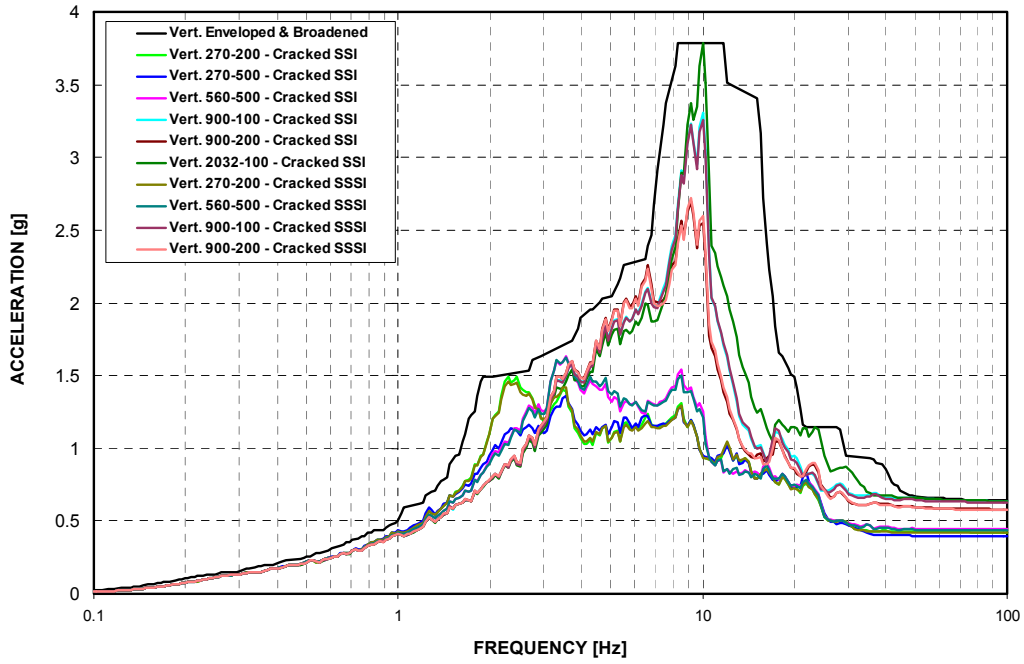

Figure 3-F.2.0-30 ISRS at SFP - 4% Damped Response in Vertical Direction (Z) - Cracked

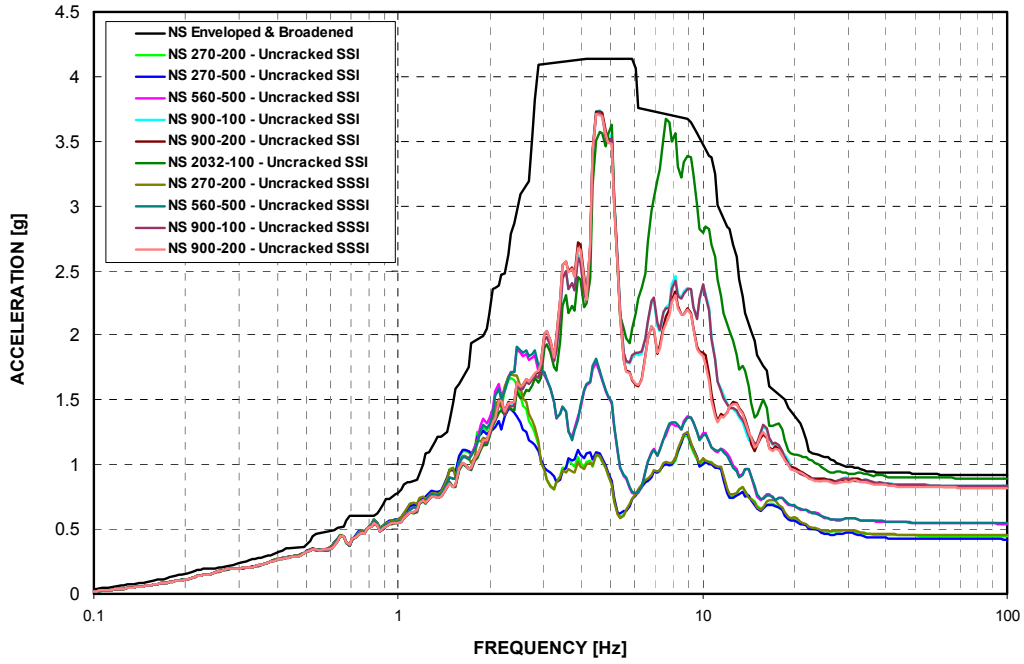

Figure 3-F.2.0-31 ISRS at NFSP - 4% Damped Response in NS Direction (X) - Uncracked

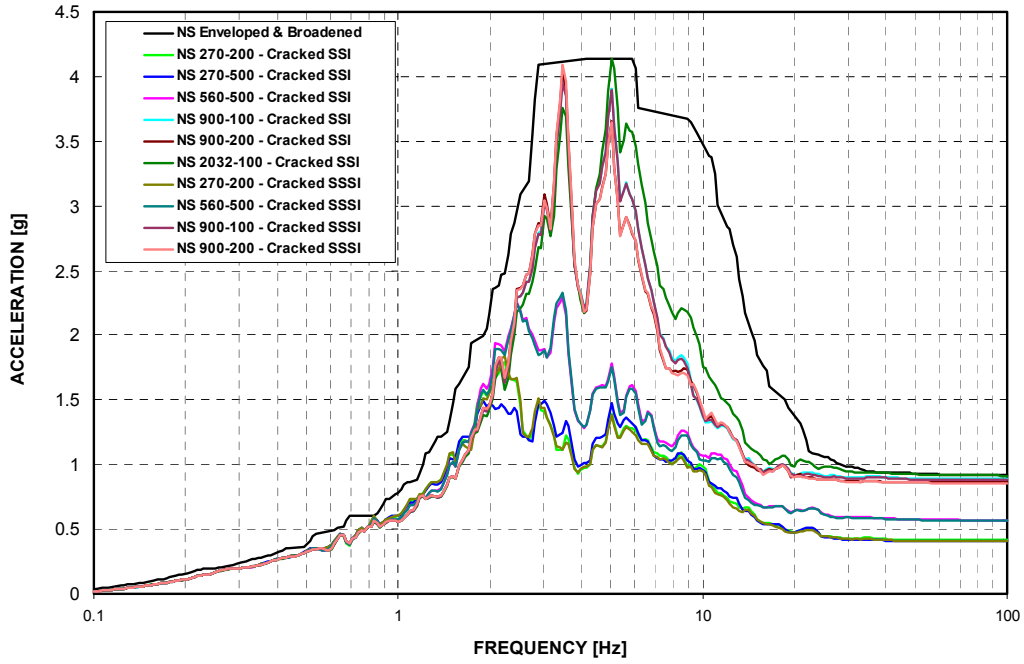

Figure 3-F.2.0-32 ISRS at NFSP - 4% Damped Response in NS Direction (X) - Cracked

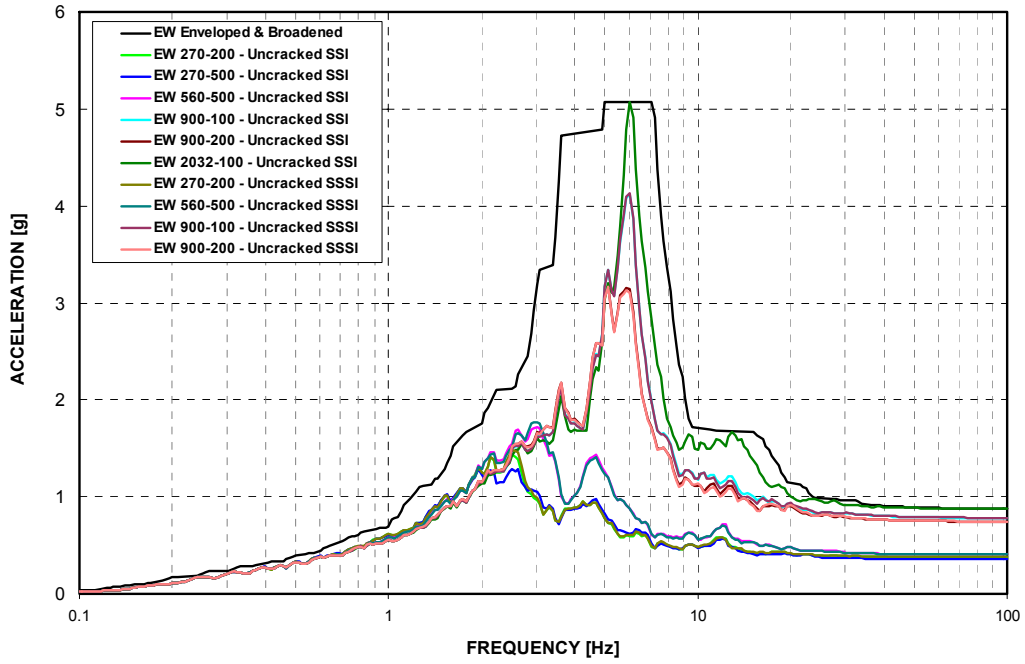

Figure 3-F.2.0-33 ISRS at NFSP - 4% Damped Response in EW Direction (Y) - Uncracked

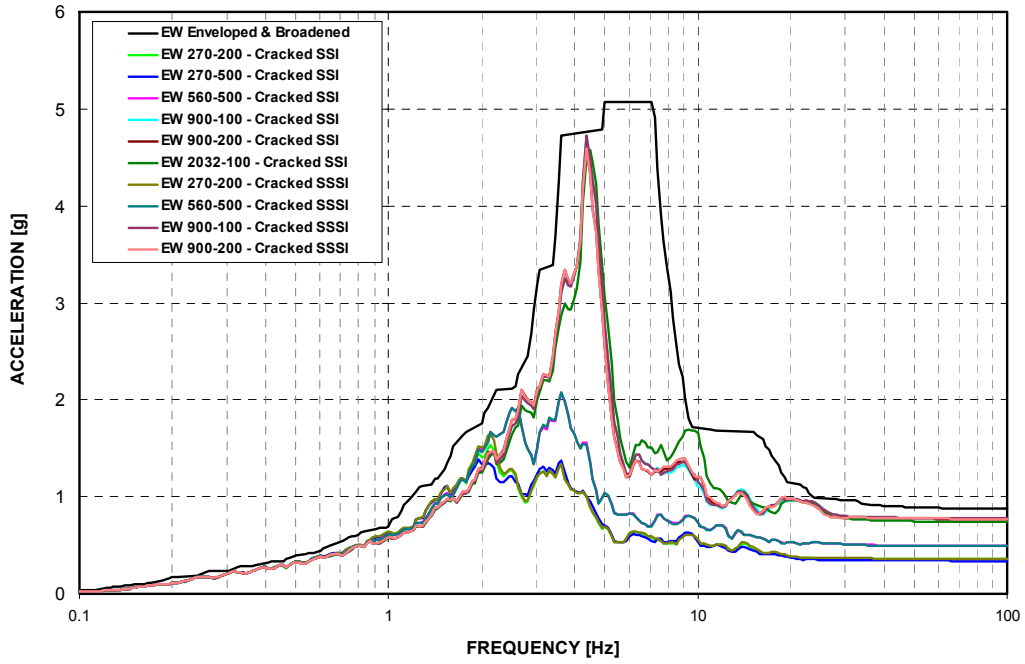

Figure 3-F.2.0-34 ISRS at NFSP - 4% Damped Response in EW Direction (Y) - Cracked

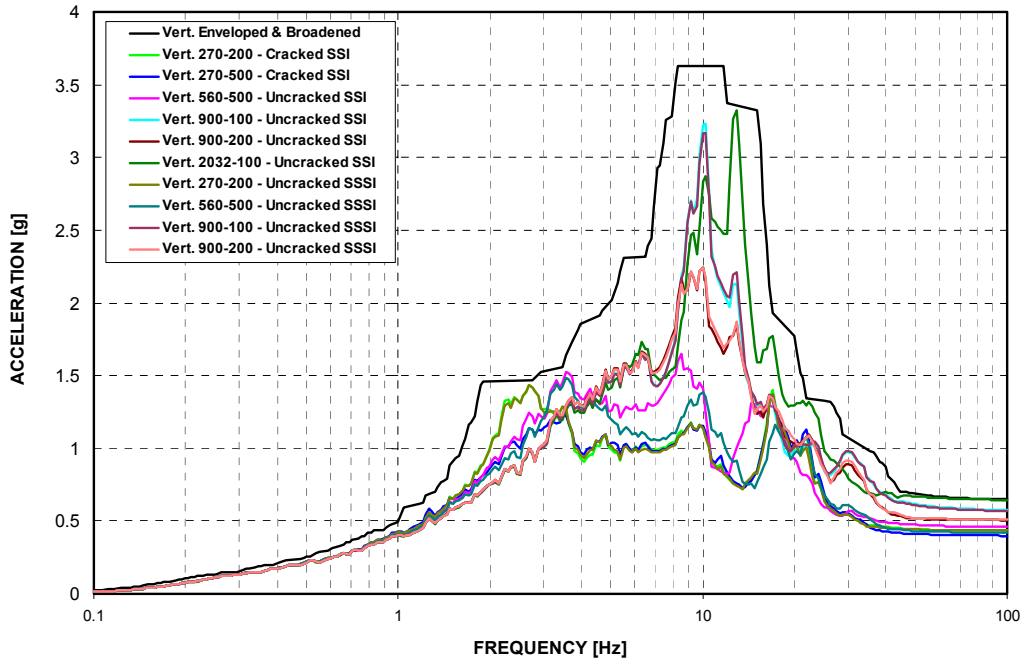

Figure 3-F.2.0-35 ISRS at NFSP - 4% Damped Response in Vertical Direction (Z) - Uncracked

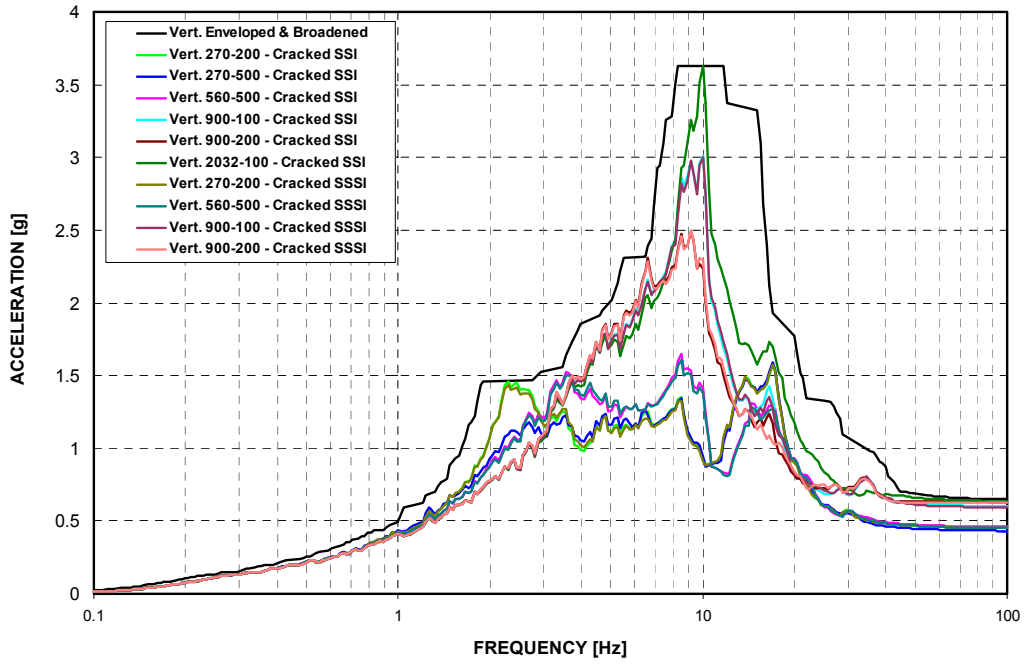

Figure 3-F.2.0-36 ISRS at NFSP - 4% Damped Response in Vertical Direction (Z) - Cracked

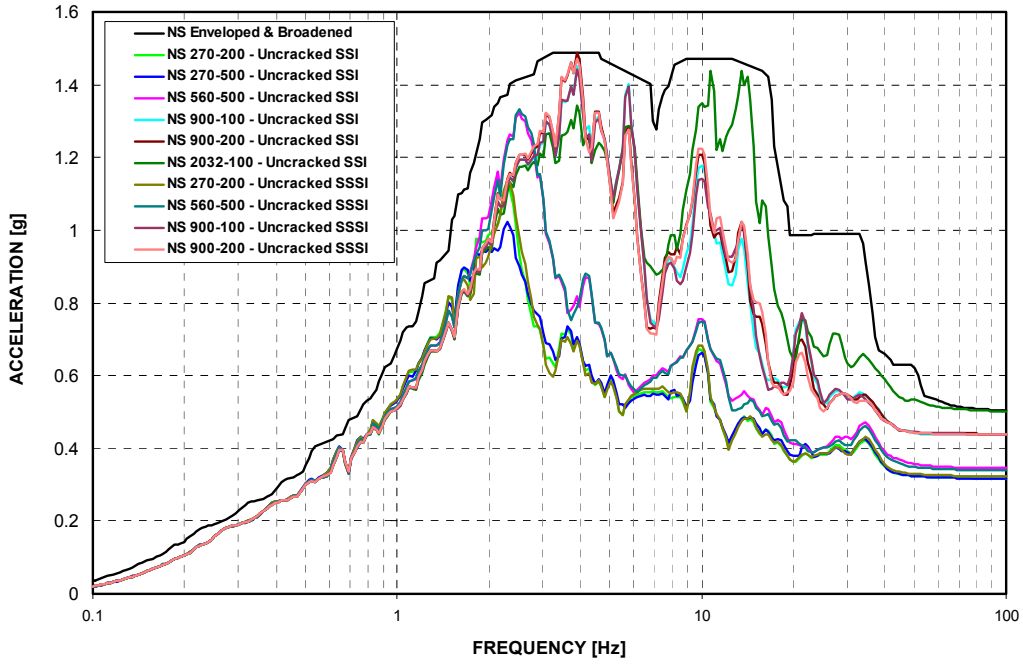

Figure 3-F.2.0-37 ISRS at A-AAC GTG - 5% Damped Response in NS Direction (X) - Uncracked

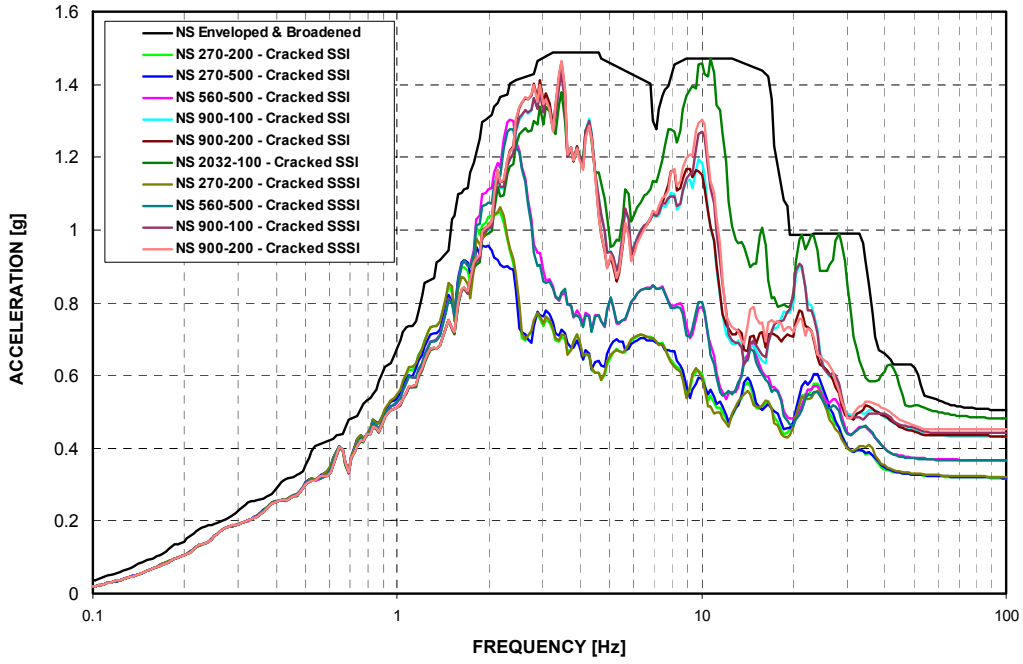

Figure 3-F.2.0-38 ISRS at A-AAC GTG - 5% Damped Response in NS Direction (X) - Cracked

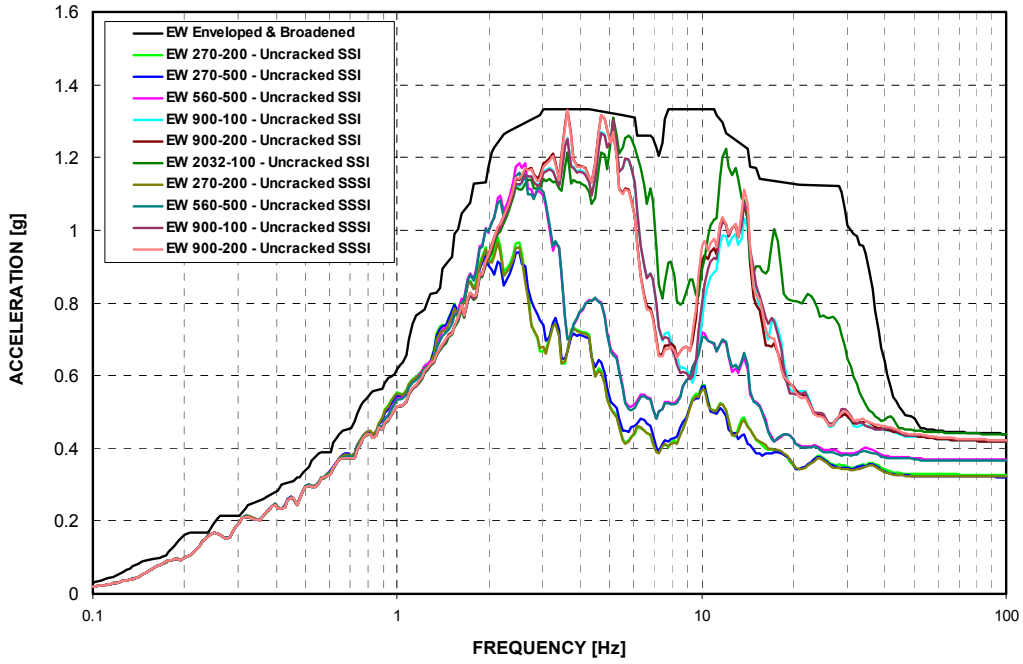

Figure 3-F.2.0-39 ISRS at A-AAC GTG - 5% Damped Response in EW Direction (Y) - Uncracked

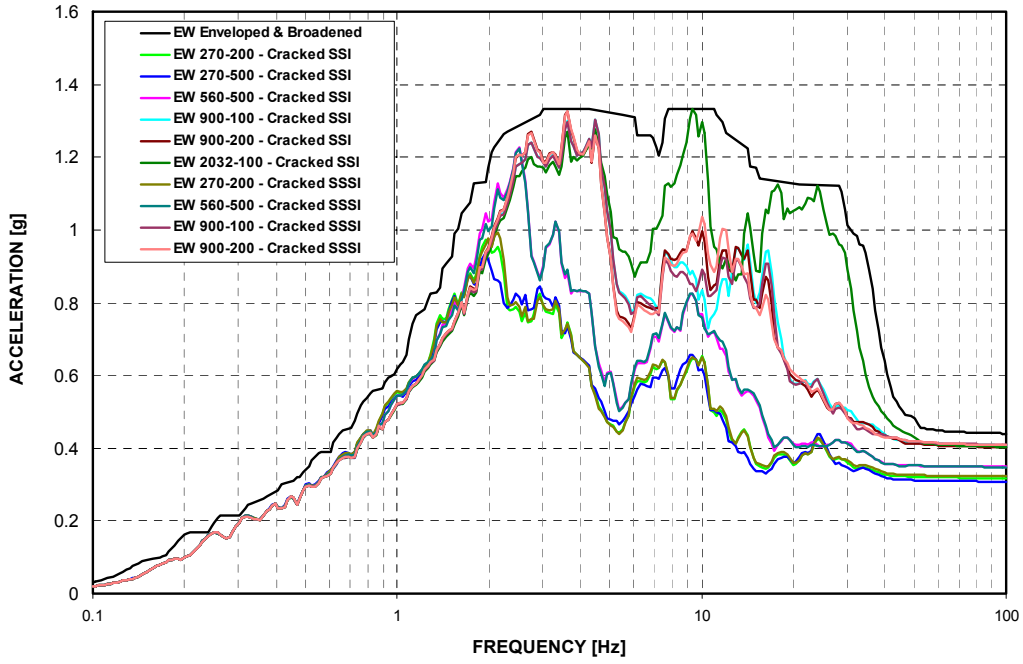

Figure 3-F.2.0-40 ISRS at A-AAC GTG - 5% Damped Response in EW Direction (Y) - Cracked

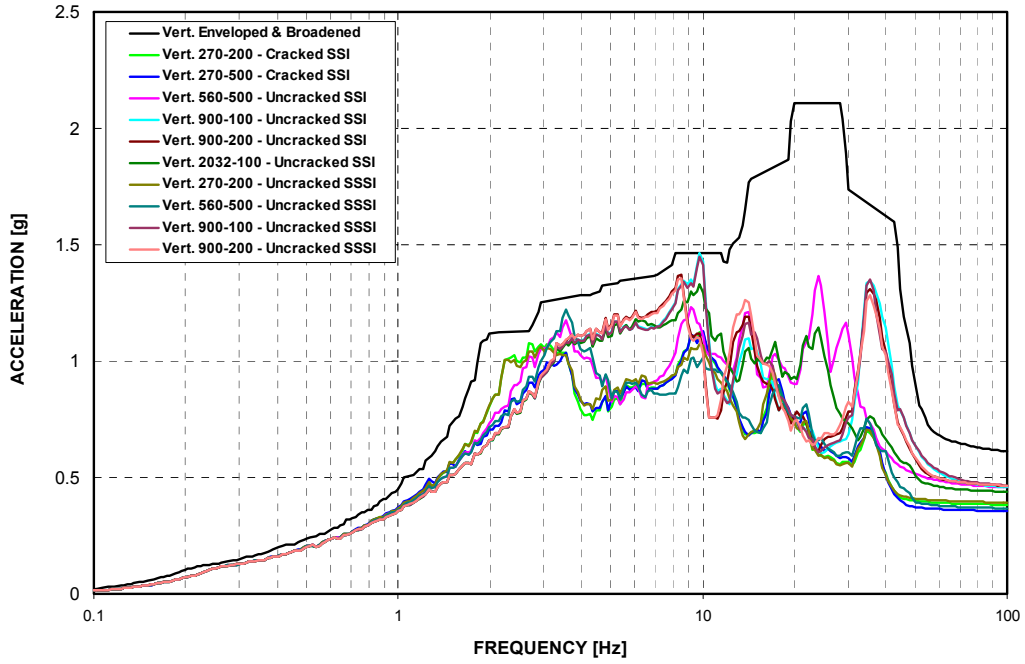

Figure 3-F.2.0-41 ISRS at A-AAC GTG - 5% Damped Response in Vertical Direction (Z) - Uncracked

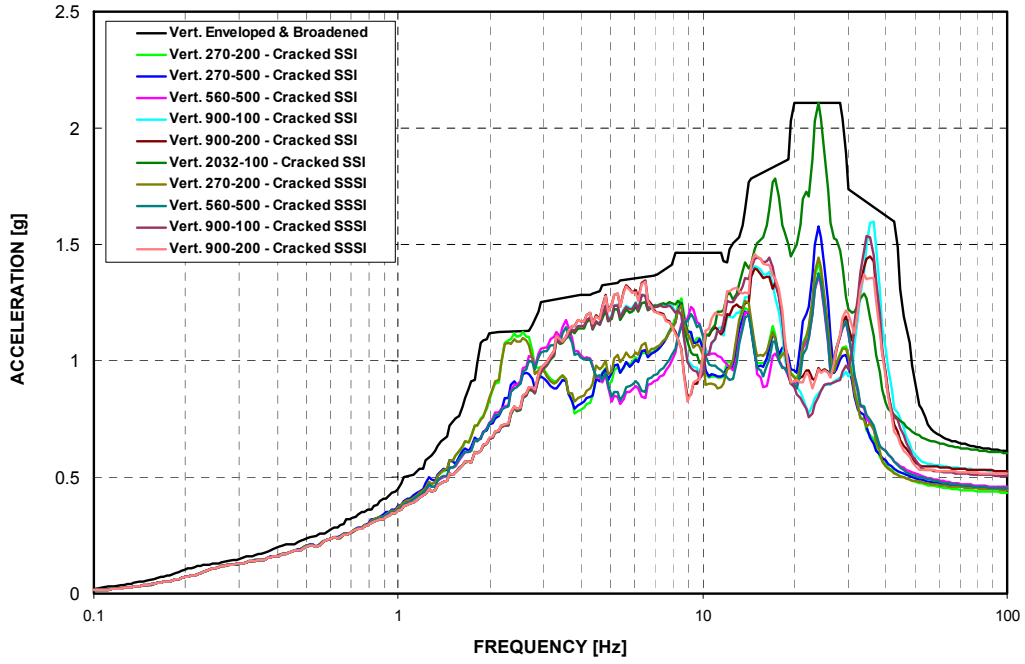

Figure 3-F.2.0-42 ISRS at A-AAC GTG - 5% Damped Response in Vertical Direction (Z) - Cracked

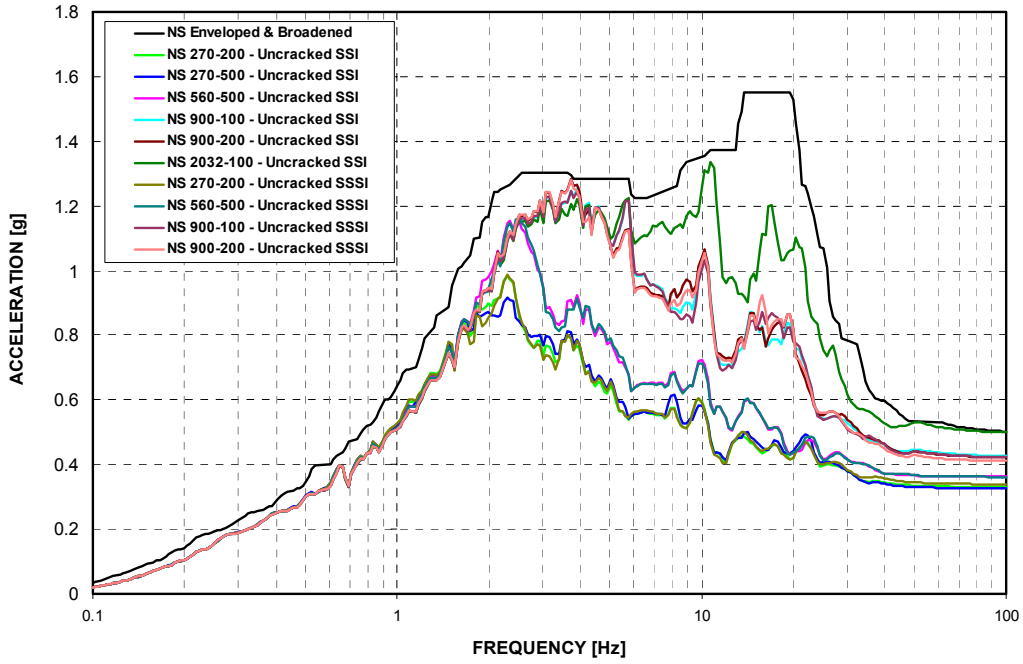

Figure 3-F.2.0-43 ISRS at B-AAC GTG - 5% Damped Response in NS Direction (X) - Uncracked

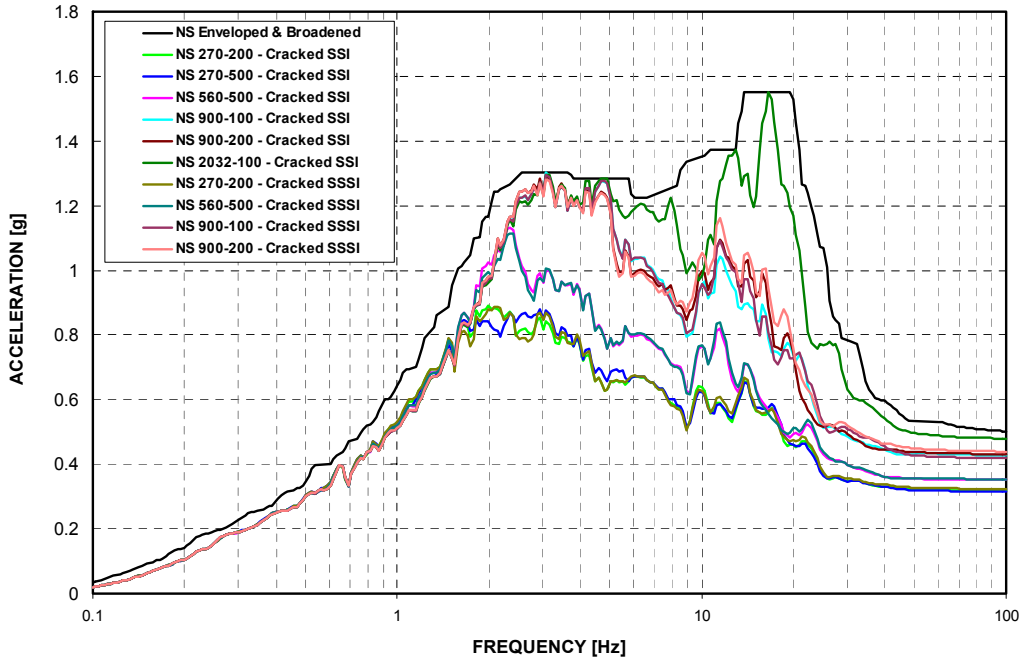

Figure 3-F.2.0-44 ISRS at B-AAC GTG - 5% Damped Response in NS Direction (X) - Cracked

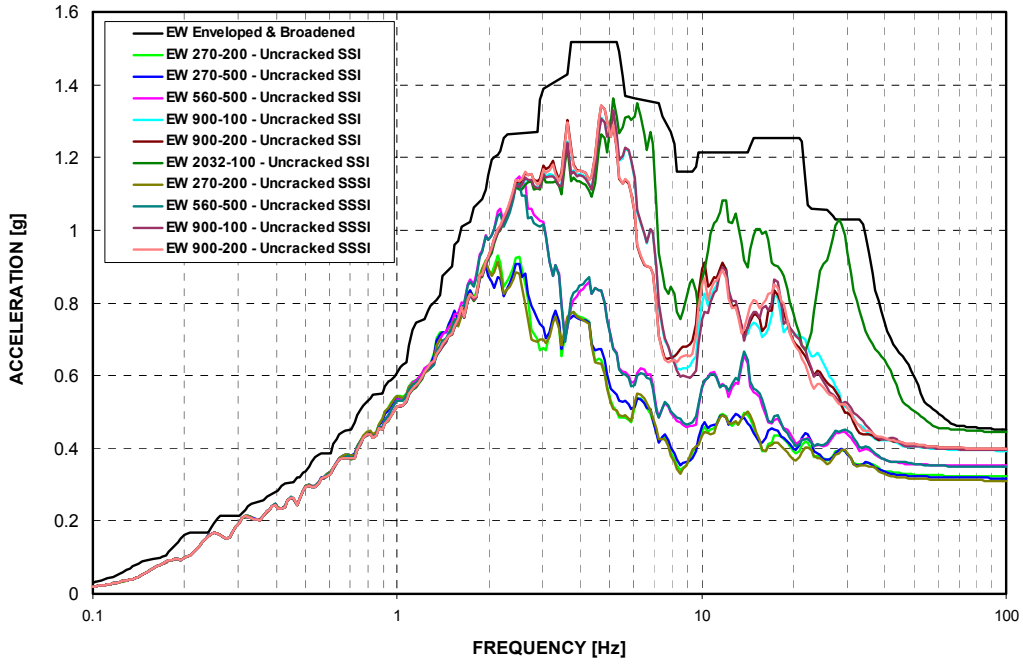

Figure 3-F.2.0-45 ISRS at B-AAC GTG - 5% Damped Response in EW Direction (Y) - Uncracked

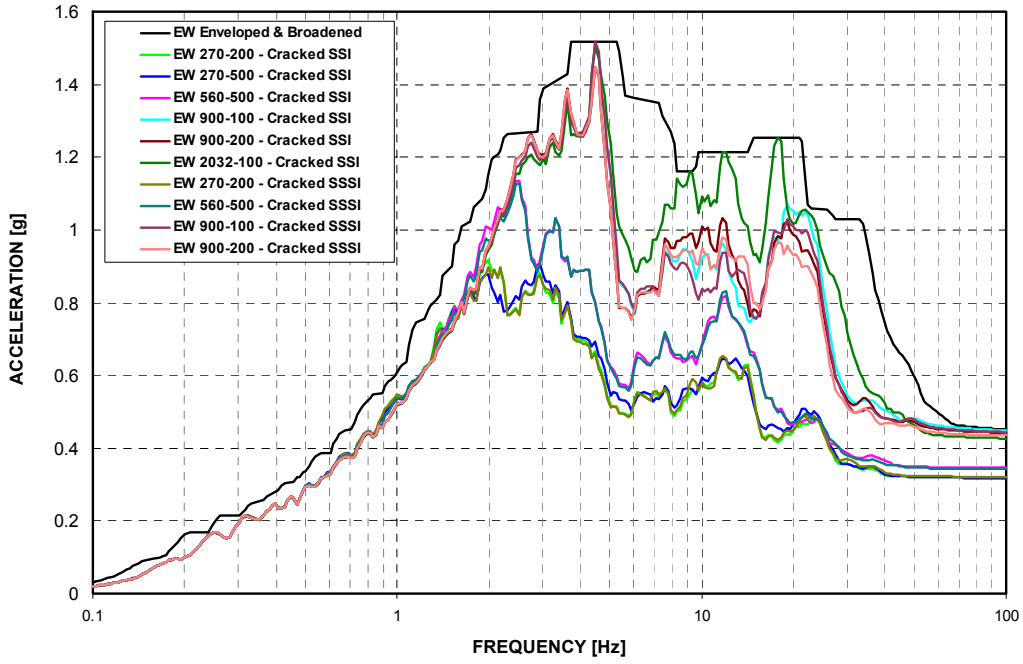

Figure 3-F.2.0-46 ISRS at B-AAC GTG - 5% Damped Response in EW Direction (Y) - Cracked

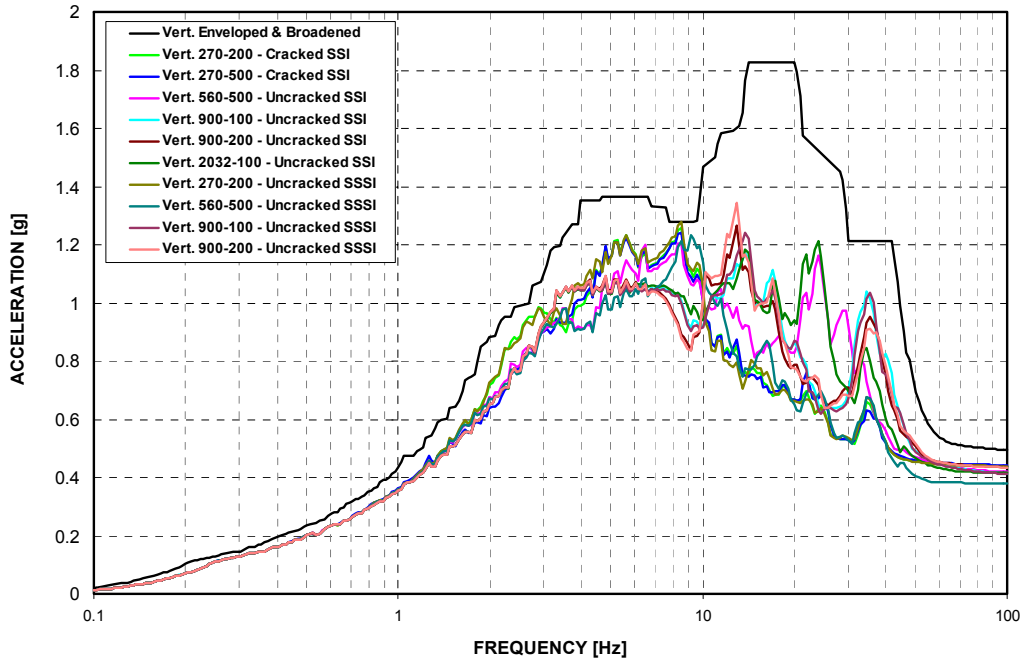

Figure 3-F.2.0-47 ISRS at B-AAC GTG - 5% Damped Response in Vertical Direction (Z) - Uncracked

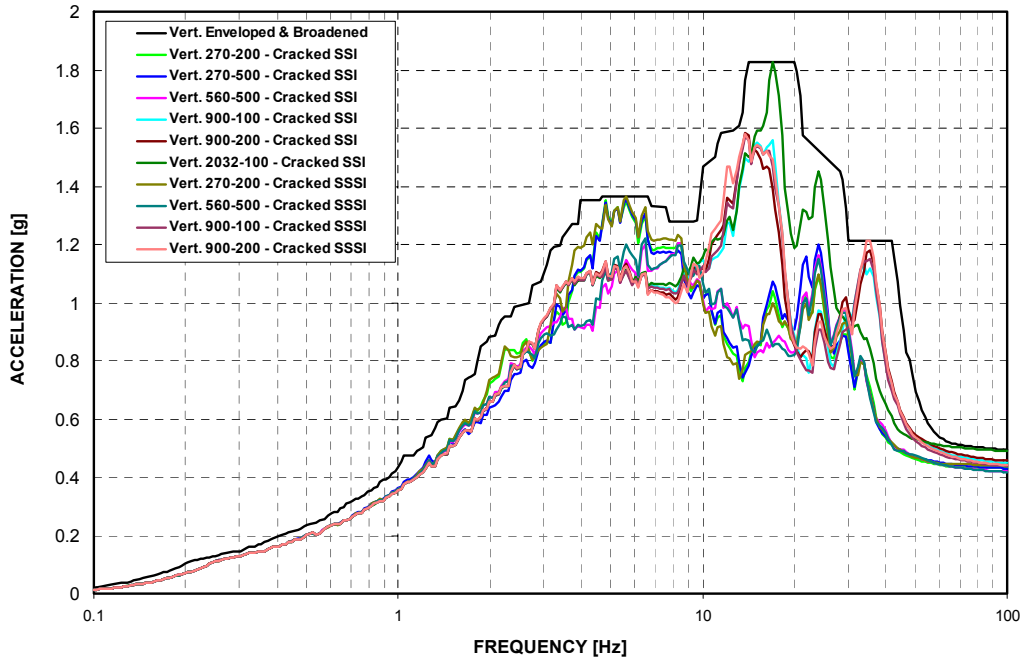

Figure 3-F.2.0-48 ISRS at B-AAC GTG - 5% Damped Response in Vertical Direction (Z) - Cracked

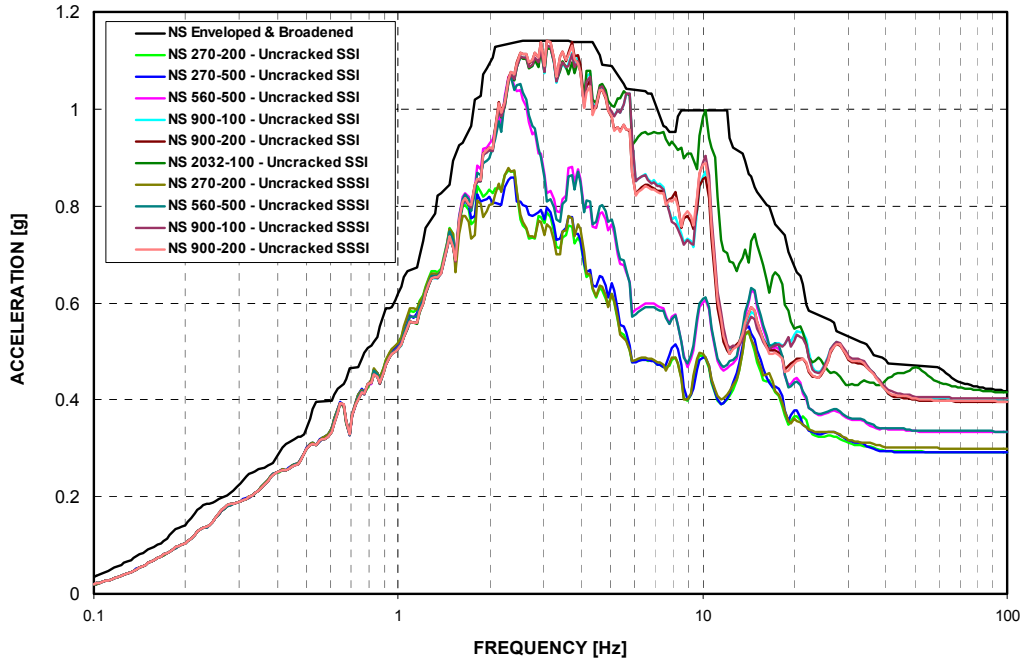

Figure 3-F.2.0-49 ISRS at A/B NW Corner Basemat - 5% Damped Response in NS Direction (X) at Model Elevation -26'-4" - Uncracked

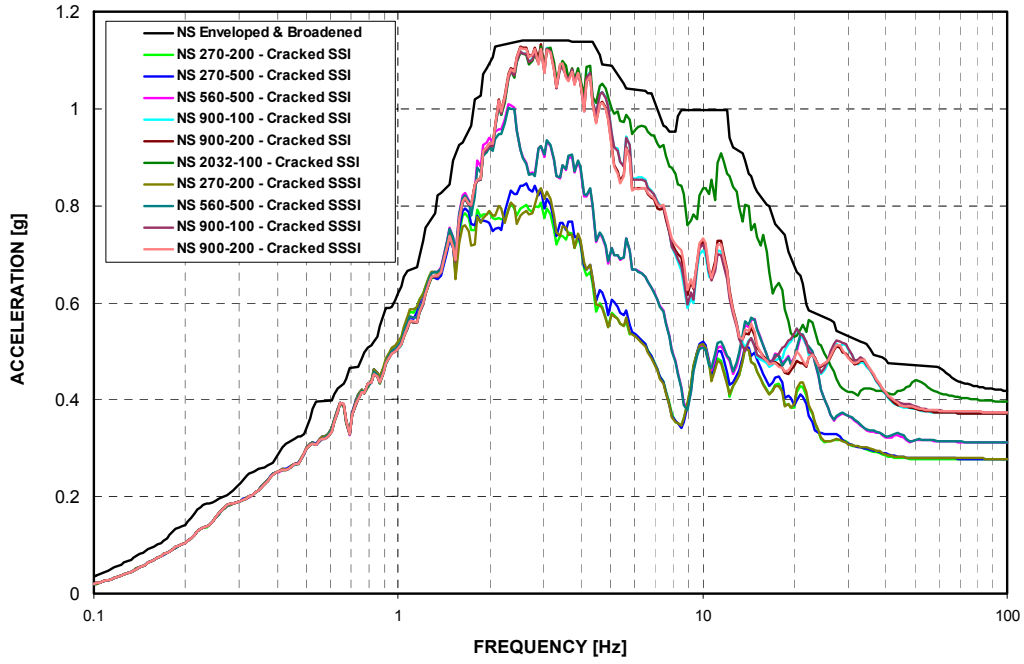

Figure 3-F.2.0-50 ISRS at A/B NW Corner Basemat - 5% Damped Response in NS Direction (X) at Model Elevation -26'-4" - Cracked

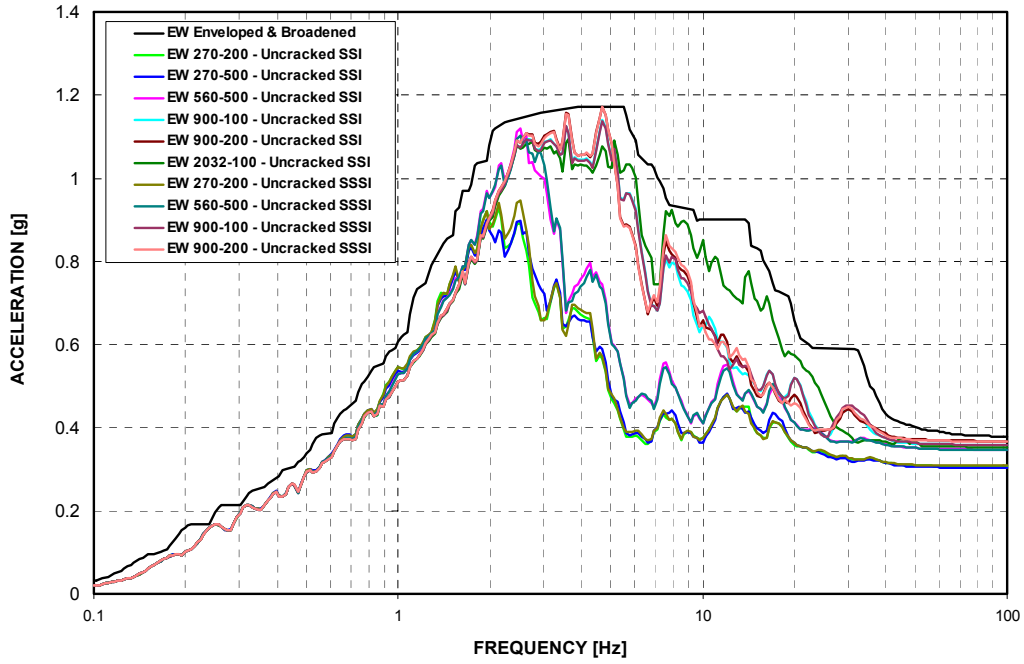

Figure 3-F.2.0-51 ISRS at A/B NW Corner Basemat - 5% Damped Response in EW Direction (Y) at Model Elevation -26'-4" - Uncracked

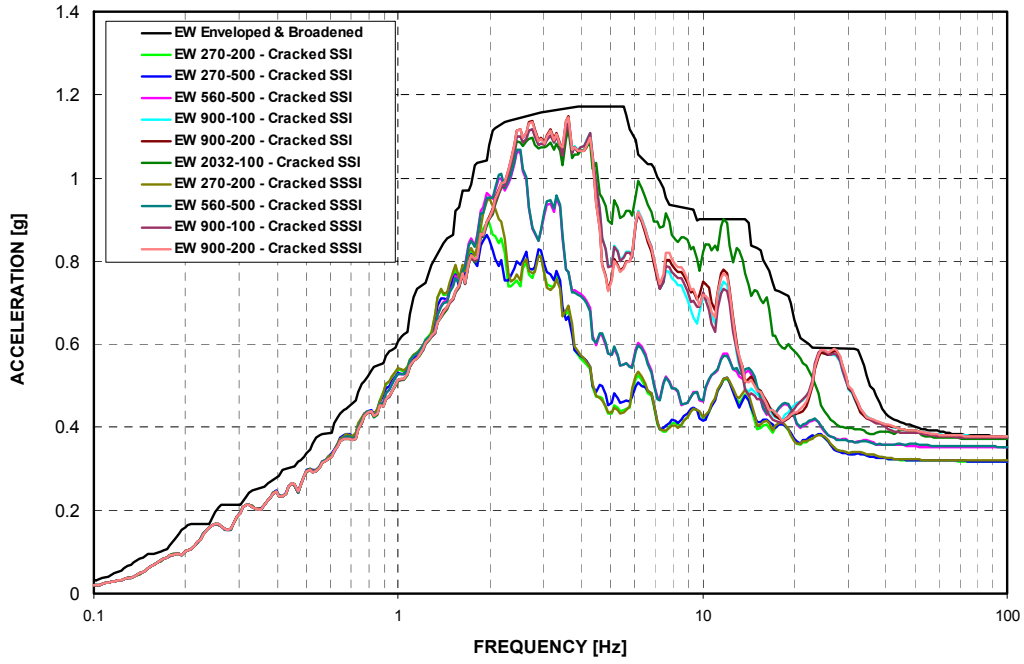

Figure 3-F.2.0-52 ISRS at A/B NW Corner Basemat - 5% Damped Response in EW Direction (Y) at Model Elevation -26'-4" - Cracked

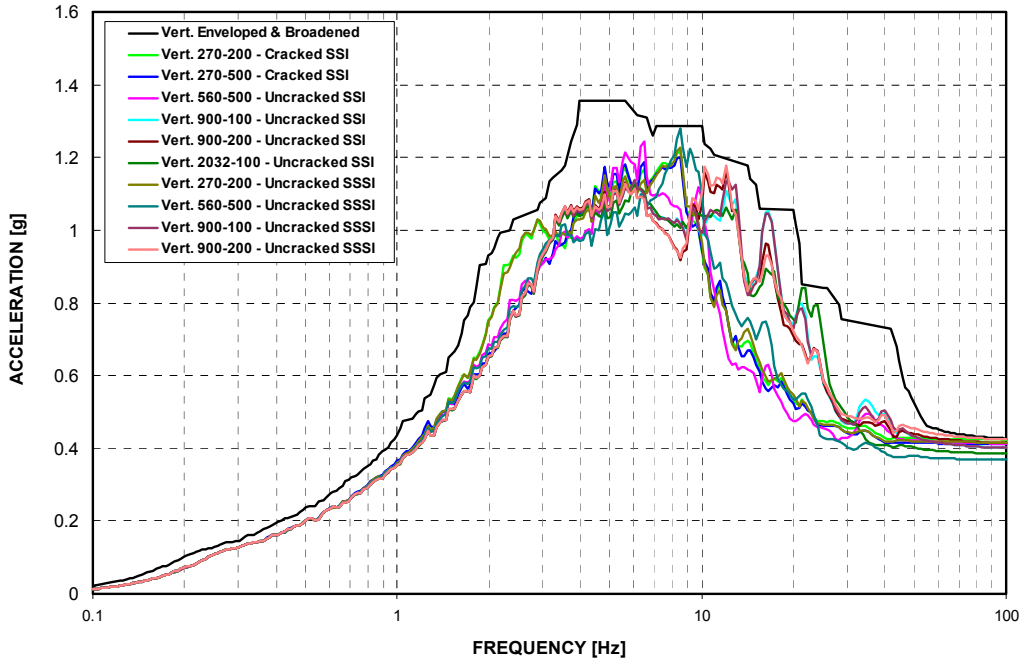

Figure 3-F.2.0-53 ISRS at A/B NW Corner Basemat - 5% Damped Response in Vertical Direction (Z) at Model Elevation -26'-4" - Uncracked

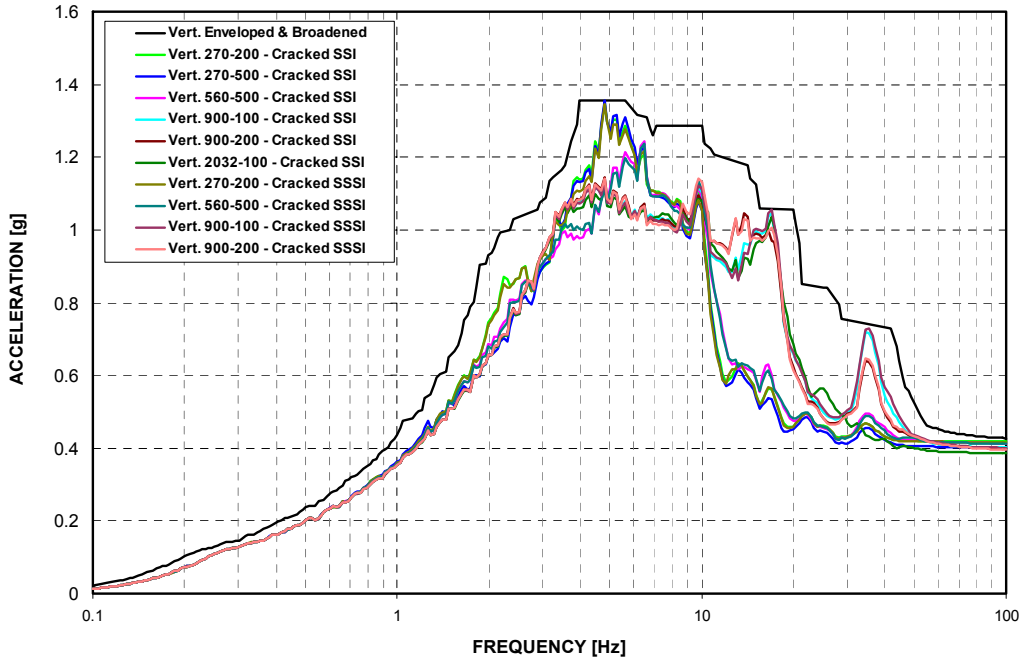

Figure 3-F.2.0-54 ISRS at A/B NW Corner Basemat - 5% Damped Response in Vertical Direction (Z) at Model Elevation -26'-4" - Cracked

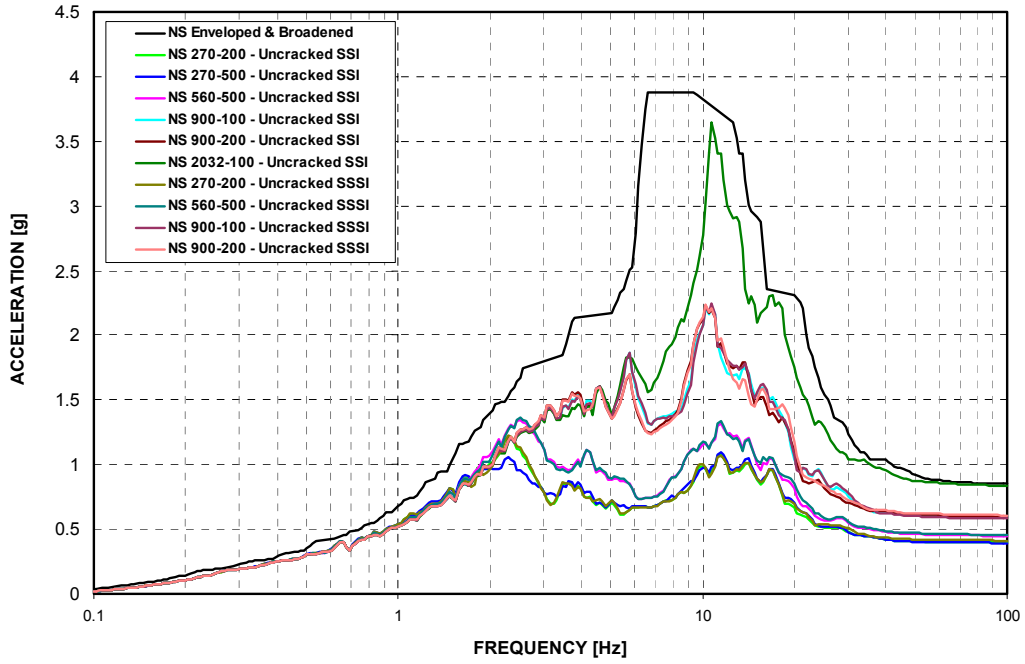

Figure 3-F.2.0-55 ISRS at A/B NW Corner Roof - 5% Damped Response in NS Direction (X) at Model Elevation 74'-10" - Uncracked

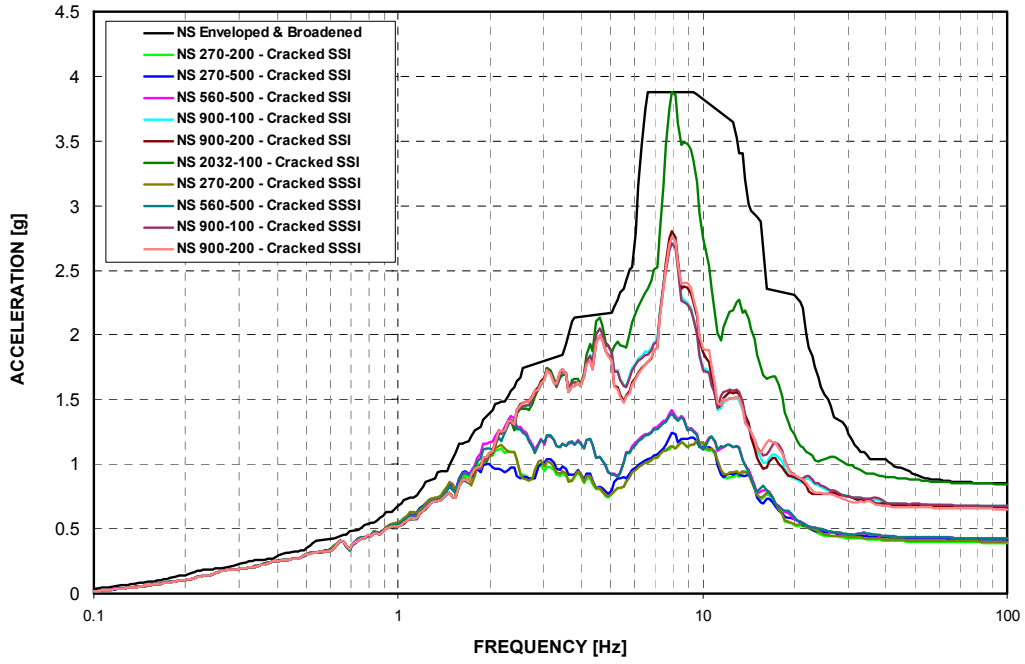

Figure 3-F.2.0-56 ISRS at A/B NW Corner Roof - 5% Damped Response in NS Direction (X) at Model Elevation 74'-10" - Cracked

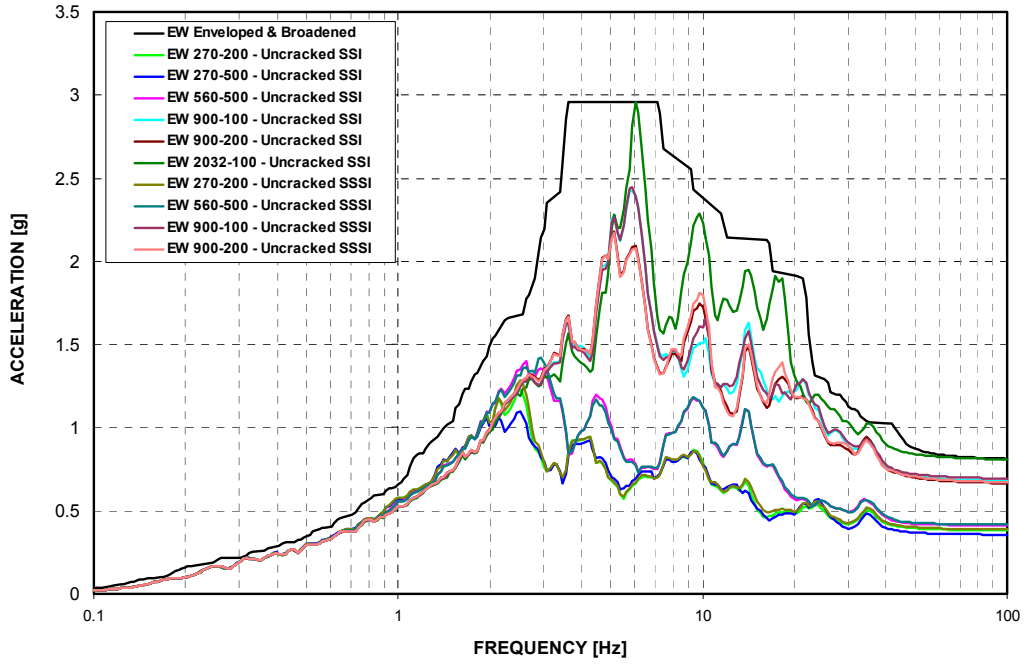

Figure 3-F.2.0-57 ISRS at A/B NW Corner Roof - 5% Damped Response in EW Direction (Y) at Model Elevation 74'-10" - Uncracked

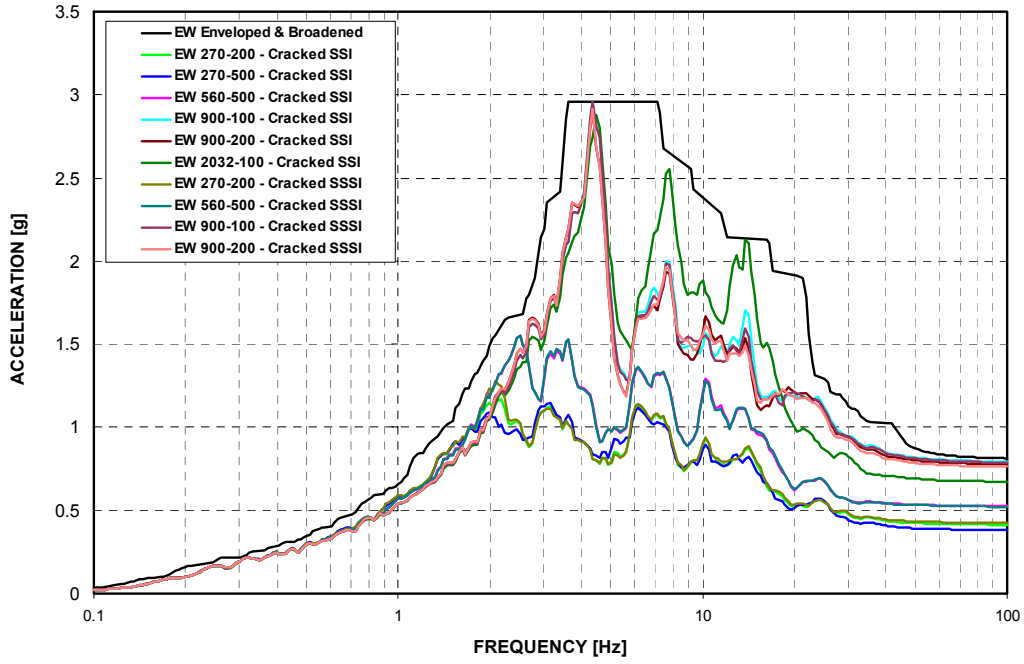

Figure 3-F.2.0-58 ISRS at A/B NW Corner Roof - 5% Damped Response in EW Direction (Y) at Model Elevation 74'-10" - Cracked

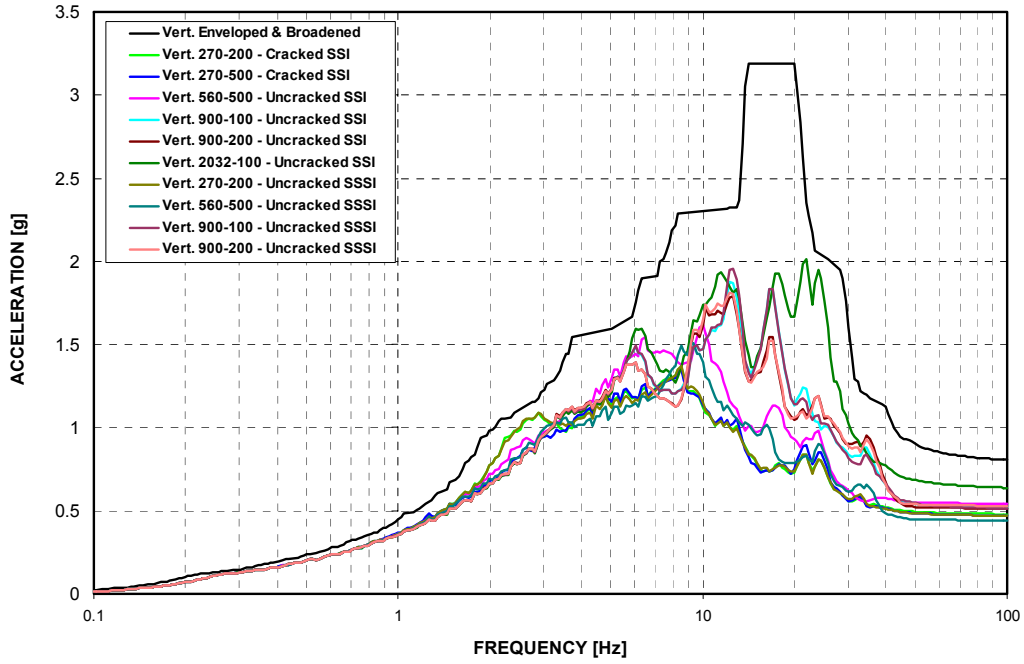

Figure 3-F.2.0-59 ISRS at A/B NW Corner Roof - 5% Damped Response in Vertical Direction (Z) at Model Elevation 74'-10" - Uncracked

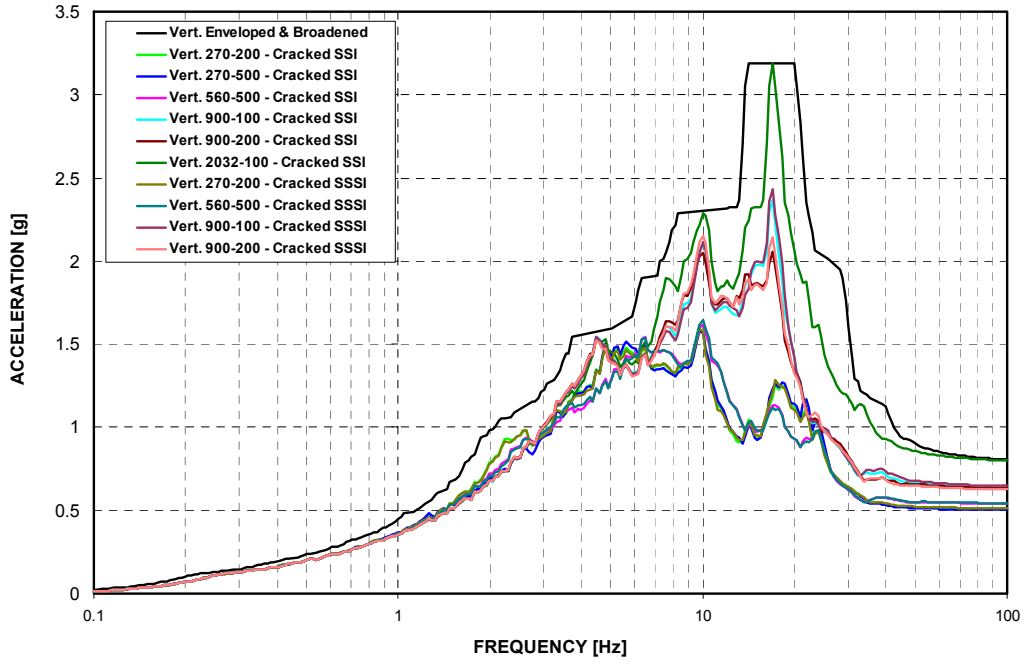

Figure 3-F.2.0-60 ISRS at A/B NW Corner Roof - 5% Damped Response in Vertical Direction (Z) at Model Elevation 74'-10" - Cracked

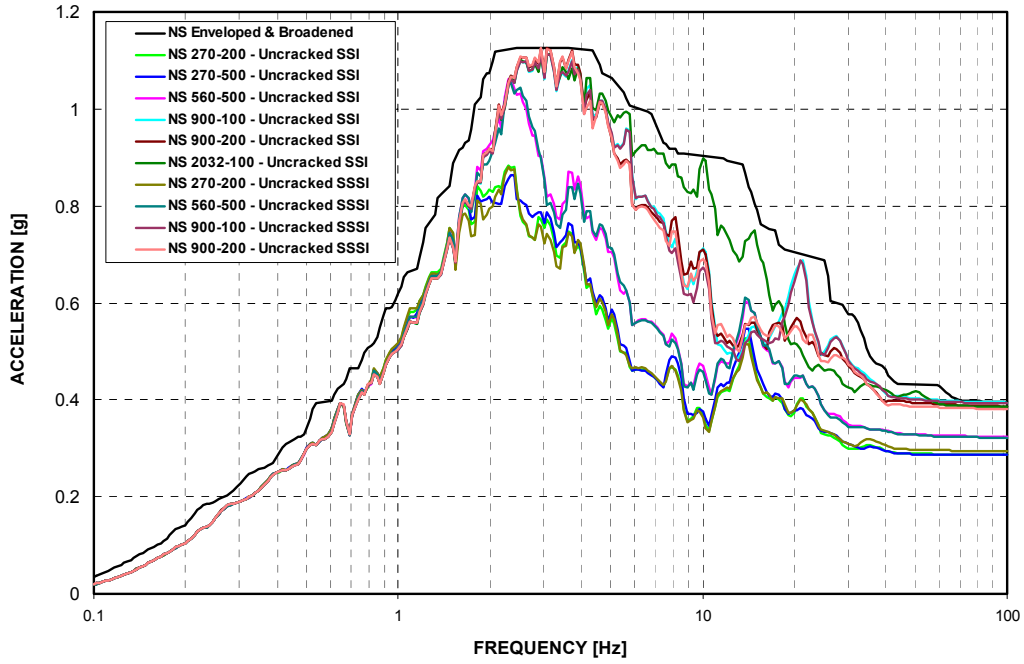

Figure 3-F.2.0-61 ISRS at West PS/B SW Corner Basemat - 5% Damped Response in NS Direction (X) at Model Elevation -26'-4" - Uncracked

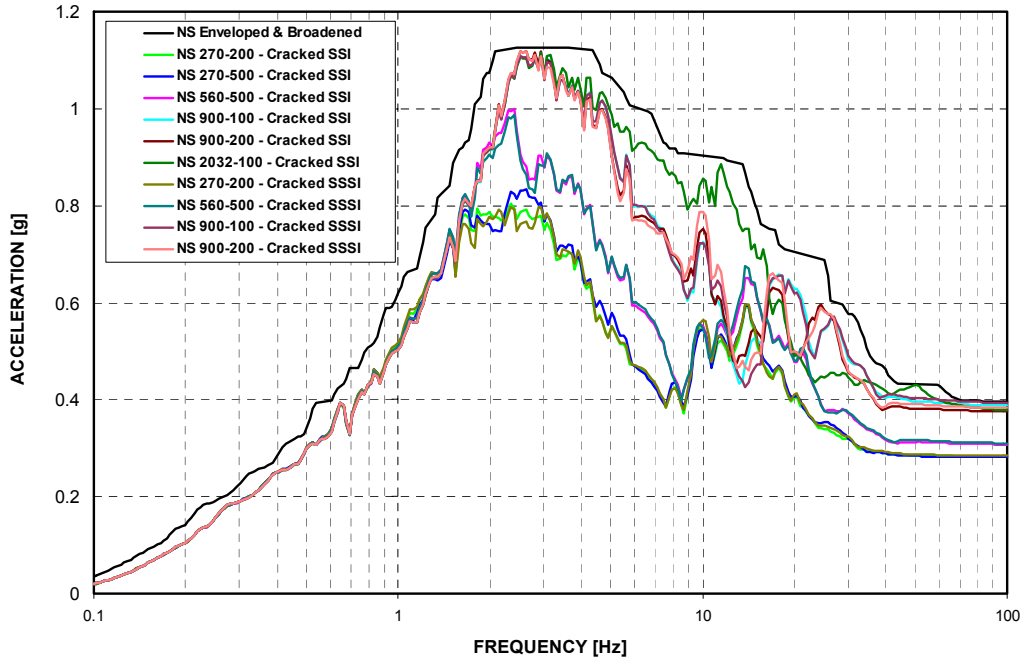

Figure 3-F.2.0-62 ISRS at West PS/B SW Corner Basemat - 5% Damped Response in NS Direction (X) at Model Elevation -26'-4" - Cracked

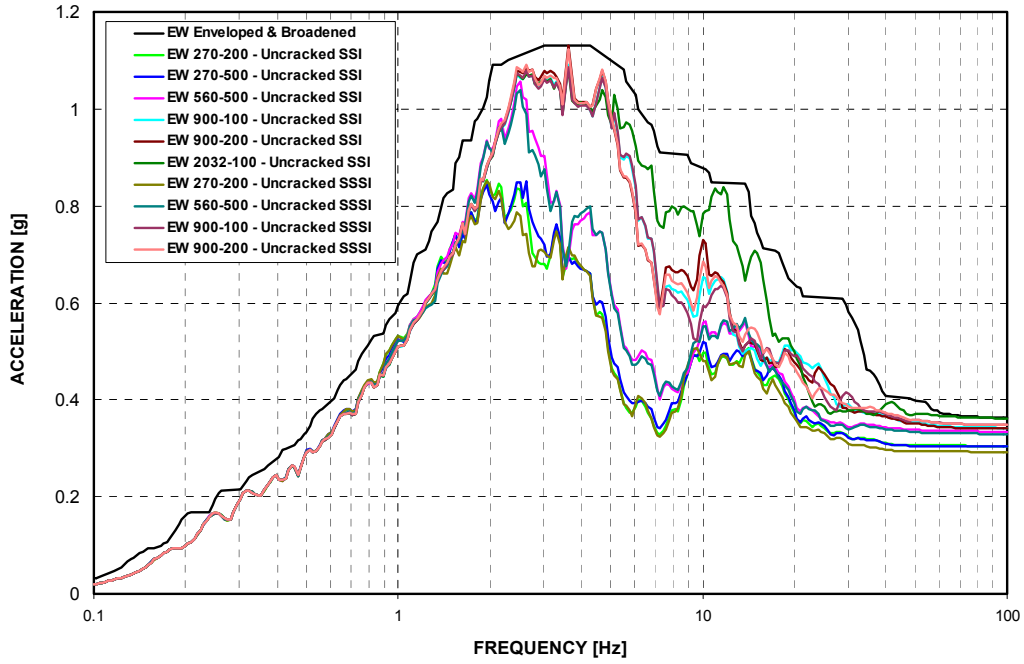

Figure 3-F.2.0-63 ISRS at West PS/B SW Corner Basemat - 5% Damped Response in EW Direction (Y) at Model Elevation -26'-4" - Uncracked

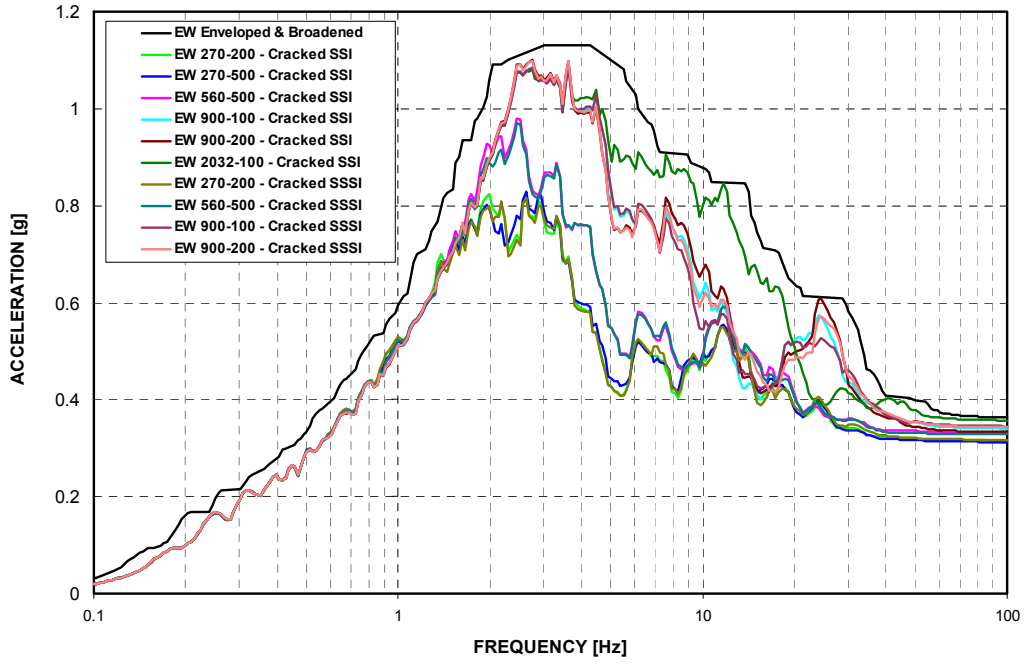

Figure 3-F.2.0-64 ISRS at West PS/B SW Corner Basemat - 5% Damped Response in EW Direction (Y) at Model Elevation -26'-4" - Cracked

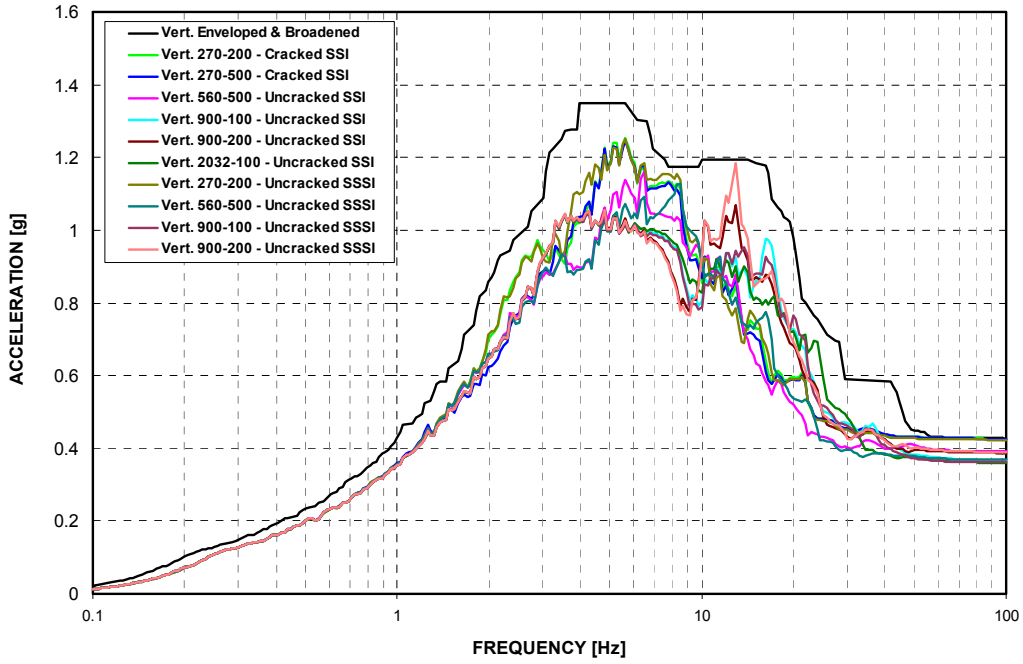

Figure 3-F.2.0-65 ISRS at West PS/B SW Corner Basemat - 5% Damped Response in Vertical Direction (Z) at Model Elevation -26'-4" - Uncracked

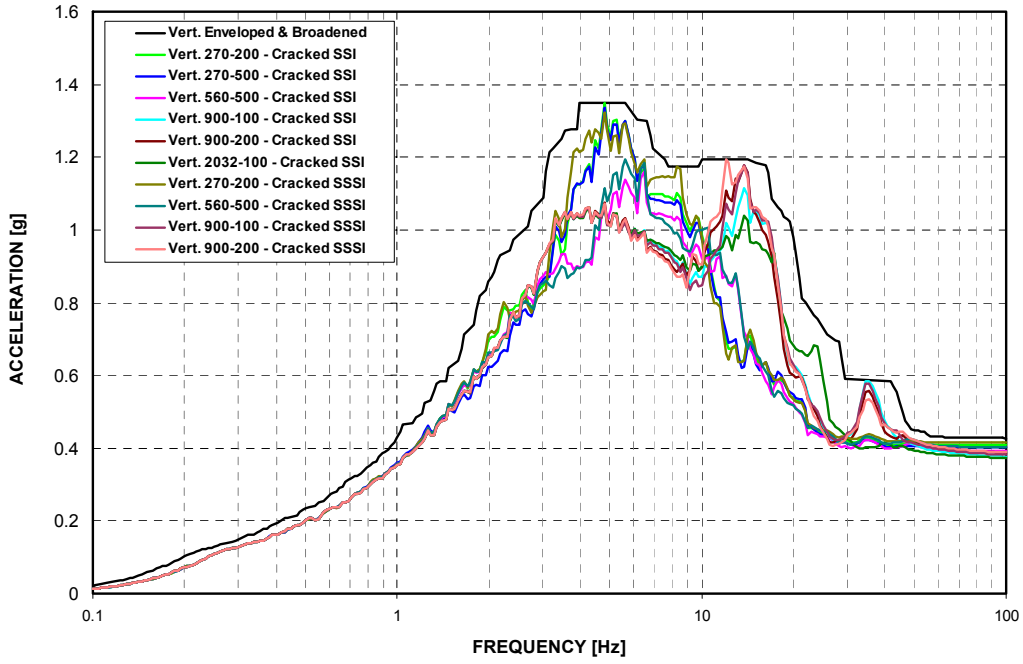

Figure 3-F.2.0-66 ISRS at West PS/B SW Corner Basemat - 5% Damped Response in Vertical Direction (Z) at Model Elevation -26'-4" - Cracked

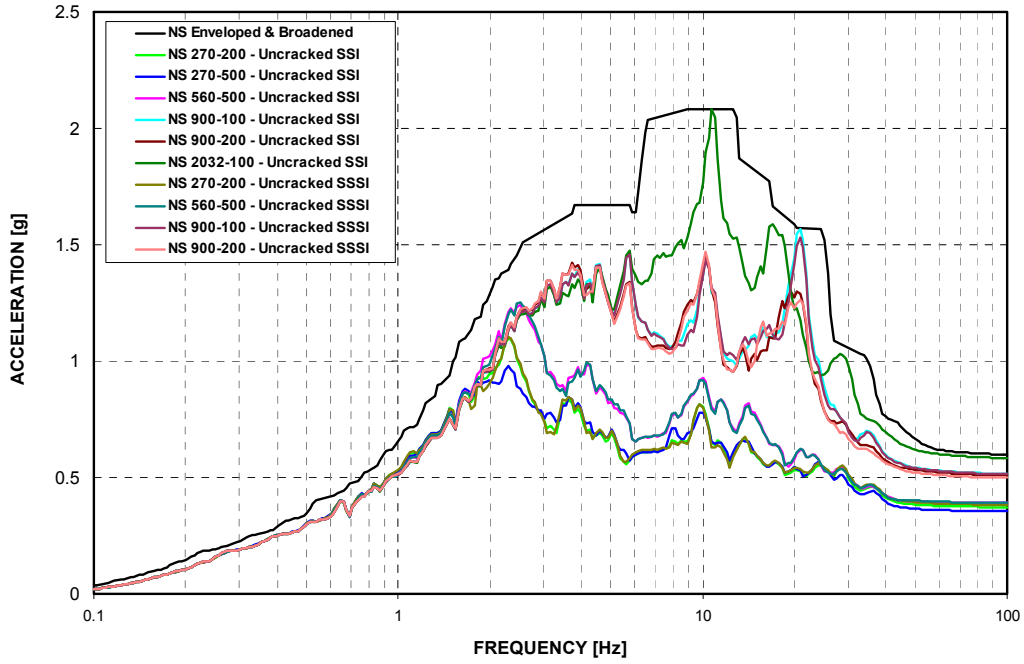

Figure 3-F.2.0-67 ISRS at West PS/B SW Corner Roof - 5% Damped Response in NS Direction (X) at Model Elevation 48'-6" - Uncracked

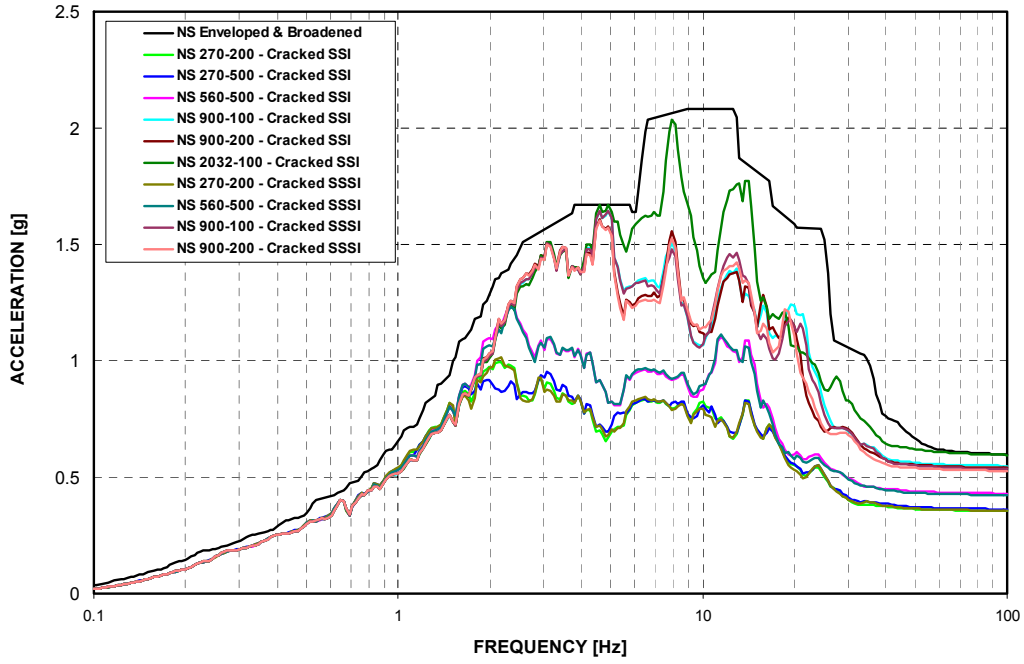

Figure 3-F.2.0-68 ISRS at West PS/B SW Corner Roof - 5% Damped Response in NS Direction (X) at Model Elevation 48'-6" - Cracked

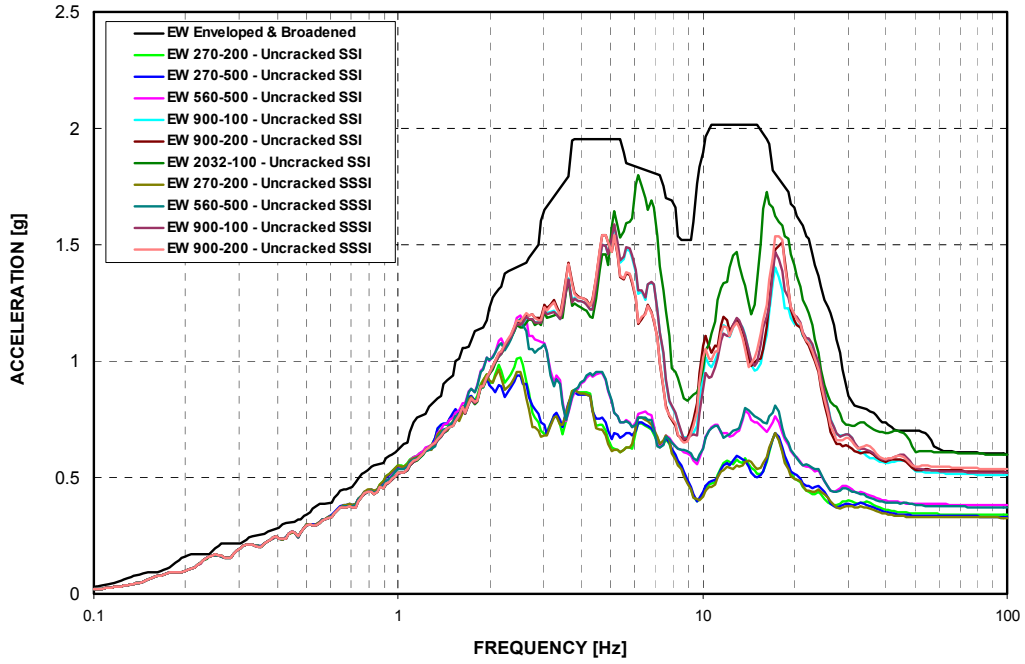

Figure 3-F.2.0-69 ISRS at West PS/B SW Corner Roof - 5% Damped Response in EW Direction (Y) at Model Elevation 48'-6" - Uncracked

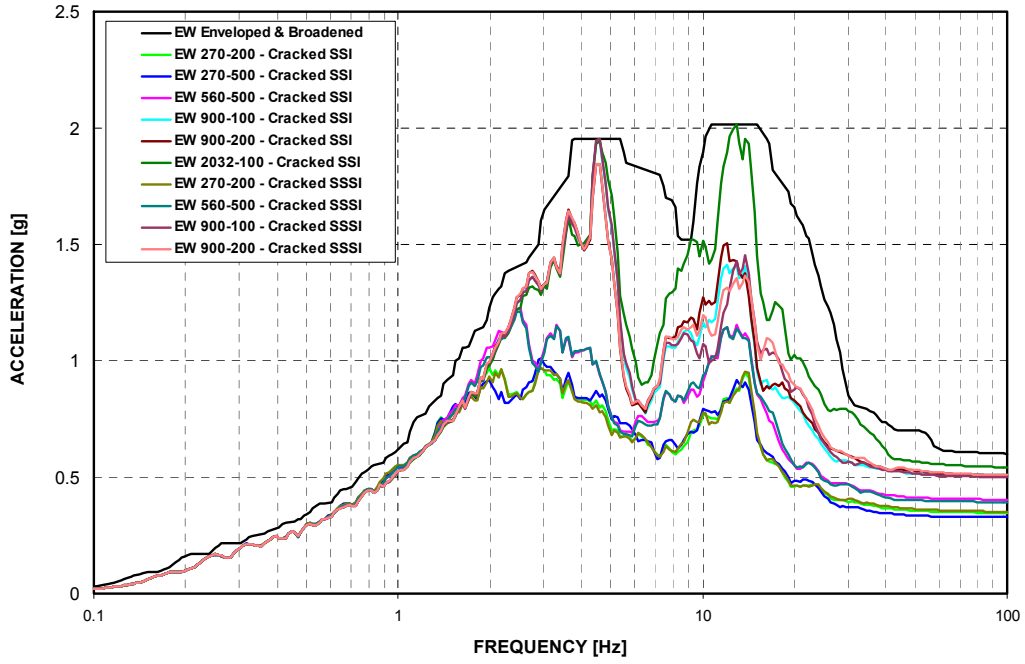

Figure 3-F.2.0-70 ISRS at West PS/B SW Corner Roof - 5% Damped Response in EW Direction (Y) at Model Elevation 48'-6" - Cracked

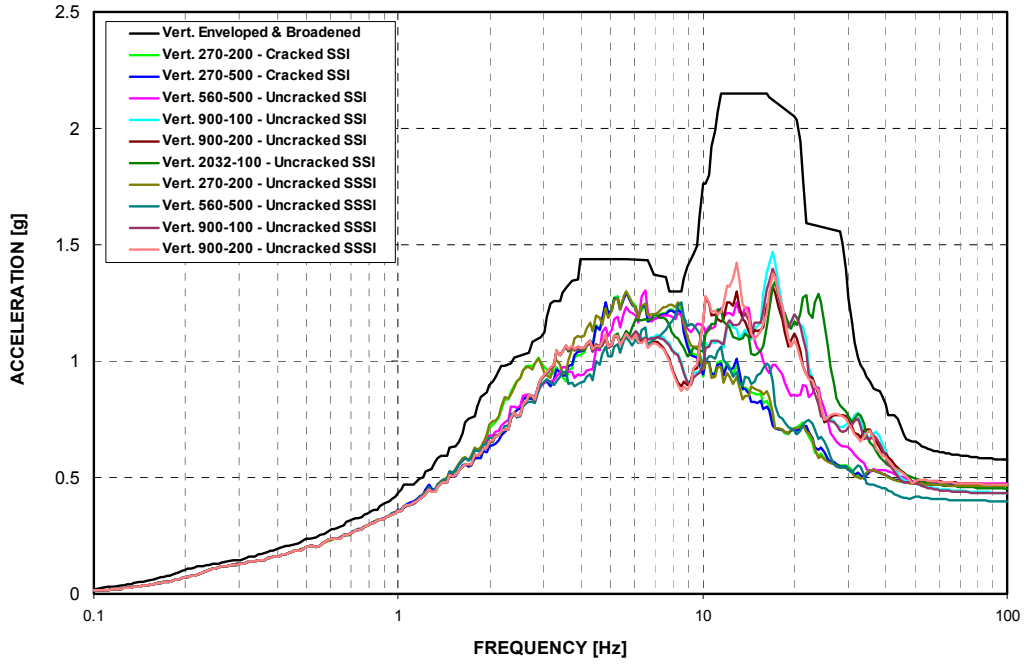

Figure 3-F.2.0-71 ISRS at West PS/B SW Corner Roof - 5% Damped Response in Vertical Direction (Z) at Model Elevation 48'-6" - Uncracked

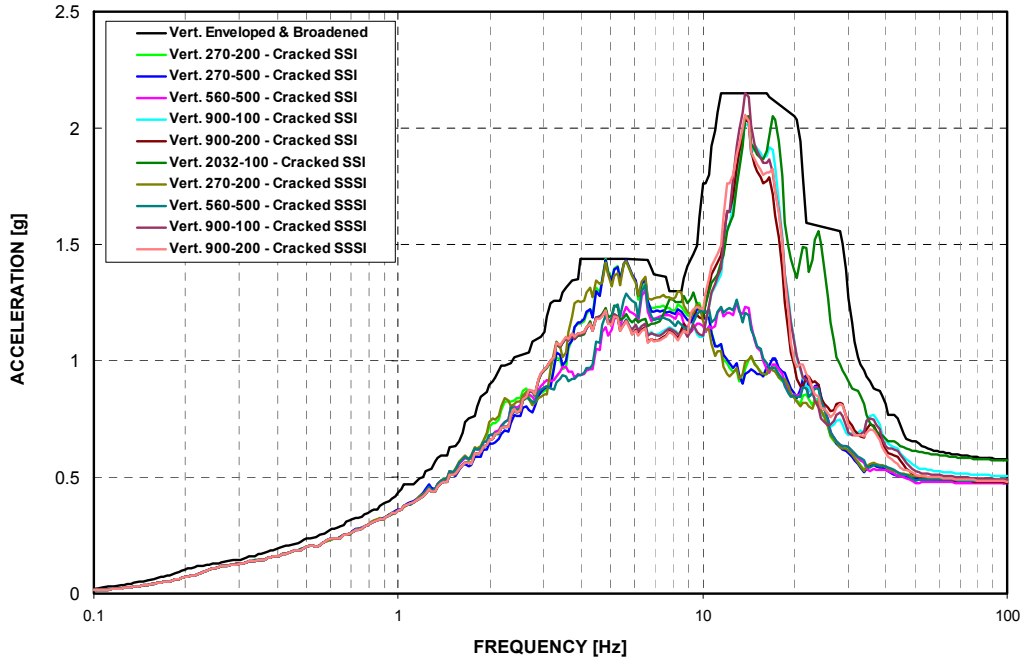

Figure 3-F.2.0-72 ISRS at West PS/B SW Corner Roof - 5% Damped Response in Vertical Direction (Z) at Model Elevation 48'-6" - Cracked

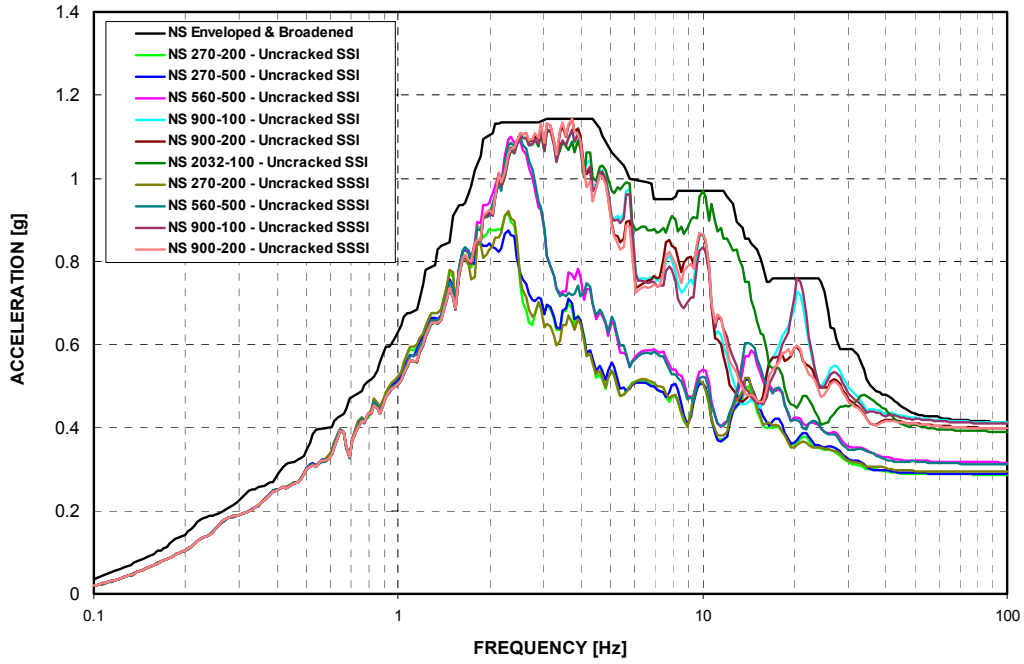

Figure 3-F.2.0-73 ISRS at East PS/B SE Corner Basemat - 5% Damped Response in NS Direction (X) at Model Elevation -26'-4" - Uncracked

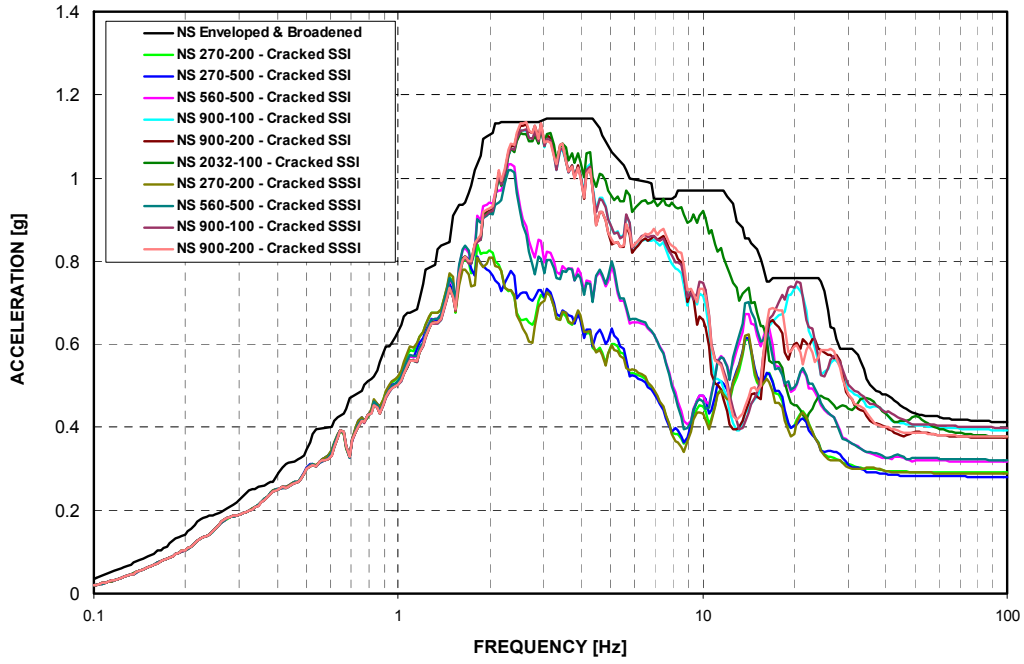

Figure 3-F.2.0-74 ISRS at East PS/B SE Corner Basemat - 5% Damped Response in NS Direction (X) at Model Elevation -26'-4" - Cracked

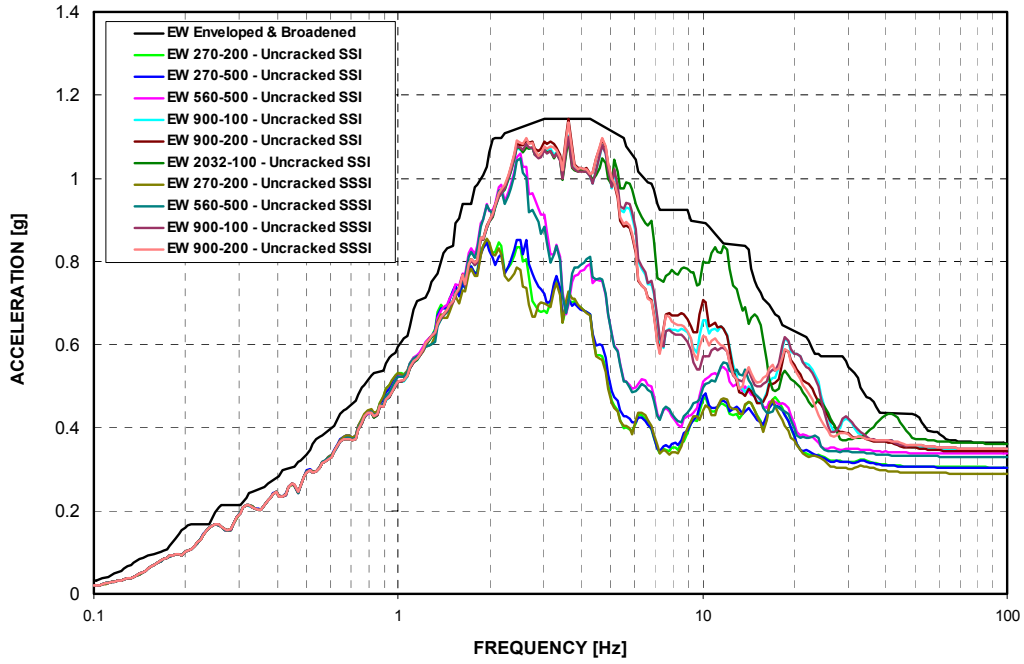

Figure 3-F.2.0-75 ISRS at East PS/B SE Corner Basemat - 5% Damped Response in EW Direction (Y) at Model Elevation -26'-4" - Uncracked

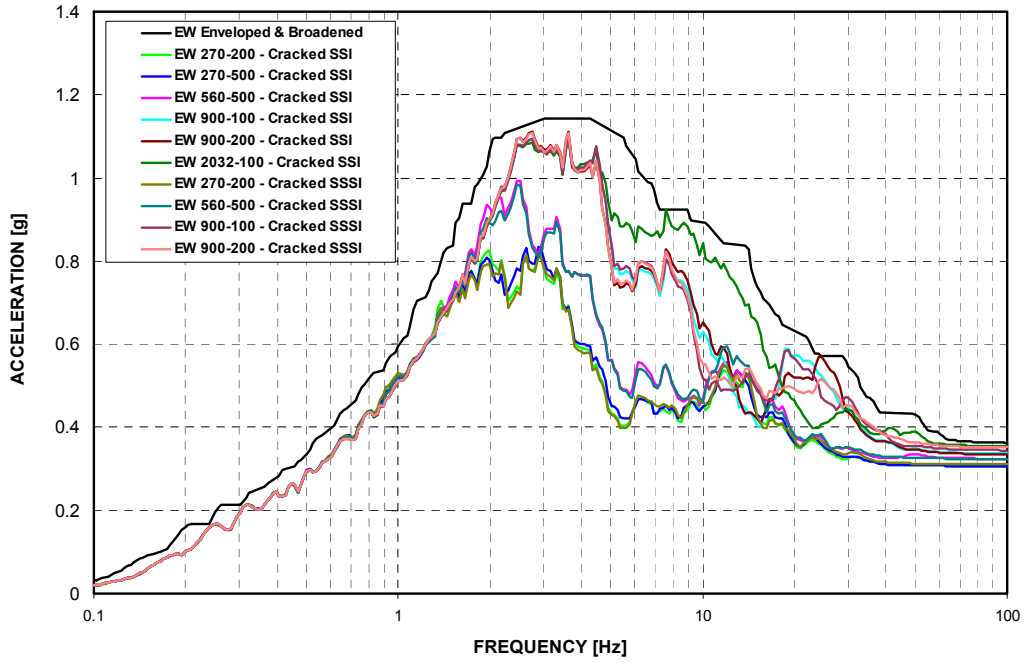

Figure 3-F.2.0-76 ISRS at East PS/B SE Corner Basemat - 5% Damped Response in EW Direction (Y) at Model Elevation -26'-4" - Cracked

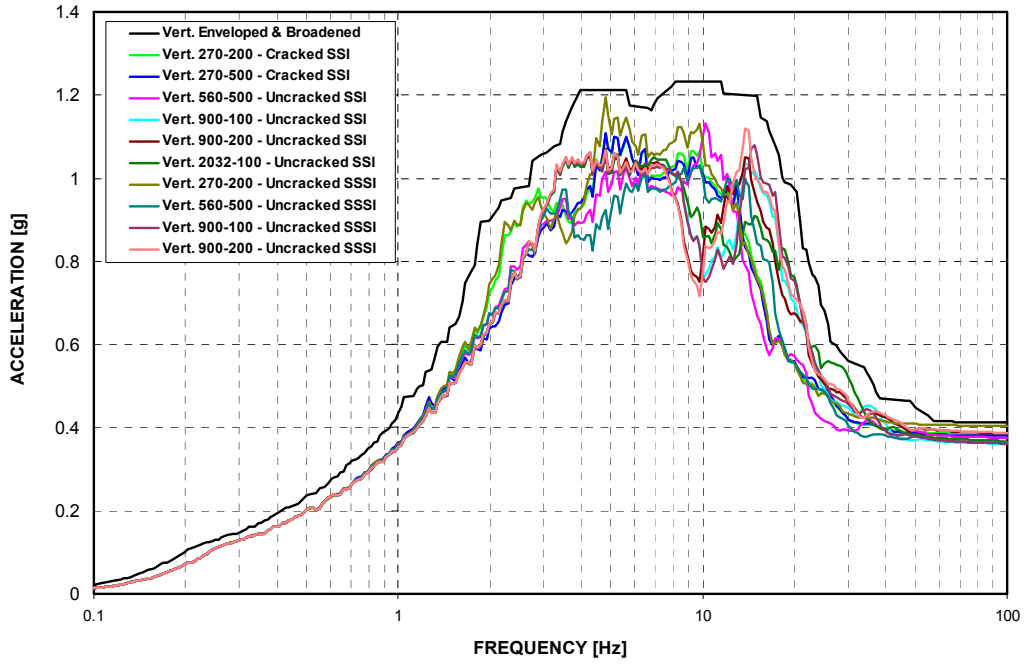

Figure 3-F.2.0-77 ISRS at East PS/B SE Corner Basemat - 5% Damped Response in Vertical Direction (Z) at Model Elevation -26'-4" - Uncracked

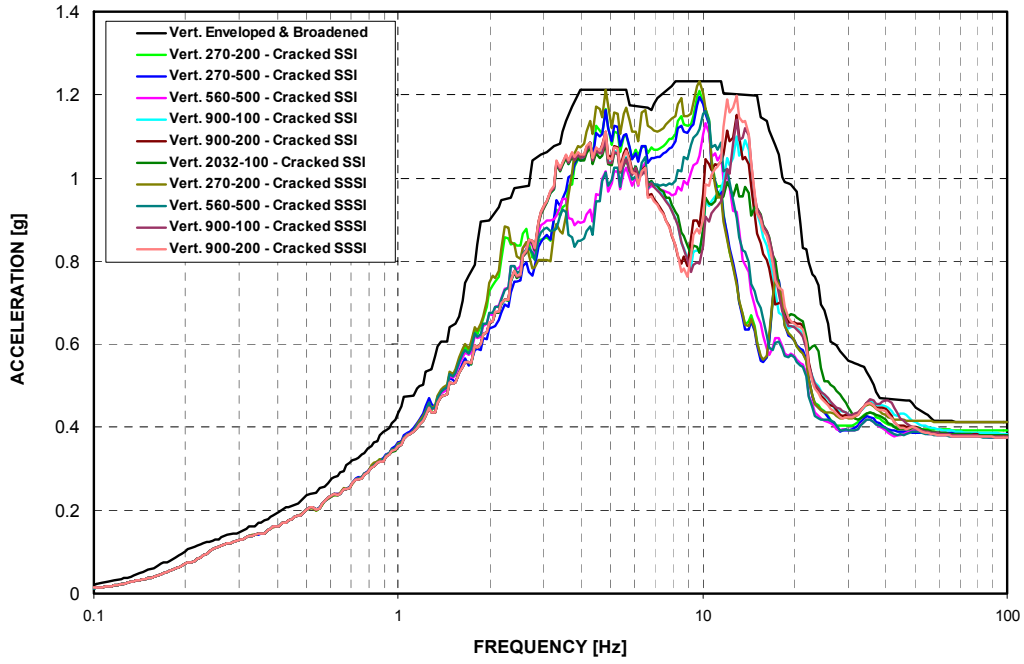

Figure 3-F.2.0-78 ISRS at East PS/B SE Corner Basemat - 5% Damped Response in Vertical Direction (Z) at Model Elevation -26'-4" - Cracked

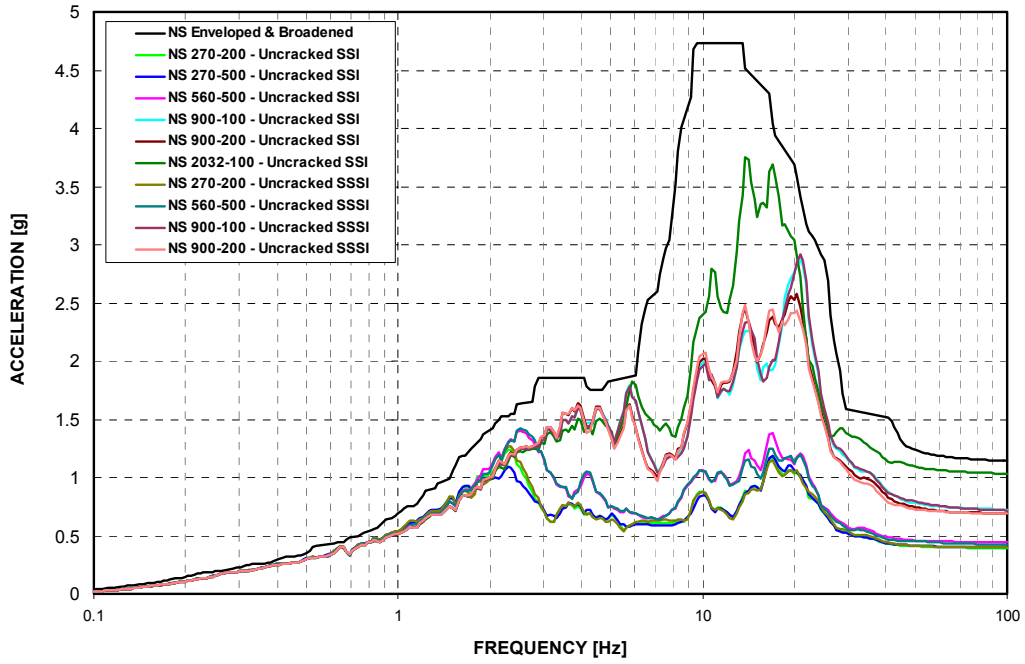

Figure 3-F.2.0-79 ISRS at East PS/B SE Corner Roof - 5% Damped Response in NS Direction (X) at Model Elevation 48'-6" - Uncracked

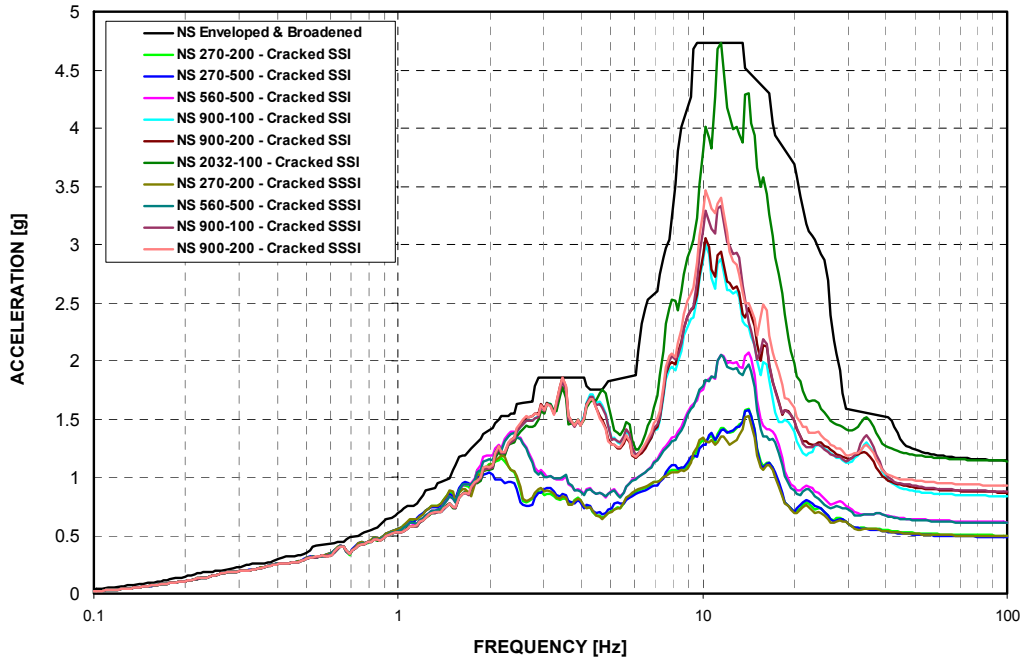

Figure 3-F.2.0-80 ISRS at East PS/B SE Corner Roof - 5% Damped Response in NS Direction (X) at Model Elevation 48'-6" - Cracked

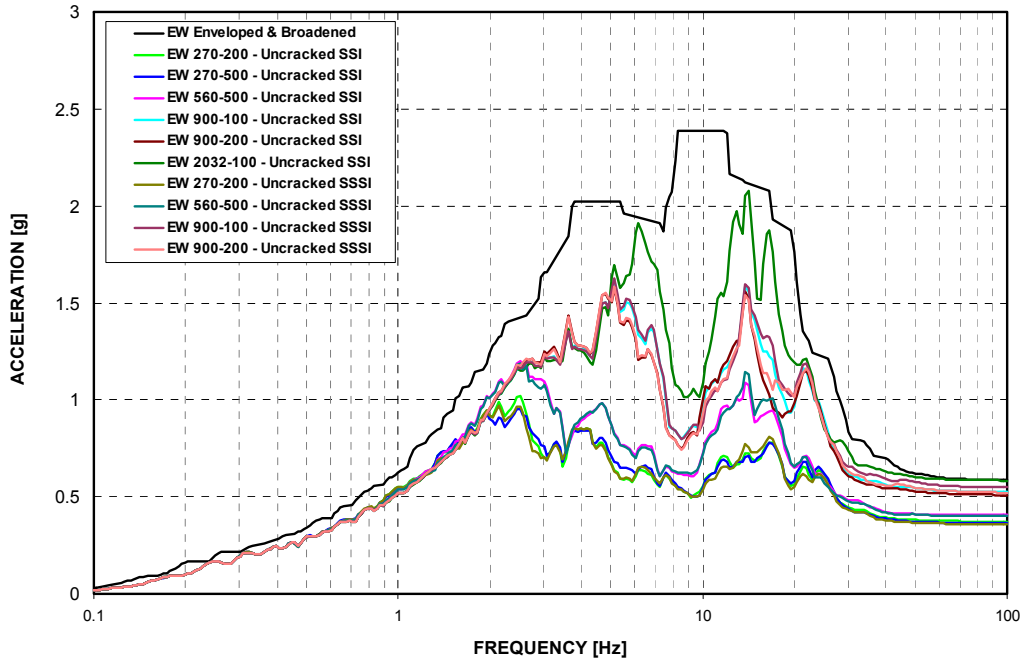

Figure 3-F.2.0-81 ISRS at East PS/B SE Corner Roof - 5% Damped Response in EW Direction (Y) at Model Elevation 48'-6" - Uncracked

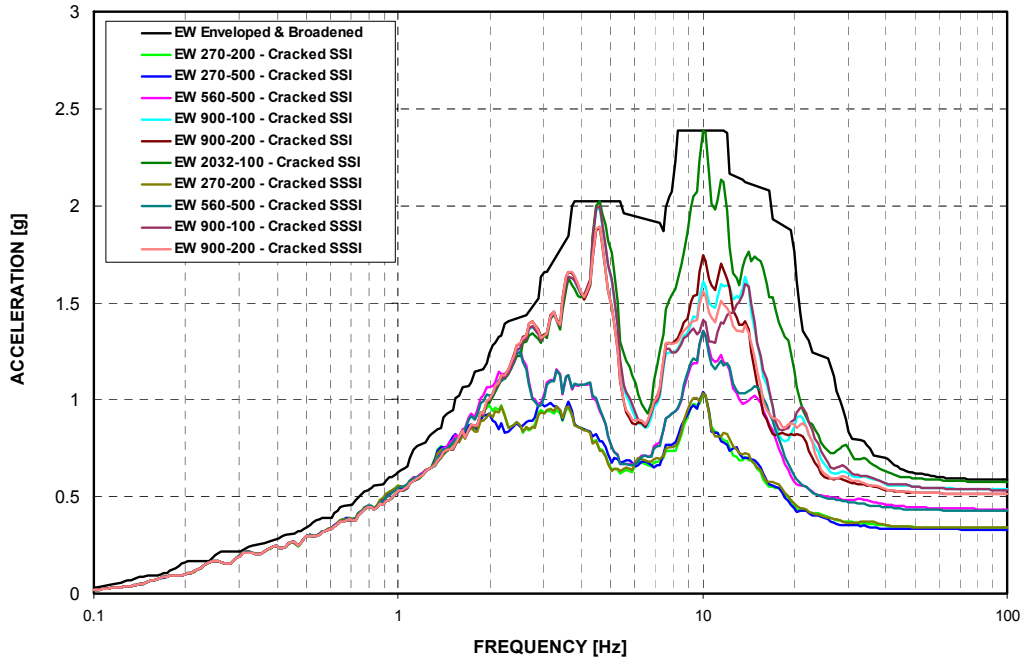

Figure 3-F.2.0-82 ISRS at East PS/B SE Corner Roof - 5% Damped Response in EW Direction (Y) at Model Elevation 48'-6" - Cracked

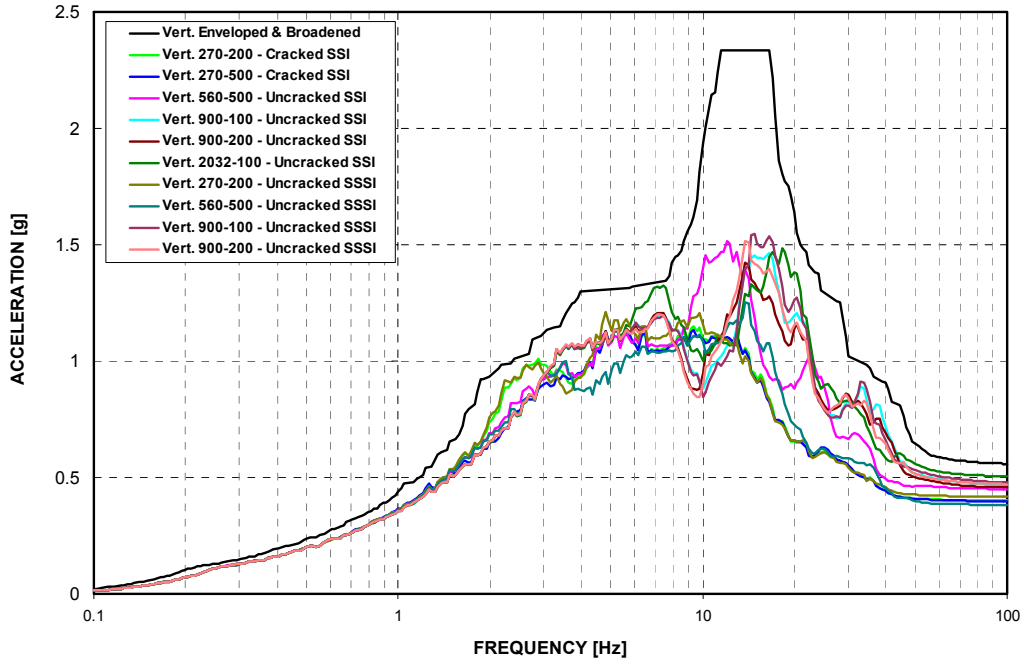

Figure 3-F.2.0-83 ISRS at East PS/B SE Corner Roof - 5% Damped Response in Vertical Direction (Z) at Model Elevation 48'-6" - Uncracked

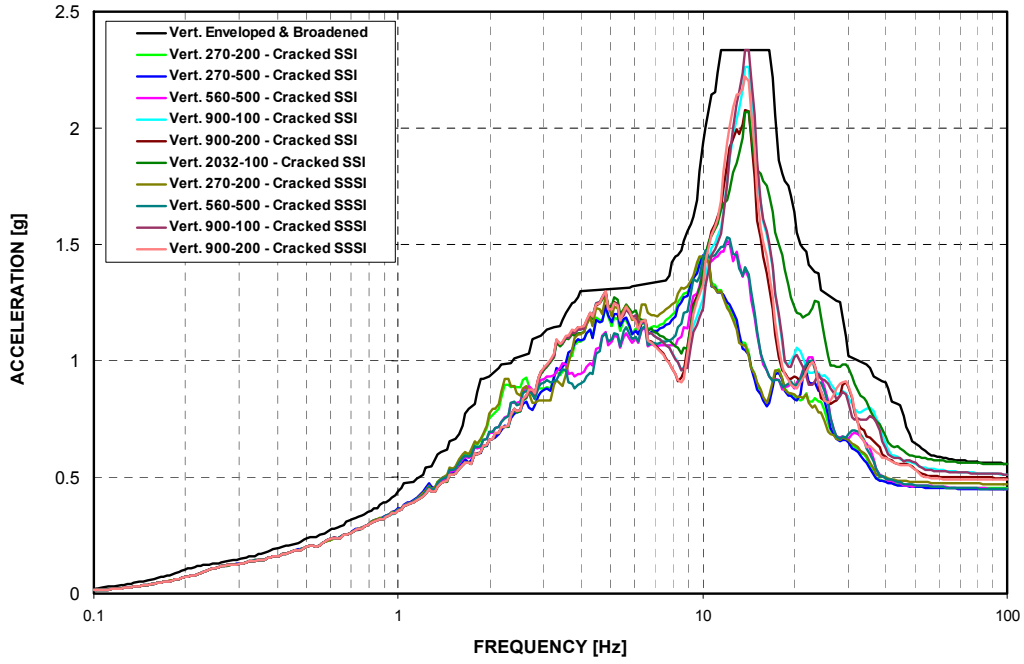

Figure 3-F.2.0-84 ISRS at East PS/B SE Corner Roof - 5% Damped Response in Vertical Direction (Z) at Model Elevation 48'-6" - Cracked

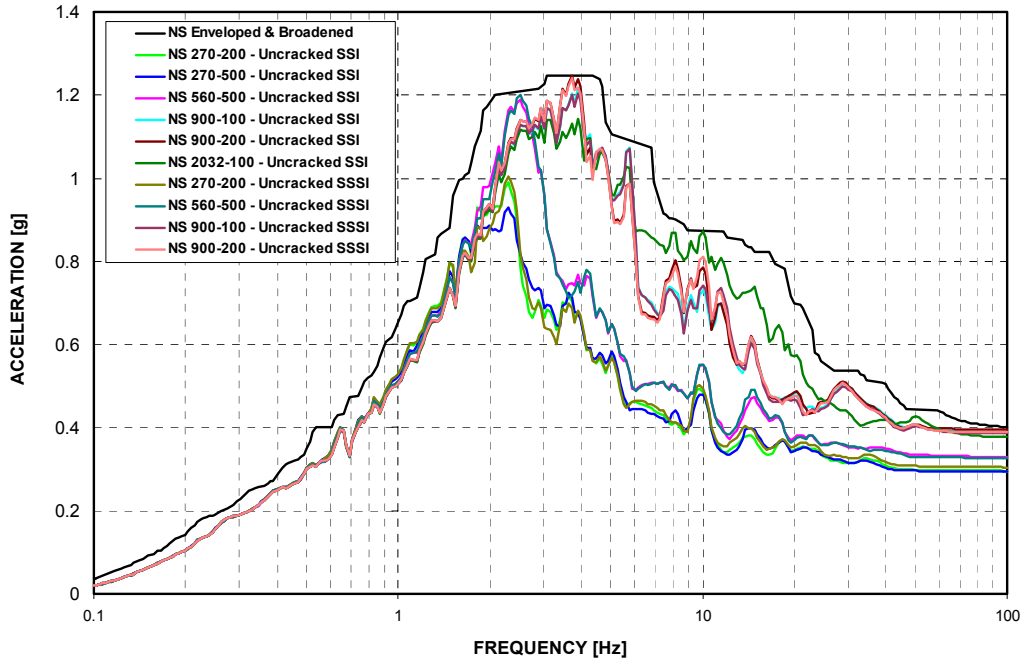

Figure 3-F.2.0-85 ISRS at R/B NE Corner Basemat - 5% Damped Response in NS Direction (X) at Model Elevation -26'-4" - Uncracked

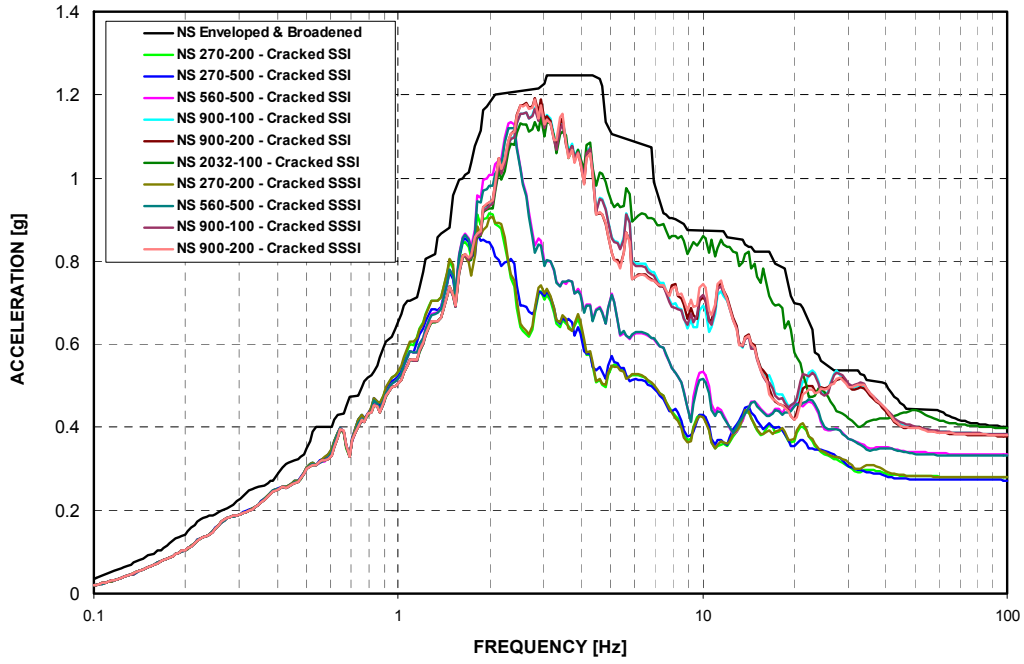

Figure 3-F.2.0-86 ISRS at R/B NE Corner Basemat - 5% Damped Response in NS Direction (X) at Model Elevation -26'-4" - Cracked

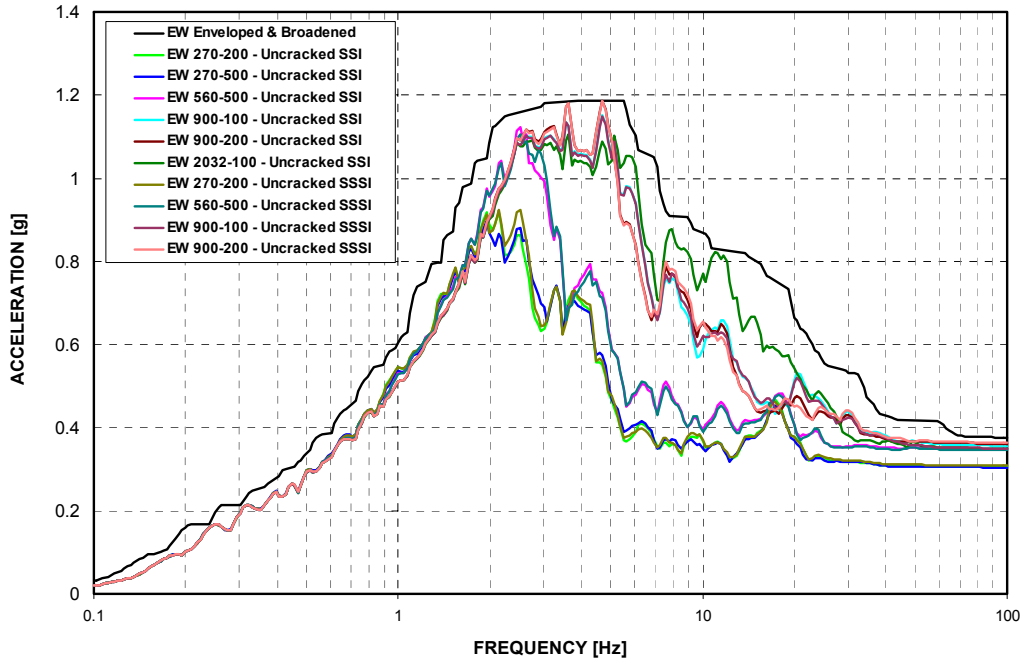

Figure 3-F.2.0-87 ISRS at R/B NE Corner Basemat - 5% Damped Response in EW Direction (Y) at Model Elevation -26'-4" - Uncracked

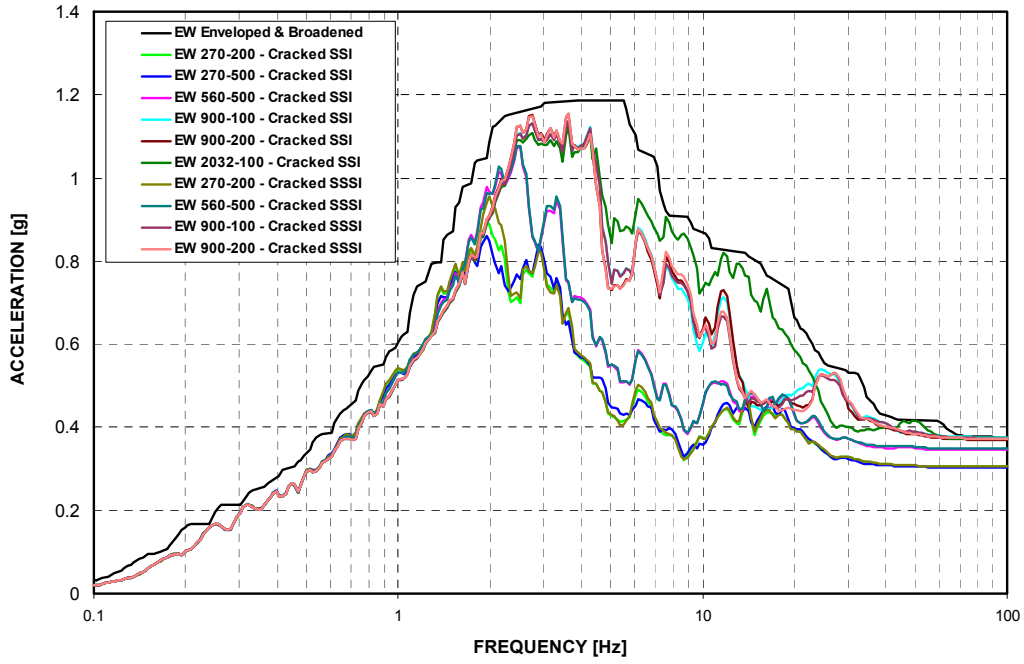

Figure 3-F.2.0-88 ISRS at R/B NE Corner Basemat - 5% Damped Response in EW Direction (Y) at Model Elevation -26'-4" - Cracked

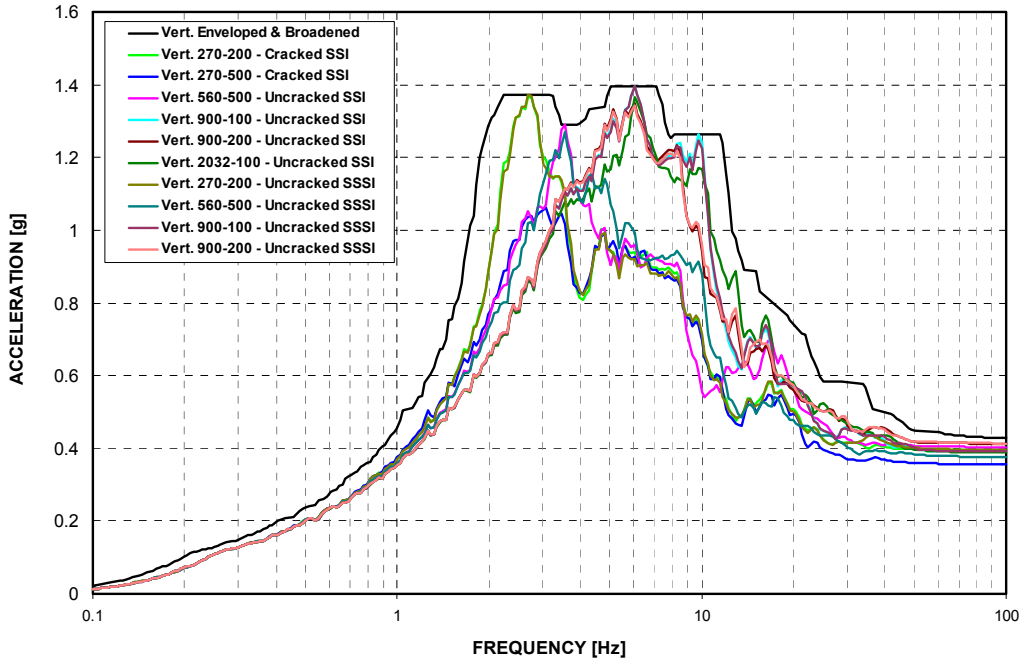

Figure 3-F.2.0-89 ISRS at R/B NE Corner Basemat - 5% Damped Response in Vertical Direction (Z) at Model Elevation -26'-4" - Uncracked

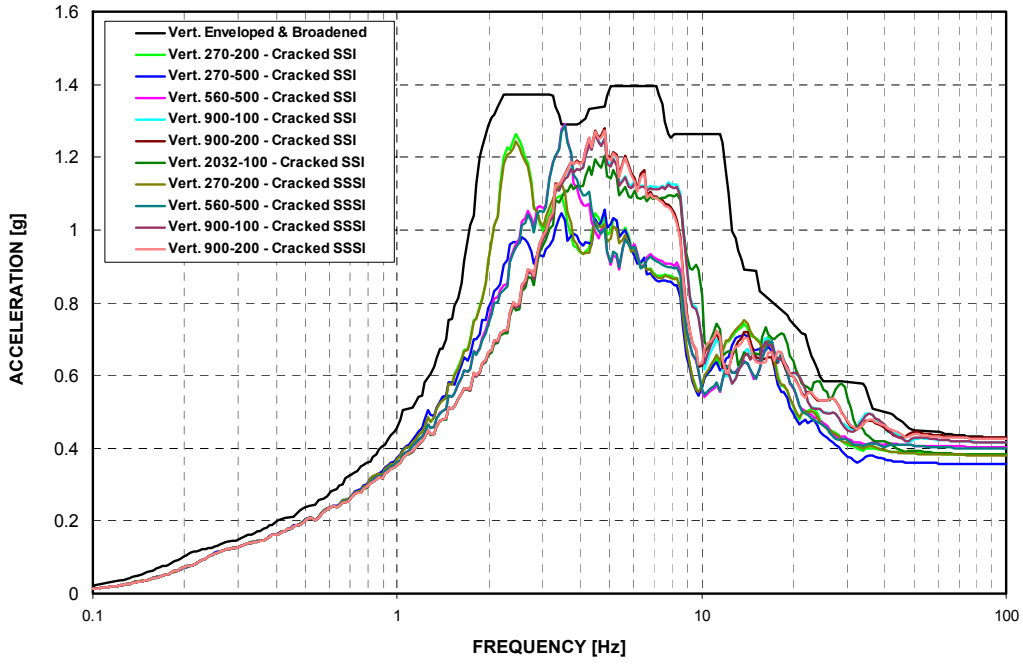

Figure 3-F.2.0-90 ISRS at R/B NE Corner Basemat - 5% Damped Response in Vertical Direction (Z) at Model Elevation -26'-4" - Cracked

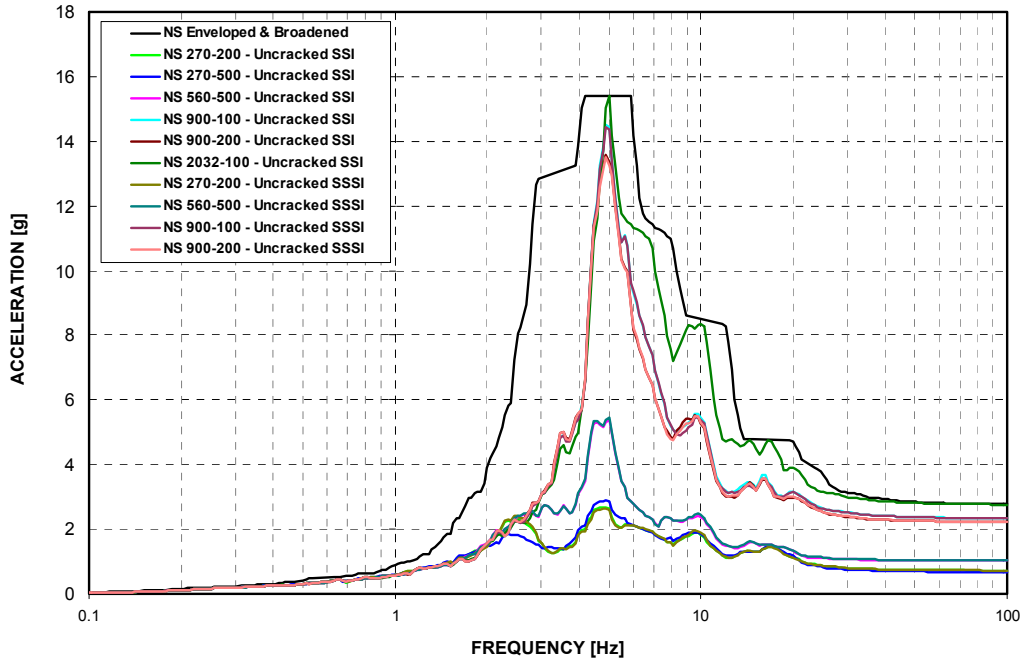

Figure 3-F.2.0-91 ISRS at FH/A NE Corner Roof - 5% Damped Response in NS Direction (X) at Model Elevation 156'-0" - Uncracked

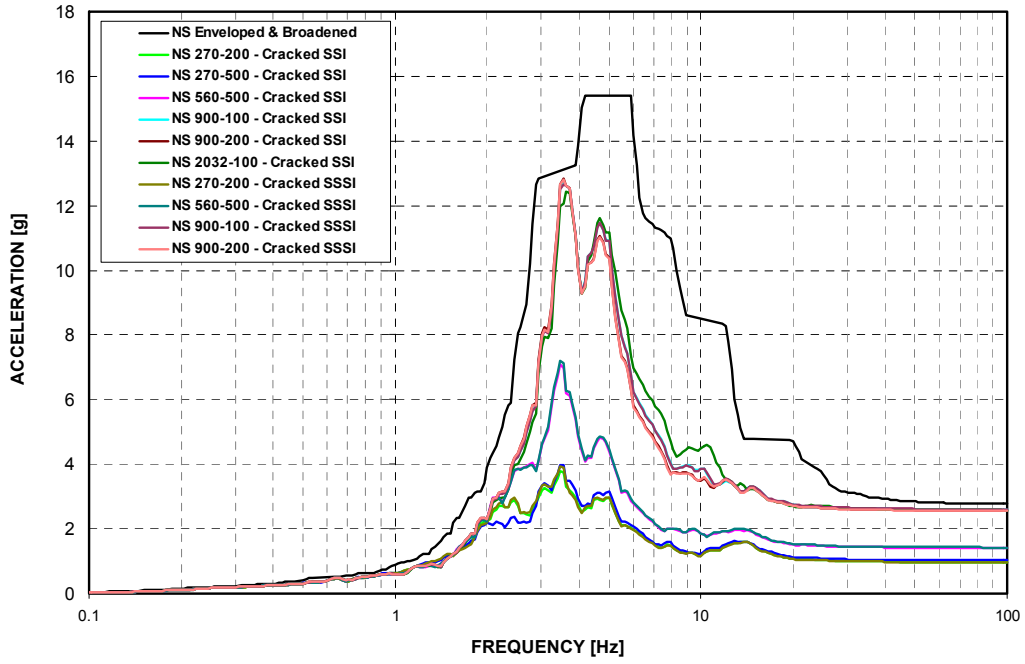

Figure 3-F.2.0-92 ISRS at FH/A NE Corner Roof - 5% Damped Response in NS Direction (X) at Model Elevation 156'-0" - Cracked

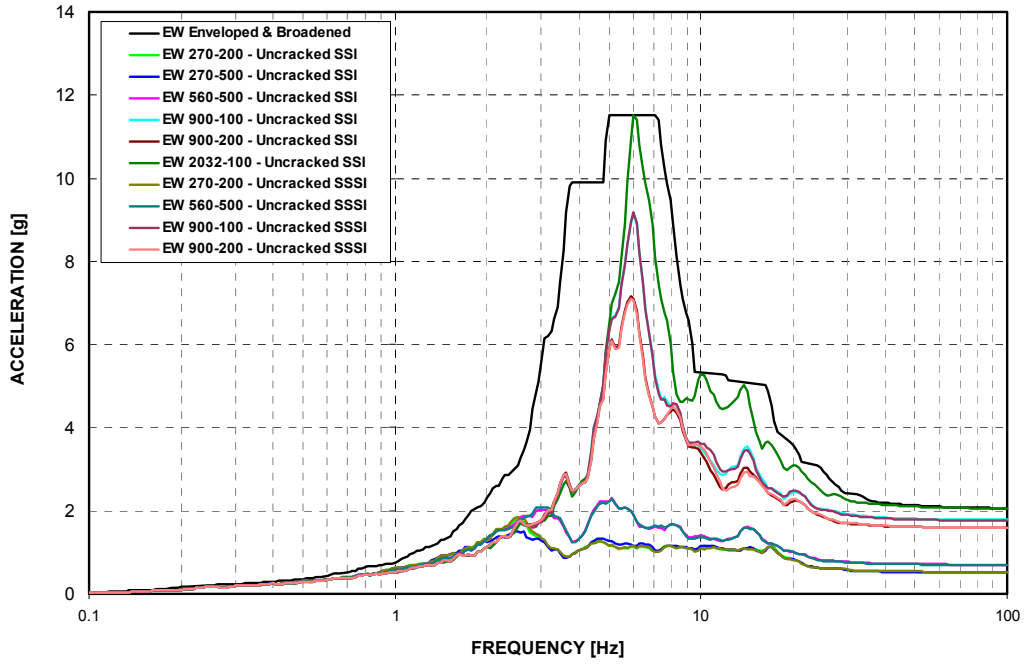

Figure 3-F.2.0-93 ISRS at FH/A NE Corner Roof - 5% Damped Response in EW Direction (Y) at Model Elevation 156'-0" - Uncracked

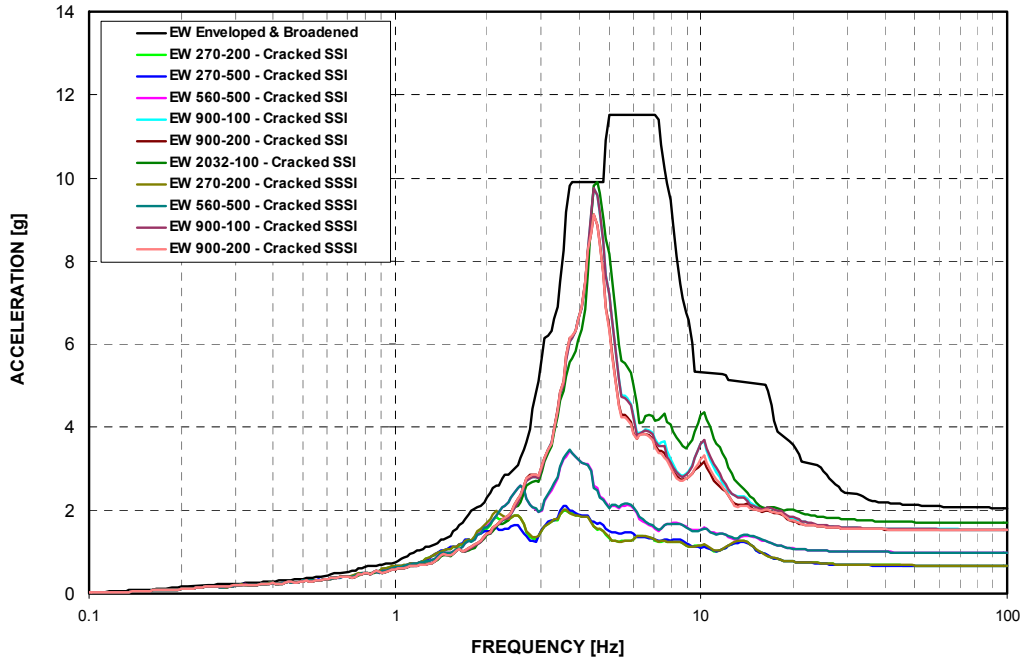

Figure 3-F.2.0-94 ISRS at FH/A NE Corner Roof - 5% Damped Response in EW Direction (Y) at Model Elevation 156'-0" - Cracked

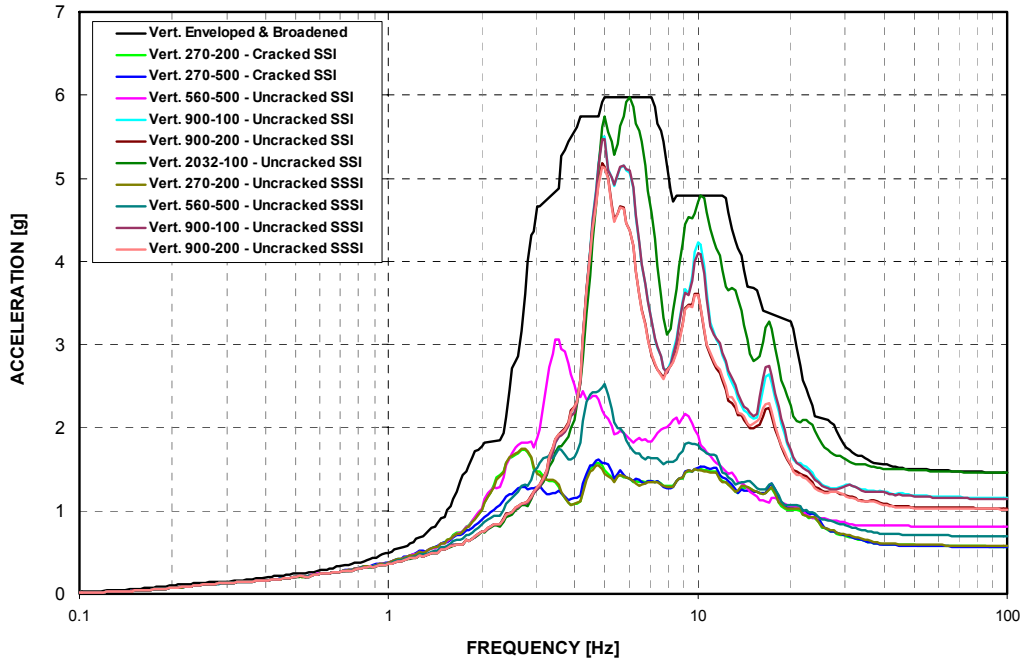

Figure 3-F.2.0-95 ISRS at FH/A NE Corner Roof - 5% Damped Response in Vertical Direction (Z) at Model Elevation 156'-0" - Uncracked

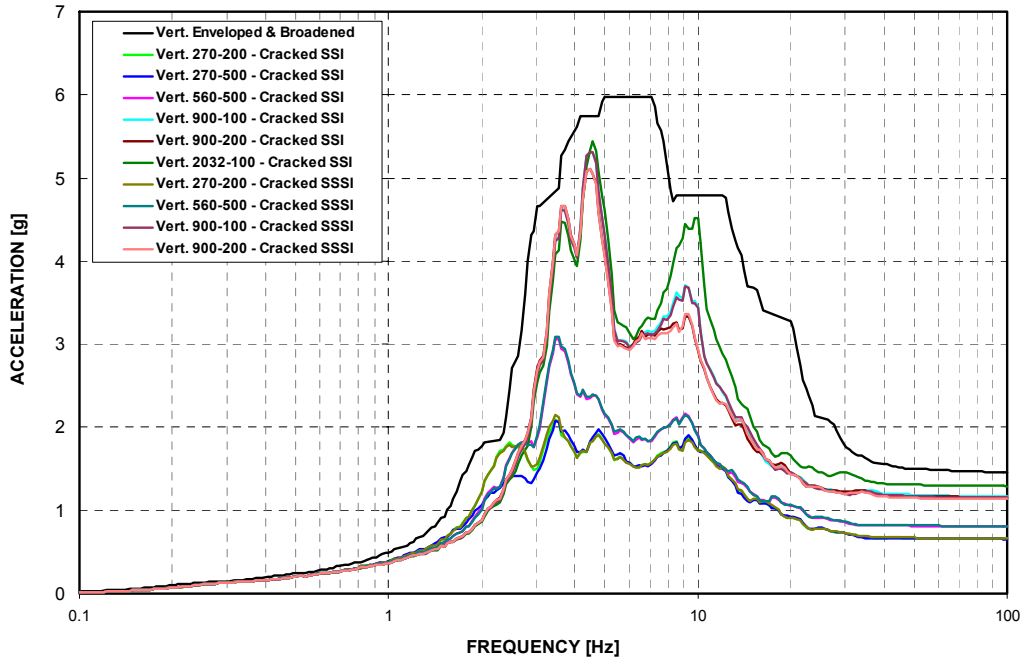

Figure 3-F.2.0-96 ISRS at FH/A NE Corner Roof - 5% Damped Response in Vertical Direction (Z) at Model Elevation 156'-0" - Cracked

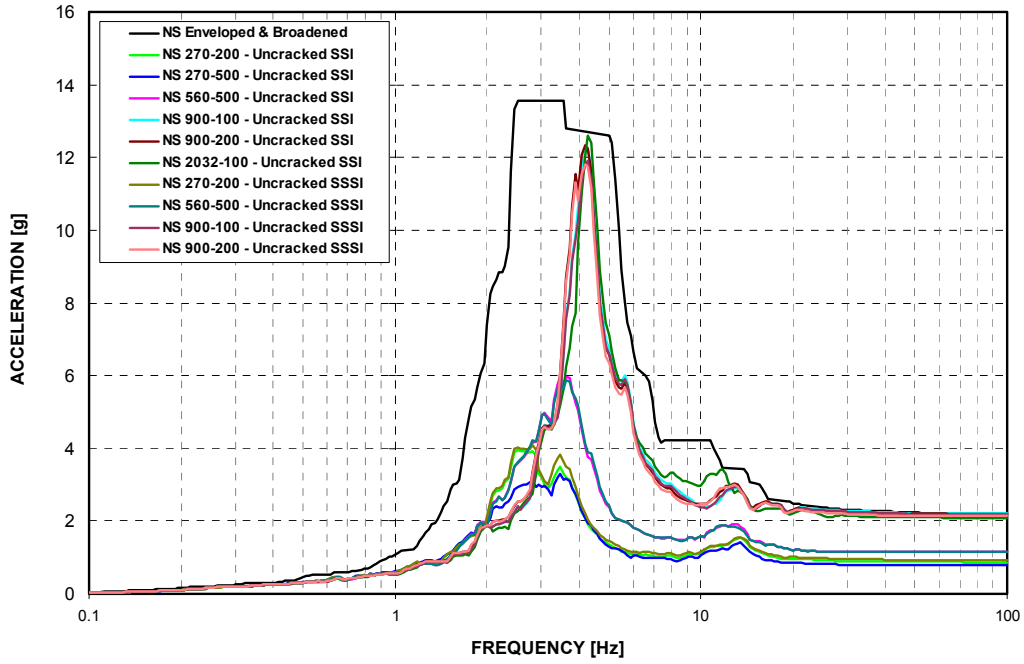

Figure 3-F.2.0-97 ISRS at Top of PCCV - 5% Damped Response in NS Direction (X) at Model Elevation 232'-0" - Uncracked

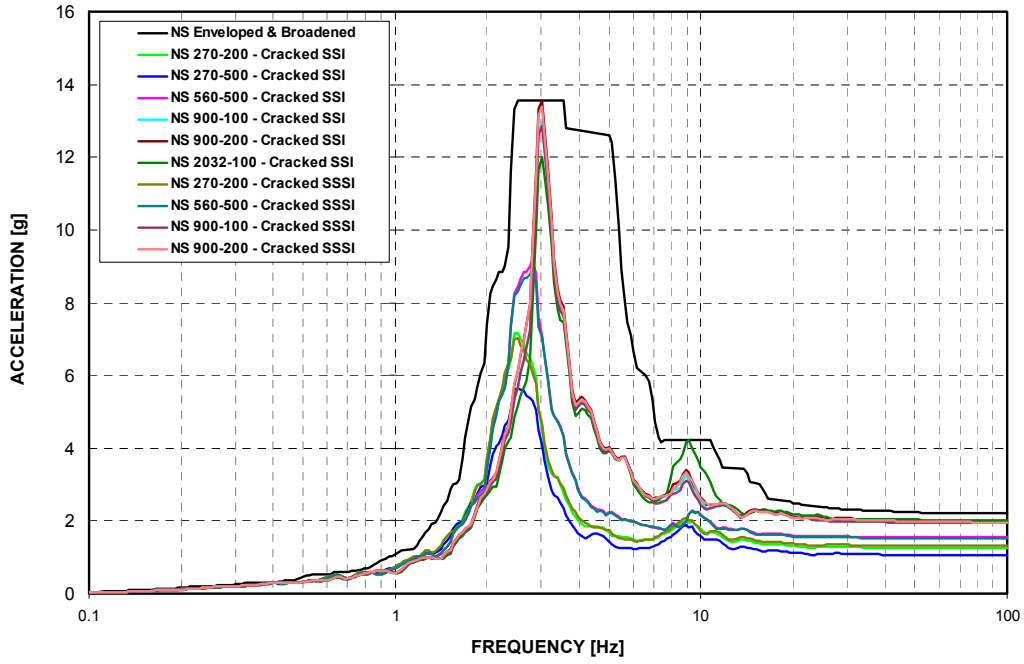

Figure 3-F.2.0-98 ISRS at Top of PCCV - 5% Damped Response in NS Direction (X) at Model Elevation 232'-0" - Cracked

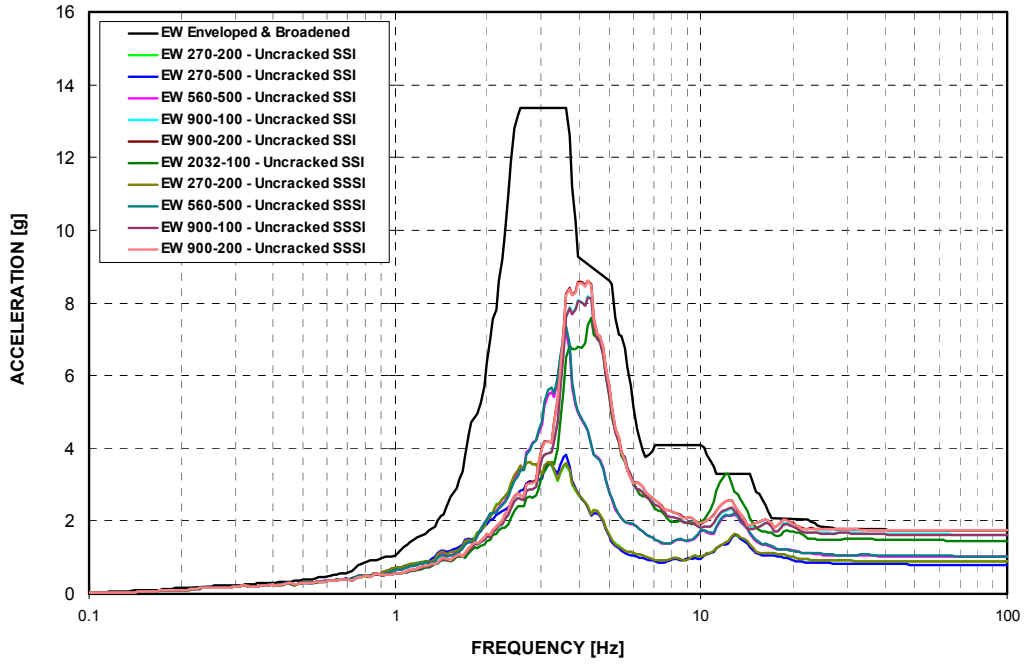

Figure 3-F.2.0-99 ISRS at Top of PCCV - 5% Damped Response in EW Direction (Y) at Model Elevation 232'-0" - Uncracked

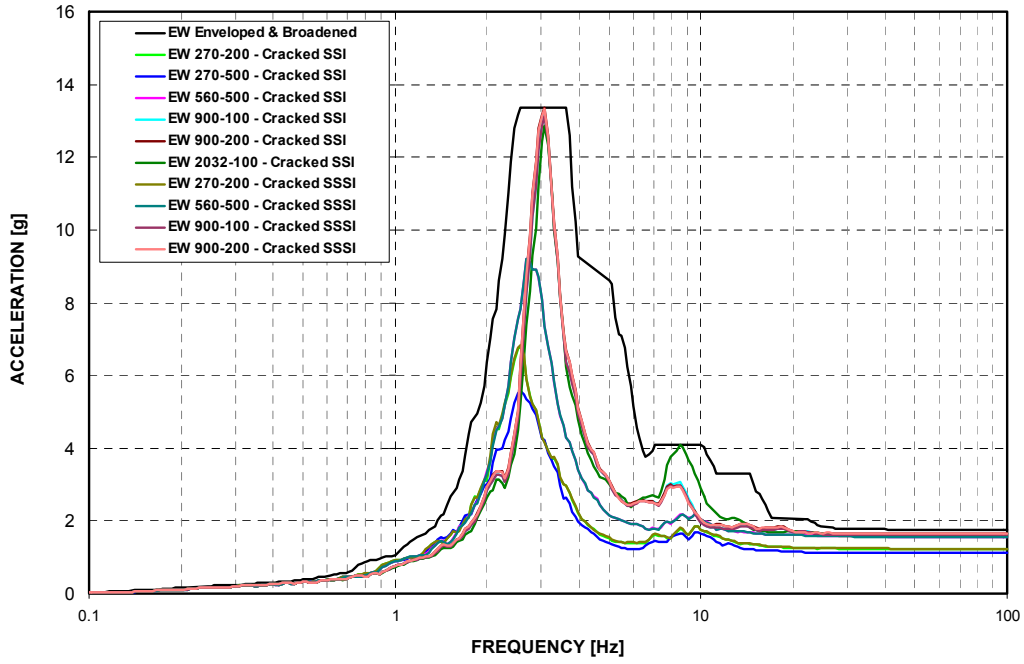

Figure 3-F.2.0-100 ISRS at Top of PCCV - 5% Damped Response in EW Direction (Y) at Model Elevation 232'-0" - Cracked

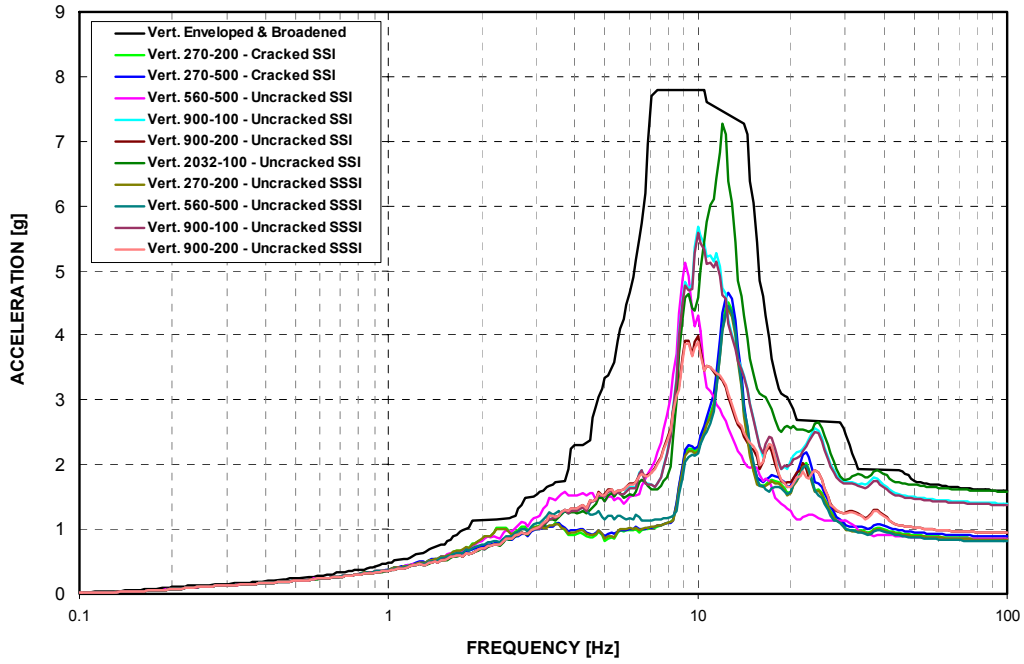

Figure 3-F.2.0-101 ISRS at Top of PCCV - 5% Damped Response in Vertical Direction (Z) at Model Elevation 232'-0" - Uncracked

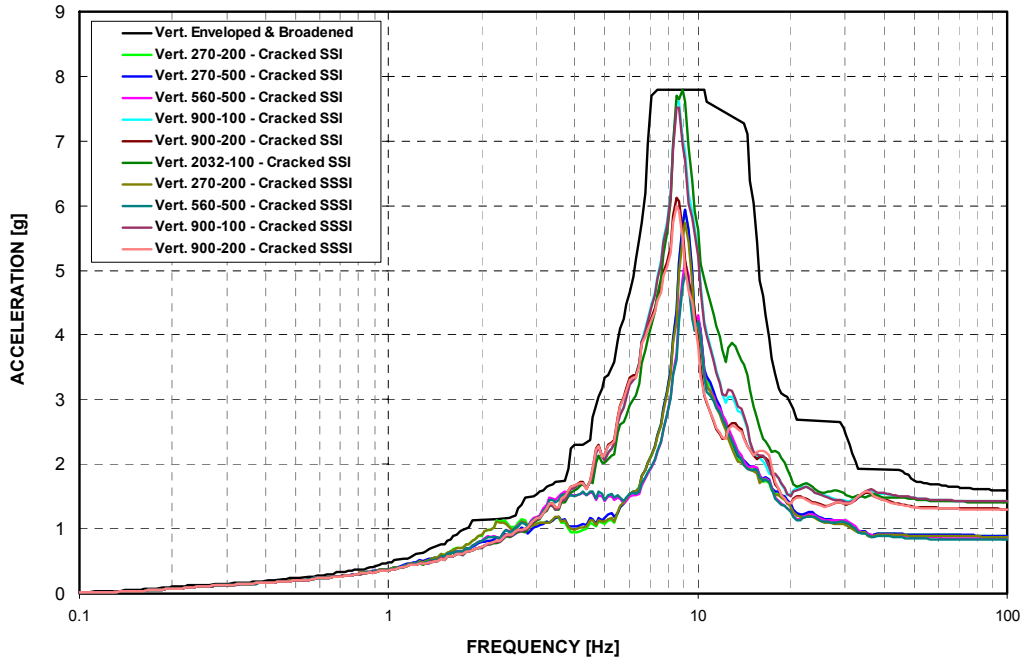

Figure 3-F.2.0-102 ISRS at Top of PCCV - 5% Damped Response in Vertical Direction (Z) at Model Elevation 232'-0" - Cracked